

2017

The Role of Lipocalin-2 in the Hepatic Microenvironment of Colorectal Cancer Metastasis

Daniel Titus Hughes
University of South Carolina

Follow this and additional works at: <https://scholarcommons.sc.edu/etd>



Part of the [Biology Commons](#)

Recommended Citation

Hughes, D. T.(2017). *The Role of Lipocalin-2 in the Hepatic Microenvironment of Colorectal Cancer Metastasis*. (Doctoral dissertation). Retrieved from <https://scholarcommons.sc.edu/etd/4334>

This Open Access Dissertation is brought to you for free and open access by Scholar Commons. It has been accepted for inclusion in Theses and Dissertations by an authorized administrator of Scholar Commons. For more information, please contact SCHOLARC@mailbox.sc.edu, dillarda@mailbox.sc.edu.

THE ROLE OF LIPOCALIN-2 IN THE HEPATIC MICROENVIRONMENT OF
COLORECTAL CANCER METASTASIS

by

Daniel Titus Hughes

Bachelor of Science
North Greenville University, 2007

Submitted in Partial Fulfillment of the Requirements

For the Degree of Doctor of Philosophy in

Biological Sciences

College of Arts and Sciences

University of South Carolina

2017

Accepted by:

Maria Marjorette O. Peña, Major Professor

Hexin Chen, Chair, Examining Committee

Franklin G. Berger, Committee Member

David Reisman, Committee Member

Michael Wyatt, Committee Member

Cheryl L. Addy, Vice Provost and Dean of the Graduate School

© Copyright by Daniel Titus Hughes, 2017
All Rights Reserved.

DEDICATION

This work is dedicated to my beautiful and intelligent wife, Erin, who is the best person I know and love. She has always been there for me through this journey and makes life so enjoyable.

ACKNOWLEDGEMENTS

To my advisor, Dr. Peña, thank you for giving me the opportunity to carry out research in your laboratory and for guiding me over the years. To my committee members Hexin Chen, Frank Berger, David Reisman, and Michael Wyatt, thank you for all your time, work, and guidance over the years. To those in and around the Peña lab, Yu Zhang, Grishma Acharya, Nikeya Tisdale, John Bonaparte, Karen Barbour, Sapana Shah, Vivek Vaish, Kristen Larsen, and Maydelis Minaya, thank you for being a pleasure to work with and know. To Yu Zhang and Vivek Vaish, thank you for all the hands-on teaching and experimental analysis methods you taught me. To Tia Davis, thank you for all your hard work over many years as our technician.

To Mom, Dad, Max, and Krysten, thank you for all that you have done over the years, raising me and providing a lot of great memories. To Joel and Cheryl Chandler and Pat and Jerry Neal, thank you all for proving support and kindness over the years of this journey. To the rest of my friends and family, thank you for all for your kindness over the years. I am privileged to have you all in my life. “Remember, no man is a failure who has friends (Goodrich et al.)”

Soli Deo Gloria.

ABSTRACT

Colorectal cancer (CRC) is the second leading cause of cancer deaths in the United States. The major cause of death is metastasis and the frequent target organ is the liver. When diagnosed early at a localized stage, the five year survival rate after resection is 90%. However, after metastasis has occurred, this drops to less than 12%. Metastasis is often asymptomatic and diagnosed at the final stage when therapeutic options are limited. Because of this, the genetic and cellular mechanisms regulating metastasis are still poorly understood. Recent studies have shown that prior to the arrival of cancer cells at the secondary organ, molecular signals from the tumor direct the recruitment of bone marrow derived cells (BMDCs) to create a pre-metastatic niche where cancer cells can attach and develop into a metastatic lesion. Identifying and understanding these signals can lead to the development of methods for early diagnosis or identifying targets for intervention.

Using an orthotopic mouse model of CRC liver metastasis, we performed microarray analyses of the liver microenvironment in tumor bearing mice before and after the arrival of metastatic cells in the liver. We found that Lipocalin-2 (Lcn2) was highly expressed in the liver and sera of mice bearing highly metastatic cells. Its expression is upregulated in tumors of epithelial origin, but has contrasting roles in metastasis. In the clinic, elevated LCN2 is associated

with poor prognosis. The role of LCN2 in the tumor microenvironment has not thoroughly been studied. Our studies show overexpression of Lcn2 in mouse colon cancer cells had little impact on tumor growth or invasiveness; however, invasion assays show that Lcn2 from some stromal cells increases the invasiveness of colon tumor cells. These studies will allow us to better elucidate the role of Lcn2 in tumor and stromal cells in the early stages of CRC metastasis and in anticancer therapy.

TABLE OF CONTENTS

DEDICATION	iii
ACKNOWLEDGEMENTS	iv
ABSTRACT	v
LIST OF FIGURES.....	ix
LIST OF ABBREVIATIONS	xi
CHAPTER 1: INTRODUCTION	1
1.1 COLORECTAL CANCER.....	1
1.2 METASTASIS	3
1.3 TUMOR MICROENVIRONMENT AND THE IMMUNE CELL COMPARTMENT	4
1.4 THE PRE-METASTATIC NICHE	6
1.5 MOUSE MODELS OF COLORECTAL CANCER METASTASIS	9
1.6 LIPOCALIN-2 IN COLORECTAL CANCER AND METASTASIS.....	10
1.7 GOALS OF THE PROJECT.....	13
CHAPTER 2: LIPOCALIN-2 IS OVEREXPRESSED IN THE LIVER OF COLORECTAL CANCER BEARING MICE.....	19
2.1 INTRODUCTION.....	19
2.2 RESULTS.....	20
2.3 SUMMARY AND DISCUSSION.....	22
CHAPTER 3: THE ROLE OF INTRA-TUMOR EXPRESSION OF LIPOCALIN-2 IN COLORECTAL CANCER METASTASIS	26
3.1 INTRODUCTION.....	26

3.2 RESULTS.....	27
3.3 SUMMARY AND DISCUSSION.....	31
CHAPTER 4: THE <i>IN-VITRO</i> ROLE OF TUMOR MICROENVIRONMENT DERIVED LCN2 IN STROMAL CELLS INVASION	39
4.1 INTRODUCTION.....	39
4.2 RESULTS.....	42
4.3 SUMMARY AND DISCUSSION.....	46
CHAPTER 5: THE ROLE OF LIPOCALIN-2 IN SHAPING THE METASTATIC STROMA OF COLORECTAL CANCER <i>IN-VIVO</i>	53
5.1 INTRODUCTION.....	53
5.2 RESULTS.....	54
5.3 SUMMARY AND FUTURE DIRECTIONS.....	62
CHAPTER 6: MATERIALS AND METHODS	75
REFERENCES	90
APPENDIX A – PERMISSION TO REPRINT	98

LIST OF FIGURES

Figure 1.1 The metastatic cascade	14
Figure 1.2 The seed and soil organotropism of metastasis.	15
Figure 1.3 Working model of pre-metastatic niche formation.	16
Figure 1.4 Mouse models of liver metastasis.	17
Figure 1.5 The known mechanisms of Lipocalin-2	18
Figure 2.1 Microarray analysis of genetic changes in the seed and soil of colorectal cancer bearing mice	24
Figure 2.2 Liver “soil” mRNA expression of <i>Lcn2</i> in tumor bearing mice	25
Figure 2.3 Circulating levels of <i>Lcn2</i> in tumor progression.	25
Figure 3.1 <i>Lcn2</i> overexpression in CT26 and CT26-FL3.....	34
Figure 3.2 <i>Lcn2</i> overexpression does not significantly impact growth or invasion in CT26 and CT26-FL3	35
Figure 3.3 <i>Lcn2</i> overexpression in CT26 and CT26-FL3 splenic injection	36
Figure 3.4 CT26-FL3 overexpressing <i>Lcn2</i> in WT and <i>Lcn2</i> ^{-/-} BALB/C mice.....	36
Figure 3.5 MC38-luc cells overexpressing <i>Lcn2</i>	37
Figure 3.6 MC38-luc cells overexpressing <i>Lcn2</i> invasion assay	37
Figure 3.7 MC38-luc cells overexpressing <i>Lcn2</i> injected via spleen in C57BL/b mice	38
Figure 3.8 ELISA data of secreted <i>Lcn2</i> in CT26 and MC38 lines.....	38
Figure 4.1 <i>Lcn2</i> is overexpressed by transfecting TIB-73 with pCMV6- <i>Lcn2</i>	48
Figure 4.2 <i>Lcn2</i> overexpression from TIB-73 cells in the “seed” compartment in a co-culture invasion assay increases invasiveness of CT26 and CT26-FL3	49

Figure 4.3 Lcn2 expression from TIB-73 hepatocytes directly affects invasiveness of CT26 tumor cells	50
Figure 4.4 Lcn2 overexpression in neutrophil cell line appears to increase invasiveness of CT26 tumor cells	51
Figure 4.5 Raw264.7 co-culture increases CT26 and CT26-FL3 invasiveness but Lcn2 dampens MC38-luc invasiveness shown by a co-culture invasion assay with Lcn2 knockout BMDMs polarized to an M2 phenotype	52
Figure 5.1 Electroporation of pV1J-Lcn2 increases tumor burden in a breast cancer and melanoma cell lines.....	64
Figure 5.2 IHC Staining of liver metastasis tissue for Lcn2 and Mpo	65
Figure 5.3 Liver metastasis tissue stained by H&E and <i>in-situ</i> RNA hybridization of Lcn2 mRNA.....	66
Figure 5.4 <i>In-situ</i> RNA stain for Lcn2 compared to IHC stained for immune cells in liver metastasis tissue	67
Figure 5.5 Confocal microscopy adjacent sections from liver metastasis of MC38-luc bearing mice electroporated with pV1J or pV1J-Lcn2 showing liver (L) and tumor metastasis (M) regions and MPO+, F4/80+, MCT+, and CD45+ cell populations	67
Figure 5.6 Quantification of confocal results at metastatic tumor-liver periphery from pV1J and pV1J-Lcn2 electroporated MC38-luc bearing mice	68
Figure 5.7 Quantification of flow cytometry results shows fold change of pV1J-Lcn2 over pV1J electroporation in cell populations of the spleen, liver, and liver metastasis compartments of tumor-bearing mice only.....	68
Figure 5.8 Flow analysis of Cd45+ immune cells.....	69
Figure 5.9 Flow analysis of F4/80+ macrophages	70
Figure 5.10 Flow analysis of Cd11b+/Ly-6G+ neutrophils and G-MDSCs	71
Figure 5.11 Flow analysis of Cd117+/FcεR1α+ mast cells.....	72

LIST OF ABBREVIATIONS

24p3.....	Lipocalin-2
24p3R.....	Lipocalin-2 receptor
BMDM	Bone Marrow Derived Macrophage
CRC	Colorectal Cancer
DFO	Deferoxamine
ELISA	Enzyme-Linked Immunosorbent Assay
FeCl ₃	Ferric Chloride
IHC	Immunohistochemistry
Lcn2	Lipocalin-2
MCT	Mast Cell Tryptase
M-CSF	Macrophage Colony Stimulating Factor
MMP-9.....	Matrix Metalloproteinase 9
MPO.....	Myeloperoxidase
NGAL	Neutrophil Gelatinase Associated Lipocalin
RCF	Relative Centrifugal Field
siRNA	Short Interfering RNA
Slc22a17	Lipocalin-2 receptor

CHAPTER 1

INTRODUCTION

1.1 COLORECTAL CANCER

Colorectal cancer (CRC), which consists of cancers originating in the colon or rectum, is one of the deadliest cancers both in the United States and in the world. The tumors are often slow growing, beginning as a benign polyp and developing into a malignant tumor over multiple years or even decades. Three types of polyps, adenomatous, hyperplastic, and dysplastic, may all form, but adenomatous polyps most frequently develop into a harmful adenocarcinoma (American Cancer Society, 2015).

In the United States, CRC ranks as the fourth most diagnosed cancer and the second leading cause of cancer related deaths (Howlader et al., 2014). According to the 2012 GLOBOCAN report by the World Health Organization (WHO), CRC was diagnosed in 1,361,000 cases and responsible for 694,000 deaths worldwide, accounting for approximately 10% of all cancer cases (WHO). As the global population continues to live longer due to better healthcare, the incidence of colorectal cancer will, as a result, also rise significantly.

Colorectal cancer is problematic not only because of its slow early growth, but also due to a lack of symptoms until the tumor is large enough to be symptomatic and clinically detectable. When diagnosed early, colorectal tumors

are usually well contained in the colon and the localized tumors can easily be surgically resected, contributing to a five year survival rate of 90.1% (Howlader et al., 2014). However, if the diagnosis occurs after the tumor has spread to the lymph nodes, the tumor is classified as stage II or III and the five-year survival drops to 60% and 40%, respectively. In Stage IV cancer where the tumors have metastasized to distant organs, surgical resection of disseminated metastatic lesions is difficult and tumor cell populations have increased heterogeneity and drug resistance. The average five-year survival for all colorectal cancer diagnoses is 64.9%, but for patients with metastatic disease, the survival rate is a mere 13.1% (Howlader et al., 2014). Furthermore, nearly 70% of patients dying from CRC burden have metastasis present as revealed by autopsy (Hugen et al., 2014; Welch and Donaldson, 1979). Colonoscopies currently remain as the best screening method for early detection of colorectal cancer development and the removal of polyps; however, less invasive methods such as stool DNA testing (e.g. Cologuard) are quickly becoming reliably accurate and significantly cheaper, providing a viable alternative to a colonoscopy (American Cancer Society, 2014). The primary reason for mortality in CRC and many other solid tumors, which includes all non-leukemic and non-lymphoma tumors, is the presence of metastatic disease and understanding the underlying molecular and cellular mechanisms that drive metastasis may lead to therapeutic strategies and interventions to improve patients' clinical outcomes (Obenauf and Massagué, 2015).

1.2 METASTASIS

One of the hallmark properties of cancer cells is the ability to activate invasion and metastasis (Hanahan and Weinberg, 2011). This is the ability of cancer cells to spread from the primary tumor to lymphatic organs and into circulation and subsequently grow in distant organs. Treatment of a primary tumor frequently only requires surgery and/or adjuvant chemotherapy; however, metastatic tumors that have spread throughout the body are difficult to remove surgically. They form heterogeneous populations that typically harbor additional mutations as compared to the primary tumor cells and that confer variable responses to chemotherapy. Patients with solid tumors that already present with metastasis upon diagnosis are given a stage IV diagnosis that correlates with low five-year survival rate as seen in the following cancers: ovarian (28.3%), breast (25.2%), colon (13.1%), and lung (4.2%) (Howlader et al., 2014).

Metastasis is a complex, multistep process that involves growth and vascularization of the primary tumor, invasion and entry into the submucosal stromal compartment, intravasation into and survival in circulation, avoidance of immune surveillance, arrest at a distant site, extravasation into the host tissue bed, and development and proliferation into a clinically detectable metastatic lesion (>2mm) (Figure 1, Valastyan and Weinberg, 2011).

The most detrimental aspect of metastasis is the general lack of symptoms until the metastatic tumor is well established and becomes clinically detectable. At that time, treatment options are limited; therefore, it is therefore important to understand the underlying mechanisms particularly in the early

stage of the disease when intervention can have an impact on its progression. This might also lead to the identification of critical biomarkers that might be used for early diagnosis or as therapeutic targets to block progression or alleviate morbidity and mortality from the disease.

1.3 TUMOR MICROENVIRONMENT AND THE IMMUNE CELL COMPARTMENT

It is now fully appreciated that a tumor is not simply comprised of a mass of rapidly proliferating malignant cancer cells (Hanahan and Weinberg, 2011). Rather, a tumor is comprised of both neoplastic tumor cells and normal non-neoplastic stromal cells that are recruited into and infiltrate the tumor bed. These supporting stromal cells comprise the tumor microenvironment (TME) and play a significant role in the growth of all solid tumors.

Host tissue is comprised of two primary cell types, parenchymal and stromal. Parenchymal cells carry out the primary function of a specific organ; for example, hepatocytes in the liver and splenocytes in the spleen. Stromal cells, are located throughout the organ and provide support for the biological function of the parenchymal cells. In the tumor, stromal cells include blood and lymphatic endothelial cells, mesenchymal stem cells, cancer-associated fibroblasts, pericytes, and immune cells, but the stromal composition can vary depending on tumor location and the origin of the tumor (Sebens and Schafer, 2012). The stromal cells are recruited to the tumor and support its growth and progression through the secretion of a diverse collection of cytokines, chemokines, growth factors, and reactive oxygen species that interact with various signaling pathways

to activate transcriptional programs that promote uncontrolled proliferation. They create a permissive tumor microenvironment that is essential to the development and advancement of many tumors. In a metastatic lesion, parenchymal cells are infiltrated both by tumor and stromal cells, all of which are involved in signaling crosstalk which can both promote and inhibit tumor growth. Additionally, many of these stromal cells, such as the immune cells, can be polarized into either a pro-tumor/immune-suppressive or anti-tumor phenotype and recent clinical evidence indicates that polarizing normal cells towards their anti-tumor phenotype has drastic effects on improving survival rates (Suzuki et al., 2016).

The immune cell component of the stroma is highly important to understanding the tumor microenvironment. In a classic immune response to an infection with a foreign antigen, T-cells, B-cells, and myeloid lineage cells are mobilized to clear the infection and then return to an inactivated state (Chaplin, 2010). In the context of cancer, however, immune cells are recruited to a tumor that they infiltrate where they may exert a pro-tumor phenotype as a consequence of their plasticity. The primary immune cells found in the tumor microenvironment include mast cells, myeloid-derived suppressor cells, macrophages, neutrophils, and T-regulatory cells among other immune cell types (Hanahan and Weinberg, 2011). Mast cells, the primary cell type responding to an allergy stimulus, often infiltrate a tumor, correlate with poor prognosis, and assist in chemotherapeutic drug resistance (Maciel et al., 2015; Oldford and Marshall, 2015). Myeloid-derived suppressor cells (MDSCs) are immature myeloid cells found in most tumors which can suppress the T-cell response to the

growing tumor (Arbab and Achyut, 2016; De Vlaeminck et al., 2016; Moses and Brandau, 2016). Macrophages and neutrophils arise from the myeloid lineage and are both highly plastic. Macrophages and neutrophils have a classically activated M1/N1 anti-infection and anti-tumor phenotype, and an alternatively activated M2/N2 wound healing and pro-tumor phenotype (Galdiero et al., 2013; Kim and Bae, 2016). These activated states are extremes on a spectrum of possible phenotypes, but must be differentiated to study their biological context accurately. When infiltrating a tumor, macrophages and neutrophils are designated as “tumor associated” macrophages or neutrophils, TAMs and TANs, respectively. TAMs and TANs are frequently polarized towards a pro-tumor phenotype and thus provide a potential target for therapy. In a healthy patient, these wound healing phenotypes prevent the body from being overwhelmed by too much inflammation; however, in the context of cancer, immune cell function can be hijacked into a pro-tumor phenotype that supports the growth of the tumor.

1.4 THE PRE-METASTATIC NICHE

Metastasis is not a random process (Figure 1.2). As early as 1889 the British pathologist, Stephen Paget, found that certain primary tumors metastasize to secondary organs for which they have a specific affinity. Dr. Paget observed in autopsies of breast cancer patients that metastases developed only in the liver, bone, and ovaries (Paget, 1989). He postulated that since the spleen receives much more blood flow than the bone, it should have more metastatic growth,

however, none of his autopsy patients presented with metastasis in the spleen. He proposed the “seed and soil hypothesis,” wherein certain “seeds”, i.e., the primary tumor cells have a preference and will only grow in certain “soil”, i.e., the secondary organ that provides a permissive environment for the growth of disseminated tumor cells.

In the 1930’s James Ewing challenged Paget’s hypothesis by suggesting that metastatic dissemination can be explained solely by hematogenous circulation (Ewing, 1928). The prevailing theory was that metastasis was controlled by the pattern of blood and lymph circulation and that capillary beds, such as those prevalent in the lung, liver, or spleen, were the only targets for metastatic growth. Prior to this it was thought that tumors only metastasized purely from the vasculature of organs although some physicians had speculated such organotropism. Although it has been shown that vasculature has an effect, the seed and soil hypothesis provides a viable explanation for discrepancies between blood flow and metastatic growths in an organ (Fidler and Hart, 1982). In the 1970’s, Isaiah Fidler’s work reignited interest in the seed-and-soil hypothesis, and in 2005, David Lyden’s group was the first to show that the formation of a pre-metastatic niche (PMN) in the target organ prior to the arrival of metastatic cells promoted the establishment and progression of metastasis (Kaplan et al., 2005). He showed that clusters of immune cells, specifically bone marrow derived cells (BMDCs) expressing VEGFR1, c-kit, CD133, and CD34, were recruited to the target organ prior to the arrival of metastatic tumor cells

where they provided sites for attachment and a favorable environment for the tumor cells to grow.

The current understanding of the pre-metastatic niche in liver metastasis is well described in both Azizidoost, et al. and Obenauf and Massagué and is schematically summarized in Figure 1.3 (Azizidoost et al., 2015; Obenauf and Massagué, 2015). The liver is the most common site for metastasis of many solid tumors and is primarily seen in the metastasis of colorectal, pancreatic, and gallbladder cancers. Liver metastasis is also seen frequently in breast and lung cancers. The hepatic portal system partially explains colorectal liver metastasis because the veins of the gastrointestinal tract drain through the capillaries in the liver, which provides ample endothelial surface area for the tumor cell to extravasate, arrest, and grow.

Some of the mechanistic details of how the pre-metastatic niche is developed have begun to unfold over the past decade. Exosomes have been shown to induce TGF- β production, which activates hepatic stellate (ito) cells and leads to BMDC recruitment to the liver. IL-6 and CCL2 have also been shown to induce the recruitment of BMDCs to the liver (Obenauf and Massagué, 2015). Neutrophils can produce MMP9, which degrades collagen in the basement membrane of an organ, allowing for an increase in both intravasation and extravasation of tumor cells. CXCL1, a neutrophil chemoattractant is highly upregulated in the liver of tumor bearing mice, leading to neutrophil recruitment (Yamamoto et al., 2008). It has also been shown that neutrophils are capable of binding to tumor cells leading to their accumulation in the liver (Spicer et al.,

2012). By understanding the kinetics and cellular and molecular mechanisms regulating the organotropism of metastasis and pre-metastatic niche formation, it may be possible to develop methods to restrict the growth of metastasis in patients whose tumors have not yet metastasized.

1.5 MOUSE MODELS OF COLORECTAL CANCER METASTASIS

In order to study the cellular and molecular factors effecting metastasis during colon cancer progression, a clinically relevant and ethically appropriate model, which can recapitulate the many traits of human metastasis from the growth of the primary tumor to establishment of metastasis, is essential. Mice provide an ideal model that has been used by many researchers for cancer studies. In studies designed to test drugs directly on human tumors, a patient-derived xenograph model (PDX) using immune-deficient mice have been very useful; however to study the biological mechanisms of metastasis and the role of the tumor microenvironment, a few factors must be controlled. The mice must have an intact immune system that is able both to respond to pathogens and infiltrate the tumor and surrounding tissues. Furthermore, the tumor must be syngeneic to the host strain so that the immune system does not detect the injected tumor cells as foreign, resulting in their rejection. The tumor must also be orthotopic, or located in its tissue of origin. As shown in Figure 1.4, a cecal implantation model for colorectal cancer is ideal for this purpose and can reliably produce liver metastasis with pre-metastatic niche formation (Zhang et al., 2013).

In this experimental method, CRC tumor cells that are syngeneic are injected into the subserosa of the cecum to grow in their native environment.

Additionally a splenic injection model is a useful experimental model that can be utilized to readily assess the establishment and growth of metastatic cells upon arrival into the liver (Lim et al., 2015). These mouse models allow for the kinetics and composition of the hepatic microenvironment to be accurately studied because they recapitulate many traits of clinically observed tumors in a rapid, reproducible, and accurate manner. Most importantly for this study, the immune cells of the mice can be studied, which is vital to precisely understanding the tumor microenvironment and its interactions with tumor cells. Other mouse models in use for colorectal cancer studies include cecal and splenic implantations of human cells into mice lacking some or all cell immune cell types (Oh et al., 2016).

1.6 LIPOCALIN-2 IN COLORECTAL CANCER AND METASTASIS

Lipocalin-2 (LCN2) is a 25 kD protein that is also known as Neutrophil Gelatinase Associated Lipocalin (NGAL), oncogene 24p3, or siderocalin. It is a siderophore binding protein that is primarily associated with the innate immune response (Goetz et al., 2002). It was initially discovered in the secondary granules of neutrophils where it was bound to neutrophil gelatinase, also known as metalloproteinase 9 (MMP9) (Kjeldsen et al., 1993).

In a normal human, the principal role of LCN2 is to bind and sequester the siderophore enterobactin, primarily secreted by *Escherichia coli* and *Salmonella*

typhimurium, to inhibit bacterial growth by limiting the amount of iron that can be stolen from the mammalian host to be used in bacterial metabolism. Many bacterial cells have developed resistance to this mechanism and secrete siderophores that LCN2 cannot bind (Correnti and Strong, 2012; Neilands, 1995). During an infection, invading bacteria secrete siderophores to capture iron for use in cellular processes (Flo et al., 2004). As shown in Figure 1.5, Lipocalin-2 circumvents this hijacking by binding the siderophore and sequestering it back into a host cell expressing the receptor for Lipocalin-2, Slc22a17 (24p3R) (Bao et al., 2010; Richardson, 2005).

Not only can Lipocalin-2 bind to the bacterial siderophore, enterobactin, but it can also bind to the mammalian siderophore, catechol (Correnti and Strong, 2012; Neilands, 1995). In mammalian cells, LCN2 can both increase or decrease intracellular iron levels in response to environmental signals (Tandara and Salamunic, 2012). Upon binding iron, LCN2 binds to the cell surface receptor 24p3R which is then internalized. The iron is released causing intracellular iron levels to increase. LCN2 can also bind to intracellular iron and shuttle it out of the cell, reducing iron levels and inducing apoptosis (Bao et al., 2010; Reilly et al., 2013).

There are multiple studies with contrasting data on the role of Lcn2, which is likely context dependent; however, there is strong support in the published literature for a pro-tumorigenic role for Lcn2 in cancer progression. A number of papers show that elevated levels of Lcn2 correlate with poor prognosis, poor survival, metastasis, and invasiveness. In multiple studies, colorectal

adenocarcinoma patient samples were analyzed by IHC and high NGAL expression was seen in colorectal cancer specimens, while low or no expression was seen in adjacent normal tissue (Nielsen et al., 1996) (Lv et al., 2010) (Sun et al., 2011) (Barresi et al., 2011). Proteomic analysis via mass spectrometry showed higher LCN2 in colon cancer samples versus normal colon samples (Conrotto et al., 2008). In rectal cancer patient samples, 69/100 samples showed LCN2 overexpression which positively correlated with invasiveness, lymph node metastasis, angiogenesis, and an advanced stage (Zhang et al., 2009). LCN2 was associated with an increase in distant metastasis and advanced cancer stage in 64 surgically resected colorectal carcinoma tissues (Barresi et al., 2010). In a study of patients already presenting with hepatic metastasis, serum LCN2 was significantly higher in patients with three or more metastatic nodes and in patients with two or more hepatic lobes showing metastases (Martí et al., 2010). Furthermore, plasma LCN2 was lower in healthy patients as compared to non-metastatic and metastatic CRC patients (Marti et al., 2013).

Outside of the primary tumor, other studies have begun describing a role for stromal-derived Lcn2. In McLean et al., LCN2 was expressed in 100% of adenoma and carcinoma tumor tissues, but only in 4% of tumor adjacent normal tissue (McLean et al., 2013). This tumor adjacent tissue only expressed LCN2 in the stromal compartment, but in the tumor tissue, LCN2 was more prevalent in stroma than in epithelium. In oral squamous cell carcinoma tissue, Shinriki, et al. showed that LCN2+ neutrophils were significantly associated with lower overall survival (Shinriki et al., 2014). Recently, it has been shown that Lcn2 from the

tumor stroma promotes MCF-7 breast cancer metastasis, and is postulated to be secreted from macrophages in response to tumor cells (Ören et al., 2016).

1.7 GOALS OF THE PROJECT

The overall goal of this project is to understand the changes in the liver microenvironment prior to and after the establishment of metastases; specifically, we are interested in the role that the Lipocalin-2 protein plays in this process. We will test the hypothesis that Lcn2 promotes liver metastasis of colorectal cancer by altering the hepatic microenvironment by promoting interactions between tumor cells and cells in the hepatic microenvironment. To understand these mechanisms, we altered the levels of Lcn2 both in the seed (tumor cells) and in the soil (hepatocytes and stromal immune cells). We utilized an *in-vitro* scratch/migration and matrigel[®] transwell invasion assays to systematically delineate Lcn2-specific effects on tumor cell invasion (Corning Incorporated, 2013; Justus et al., 2014). We also utilized a cecal implantation model and splenic injection model to provide the *in-vivo* framework to recapitulate the results we have obtained using the *in-vitro* methods (Soares et al., 2014; Zhang et al., 2013). Finally, we analyzed the effects of systemic upregulation of Lipocalin-2, and its effect on the rate and stromal composition of metastasis. Together, these studies provide a large volume of data showing the effects of Lcn2 in the liver metastasis of colorectal cancer.

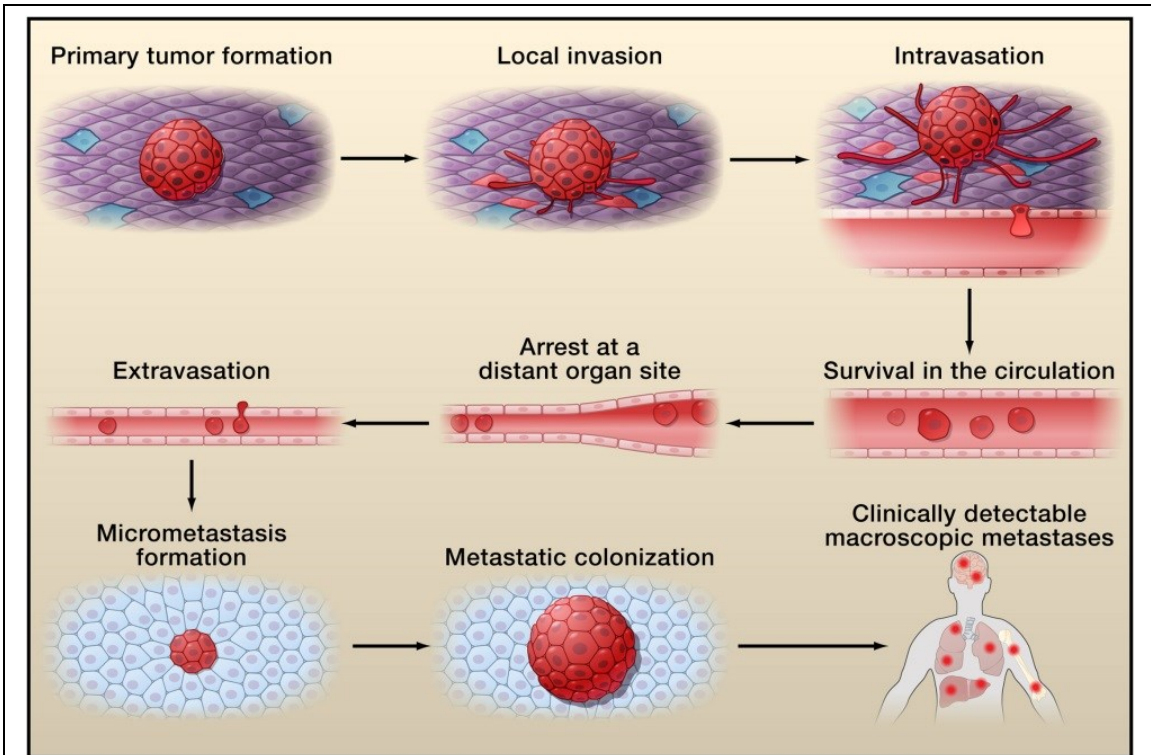


Figure 1.1: The metastatic cascade. Metastasis comprises many steps to allow tumor cells to break into circulation from the primary tumor and travel and arrest to a distant site to form a metastatic tumor. Reprinted from *Cell*, Volume 147/Issue 2, Scott Valastyan and Robert Weinberg, *Tumor Metastasis: Molecular Insights and Evolving Paradigms*, Pages 275-292, 2011, with permission from Elsevier.

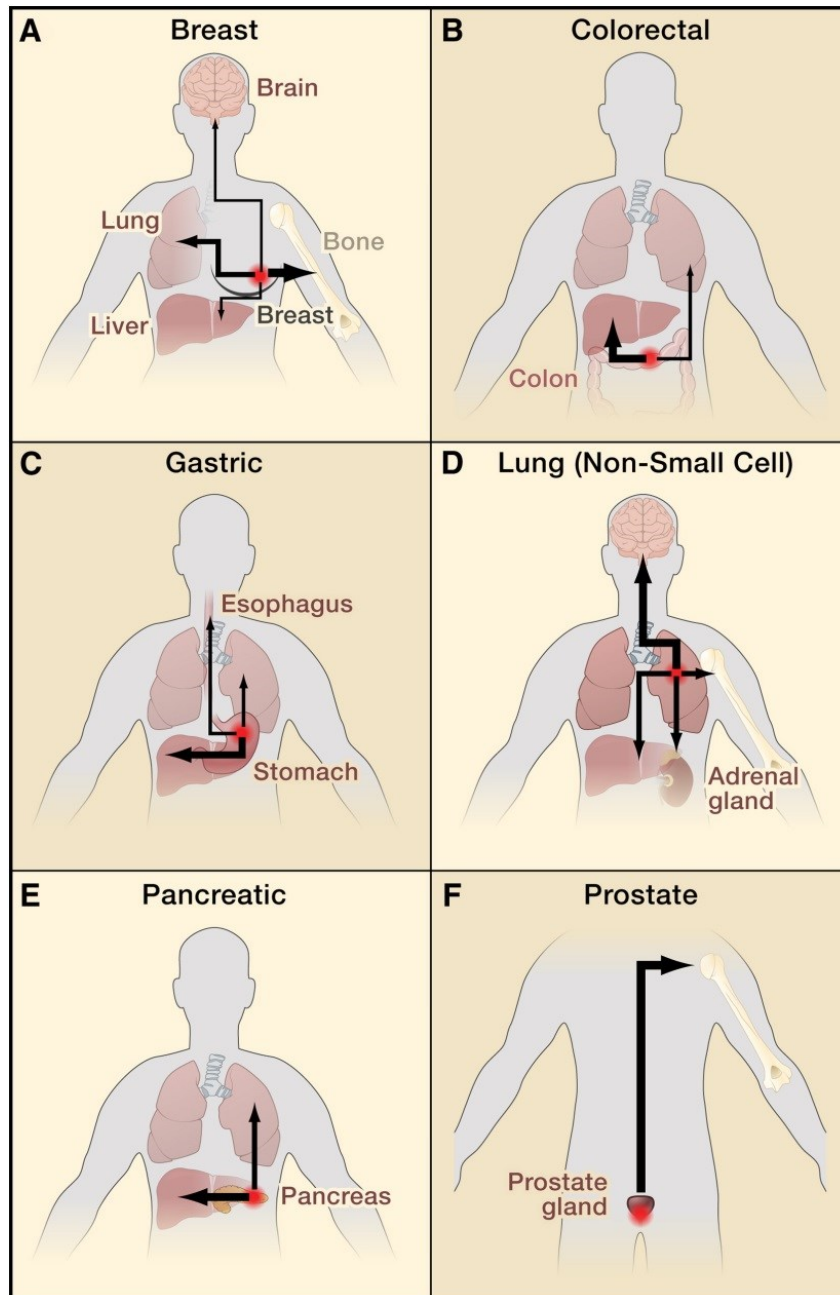


Figure 1.2: The seed and soil organotropism of metastasis. As described in (Valastyan and Weinberg, 2011), primary tumors have organotropism and an affinity for the supportive environment of certain organs for metastatic growth. Reprinted from *Cell*, Volume 147/Issue 2, Scott Valastyan and Robert Weinberg, *Tumor Metastasis: Molecular Insights and Evolving Paradigms*, Pages 275-292, 2011, with permission from Elsevier.

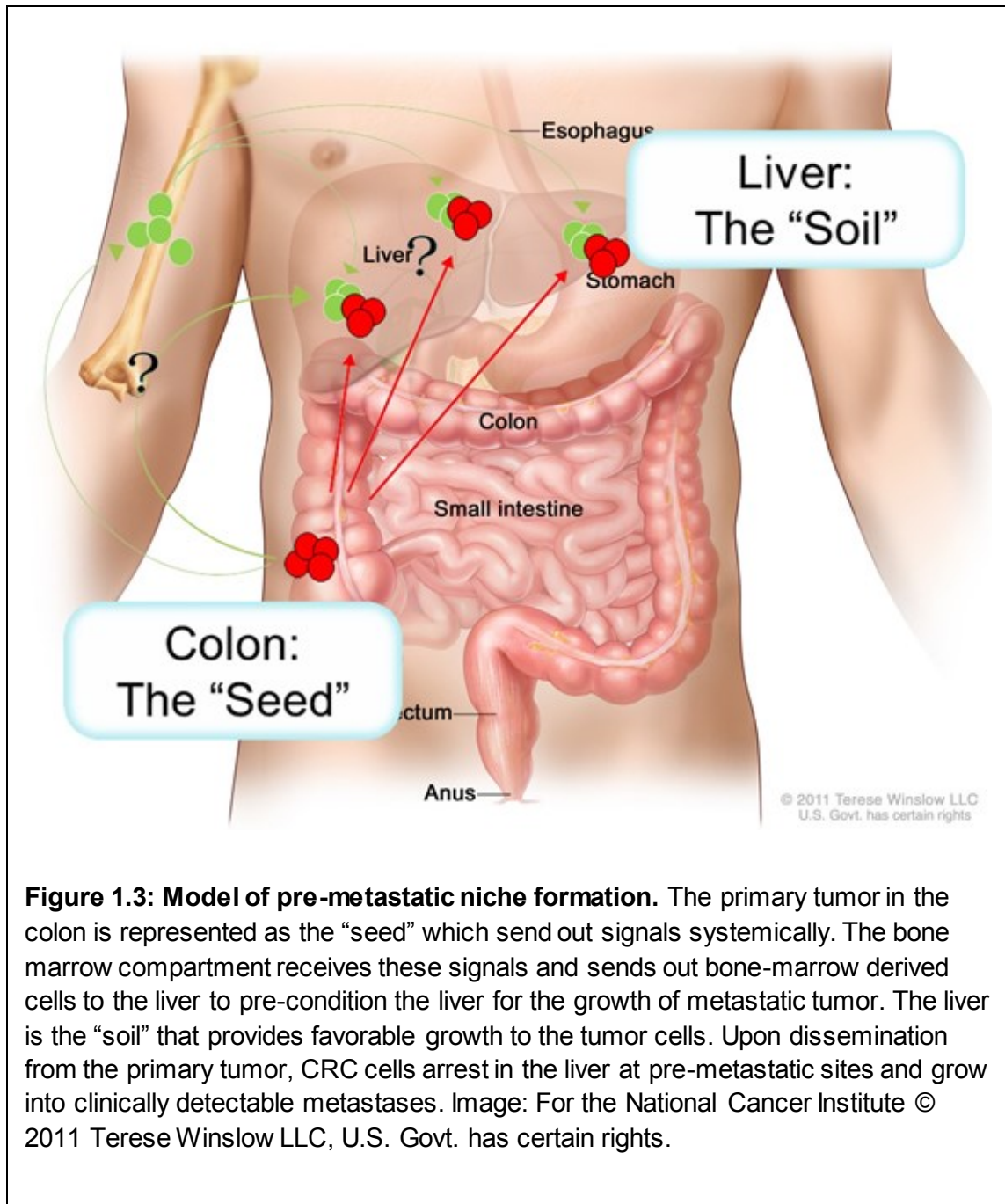


Figure 1.3: Model of pre-metastatic niche formation. The primary tumor in the colon is represented as the “seed” which send out signals systemically. The bone marrow compartment receives these signals and sends out bone-marrow derived cells to the liver to pre-condition the liver for the growth of metastatic tumor. The liver is the “soil” that provides favorable growth to the tumor cells. Upon dissemination from the primary tumor, CRC cells arrest in the liver at pre-metastatic sites and grow into clinically detectable metastases. Image: For the National Cancer Institute © 2011 Terese Winslow LLC, U.S. Govt. has certain rights.

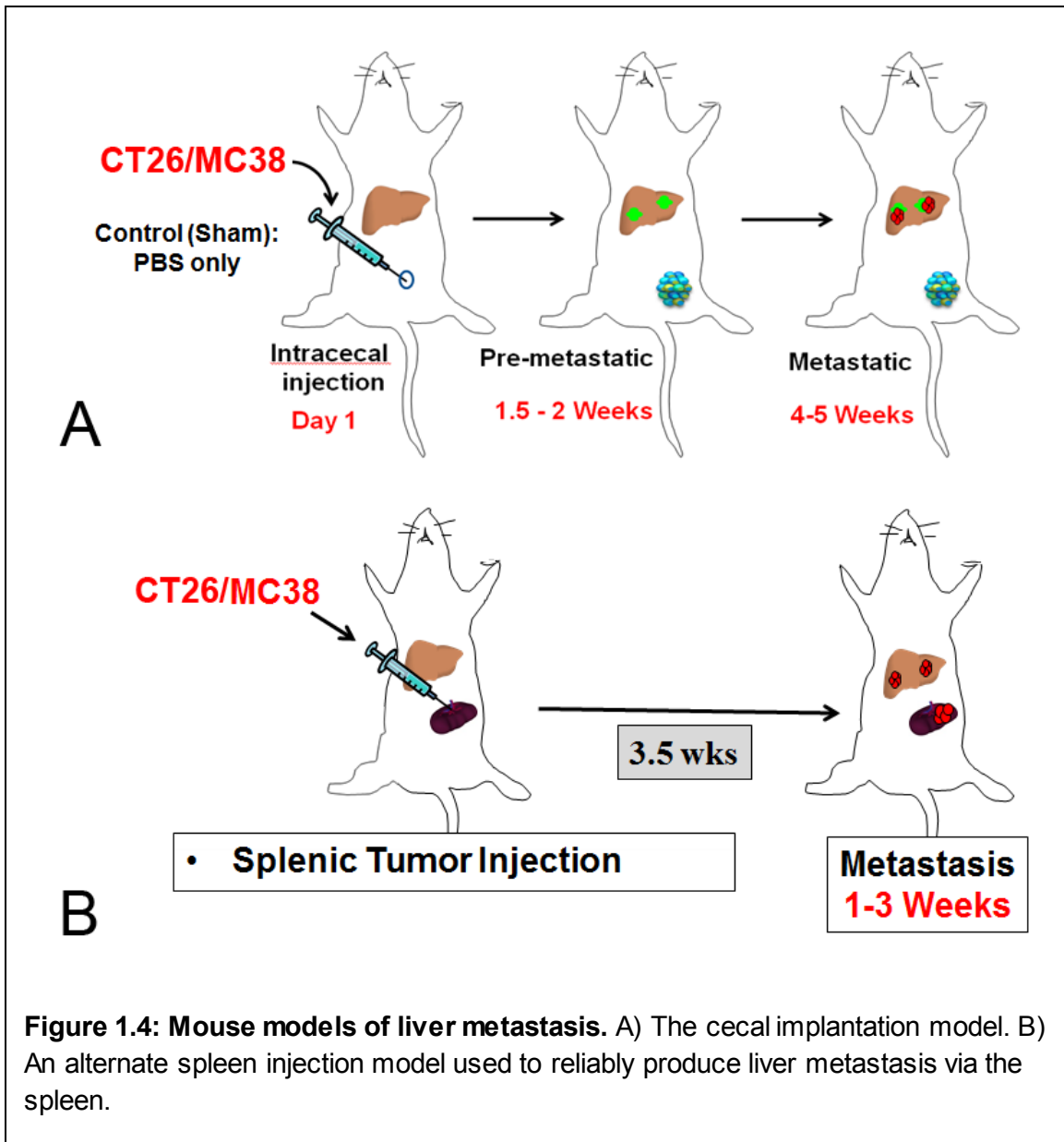


Figure 1.4: Mouse models of liver metastasis. A) The cecal implantation model. B) An alternate spleen injection model used to reliably produce liver metastasis via the spleen.

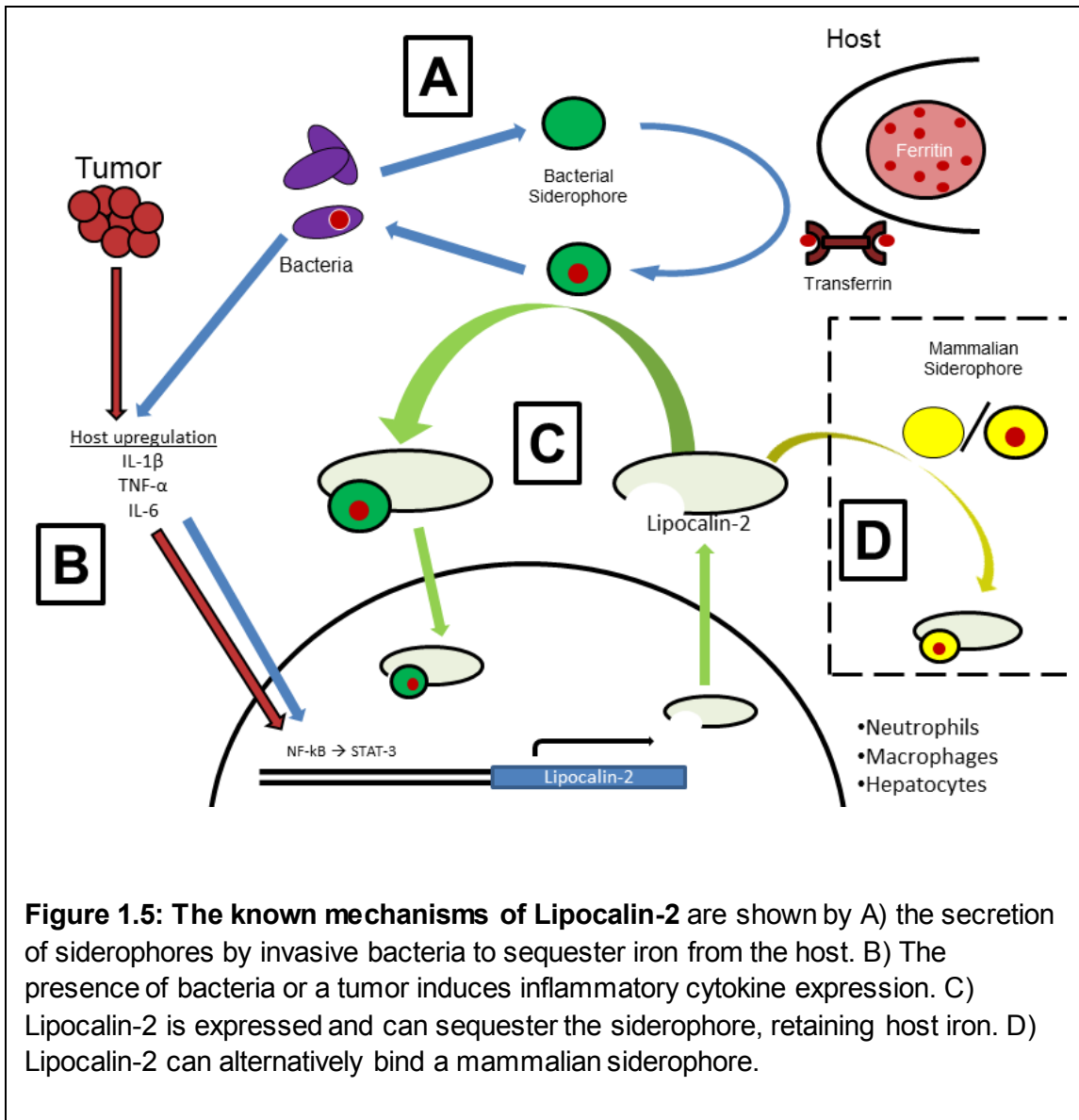


Figure 1.5: The known mechanisms of Lipocalin-2 are shown by A) the secretion of siderophores by invasive bacteria to sequester iron from the host. B) The presence of bacteria or a tumor induces inflammatory cytokine expression. C) Lipocalin-2 is expressed and can sequester the siderophore, retaining host iron. D) Lipocalin-2 can alternatively bind a mammalian siderophore.

CHAPTER 2

LIPOCALIN-2 IS OVEREXPRESSED IN THE LIVER OF COLORECTAL CANCER BEARING MICE

2.1 INTRODUCTION

Despite intensive efforts in cancer research over the past half-century, the high mortality rates of solid tumors, especially after the establishment of metastasis, remains a significant problem. In colorectal cancer, survival rates decrease drastically for patients diagnosed after metastases have grown. Therefore, it is critical to understand the biological processes occurring during tumor development prior to and after the establishment of metastasis to develop therapeutic strategies to lower the high mortality rates in patients presenting with metastasis.

The complex tumor microenvironment is composed of stromal cells that are recruited to the tumor in addition to tumor cells that are embedded in the extracellular matrix in the normal host tissue. It is critical to understand how these three cellular compartments, tumor, tumor stroma, and non-tumor parenchyma interact with one another to promote tumor growth and progression.

The overarching goal of this study is to identify genetic changes in the liver prior to, and after the establishment of metastasis in the liver during colon cancer progression. This allows us to identify genes whose products may be required to

prepare the hepatic microenvironment for the arrival of metastatic cells, and genes whose products are required to sustain metastatic growth and progression upon arrival into the liver. Using a syngeneic orthotopic cecal implantation model previously described in Zhang, et. al., we carried out a microarray analysis of liver tissue in tumor-bearing mice prior to the establishment of metastasis, and liver tissue after the establishment of CRC metastases. We found that Lipocalin-2 is highly expressed in the liver of metastasis-bearing mice and sought to determine its role in maintaining metastatic growth. In this chapter, I describe the microarray analysis and related data, which provides the basis for investigating the role of Lcn2 in the metastasis of colon cancer (Zhang, 2013).

Cellular signaling between tumor, stromal, and host cells is also of interest in this chapter as we confirm microarray data by analyzing serum of mice bearing tumors. The analysis of serum shows the systemic levels of Lcn2 throughout various stages of metastatic tumor progression.

2.2 RESULTS

2.2.1 MICROARRAY ANALYSES OF HEPATIC MICROENVIRONMENT DURING METASTATIC PROGRESSION.

A microarray analysis was performed on tumor bearing mice to determine genetic changes occurring in the liver during tumor progression (Zhang, 2013). In the tumor-bearing mice, three groups were established; sham, pre-metastatic, and metastatic. In addition, microarray analyses were performed to compare the gene expression signatures of the parental CT26 and the highly metastatic

derivative CT26-FL3 tumor cells. The following four comparisons were analyzed: Sham vs. Pre-metastatic, Sham vs. Metastatic, Pre-metastatic vs. Metastatic, and CT26 vs. CT26-FL3. From this microarray, shown in Figure 2.1, *Lcn2* was the most highly upregulated gene in the metastasis-bearing liver as compared to the sham group (388-fold higher). *Lcn2* was also one of the most highly upregulated genes in the metastatic-bearing liver versus the pre-metastatic liver (140 fold higher). *Lcn2* was found to be approximately three-fold higher in CT26-FL3 as compared to CT26; however, CT26-FL3 produces metastasis at a 10-fold higher rate as compared to CT26 (Zhang, 2013).

2.2.2 HEPATIC EXPRESSION OF LIPOCALIN-2 INCREASES DURING METASTATIC PROGRESSION

To confirm the results obtained in the microarray analysis, we quantified *mRNA* expression of *Lcn2* in liver tissue during tumor progression in mice bearing tumors from cecal-injected CT26-FL3 cells. Liver mRNA was extracted from mice at 5, 17, and 30 days after cecal implantation, representing pre-metastatic and metastatic liver, and analyzed by qRT-PCR. As shown in Figure 2.2, on day 5, *Lcn2* expression in liver tissue from mice that had undergone sham surgery was elevated due to inflammation from the surgery. By days 17 and 30, *Lcn2* expression in CT26-FL3-bearing mice was significantly higher than the sham control group, confirming the results from microarray analysis and showing that liver expression of *Lcn2* increased drastically in metastasis-bearing livers.

2.2.3 SERUM LEVELS OF LIPOCALIN-2 ARE ELEVATED DURING TUMOR AND METASTATIC PROGRESSION

To confirm the results from *mRNA* analysis, we analyzed serum protein levels to better understand how *Lcn2* is expressed and localized during tumor progression. Western blot analysis was performed on mouse sera during tumor growth and progression to metastasis. As shown in Figure 2.3, *Lcn2* protein levels progressively increased in the serum of tumor bearing mice as compared to sham injected control mice. The control mice showed an increase in *Lcn2* on day 0 immediately after surgery due to inflammation that was resolved by day 7. On the other hand, mice bearing tumors from CT26-FL3, exhibited progressively higher circulating levels of *Lcn2* by day 28, as shown in Figure 2.3. Statistical analysis using the Pearson Correlation Coefficient was performed on the western blot shown in Figure 2.3A to determine the correlation between the number of days (weeks) of tumor progression and *Lcn2* serum protein levels. The results (CT26; $r=0.6506$, $r^2=0.4233$)(CT26-FL3; $r=0.7092$, $r^2=0.503$) show that there is a stronger correlation in CT26-FL3 versus CT26 for there to be higher *Lcn2* protein expression during tumor progression. This suggests that factors in CT26-FL3 that produce higher metastasis are associated with higher *Lcn2* in circulation.

2.3 SUMMARY AND DISCUSSION

Taken together, these results show that *Lcn2* is upregulated in the liver and in mouse sera during tumor progression, prior to, and after the arrival of metastatic cells to the liver. Furthermore, the results showed that increased *Lcn2*

expression was found in non-tumor cells in the liver during tumor progression; however, it remains to be shown if this expression was from the hepatocytes or other stromal cells found in the liver as part of the pre-metastatic or metastatic niche.

The microarray study validates many of the same genes that have been shown in previous studies to be upregulated in the pre-metastatic and metastatic livers of tumor-bearing mice including *Egfr*, *S100a8*, *S100a9*, *Saa3*, and *Cxcl1* (Rafii and Lyden, 2006; Srikrishna, 2011). Many of these genes have been studied and their mechanistic contributions to metastasis mostly elucidated. However the role of *Lcn2* remains largely unstudied. As the most highly upregulated gene in the liver of metastatic-bearing mice, *Lcn2* is a potentially high yield protein of interest involved in developing a favorable organ “soil” for the colorectal tumor cells to metastasize and proliferate. Microarray analysis also showed CT26-FL3 expressed three-fold higher *Lcn2* as compared to CT26; however this was not likely to be the source of increased *Lcn2* in the serum since the *Lcn2* from the non-tumor liver was much more highly upregulated.

The goal of the subsequent chapters is to further delineate these initial findings of upregulated *Lcn2* in the progression of metastasis along the framework of the “seed and soil” hypothesis. *Lcn2* levels in the tumor “seed” must be investigated. The role of *Lcn2* in the hepatic “soil” is of high importance given the significantly upregulated *Lcn2* in the liver during metastasis in our mouse model. Delineating the immune cell, hepatocyte, and metastatic tumor cells contribution of *Lcn2*, and downstream effects of *Lcn2* in these

compartments must be determined to better understand how Lcn2 affects metastasis.

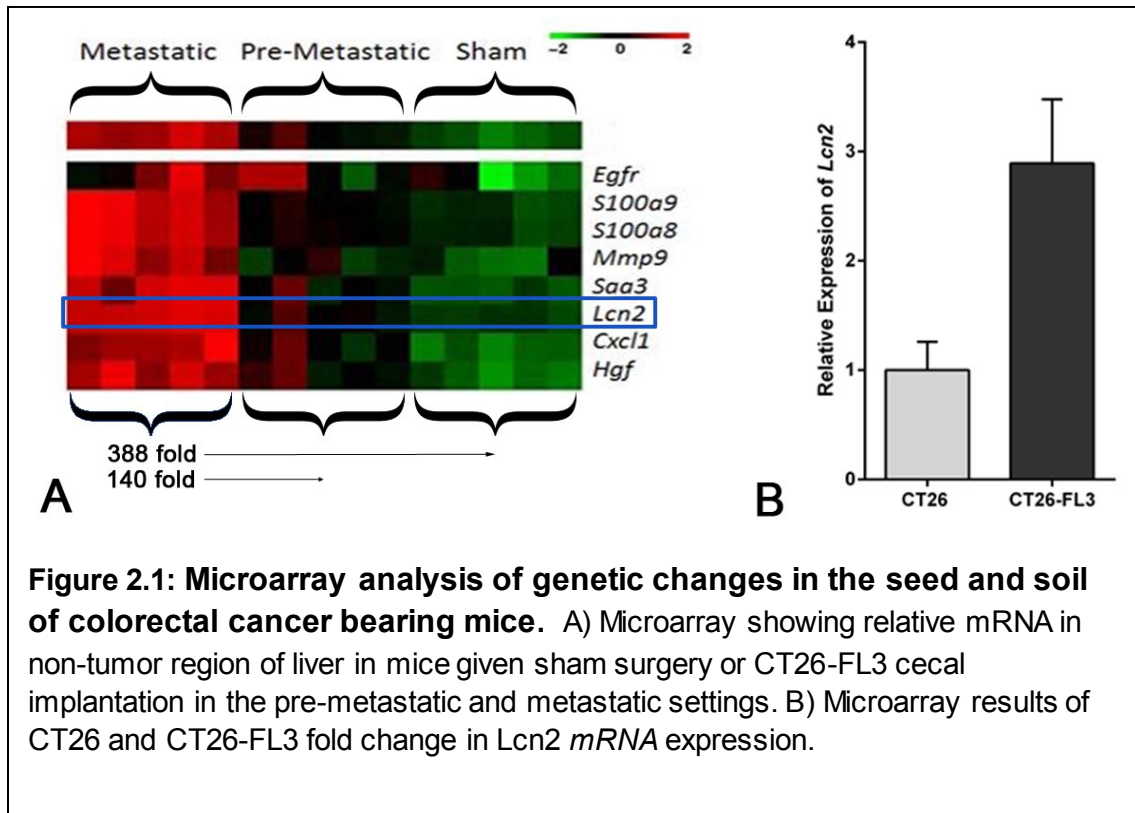


Figure 2.1: Microarray analysis of genetic changes in the seed and soil of colorectal cancer bearing mice. A) Microarray showing relative mRNA in non-tumor region of liver in mice given sham surgery or CT26-FL3 cecal implantation in the pre-metastatic and metastatic settings. B) Microarray results of CT26 and CT26-FL3 fold change in *Lcn2* mRNA expression.

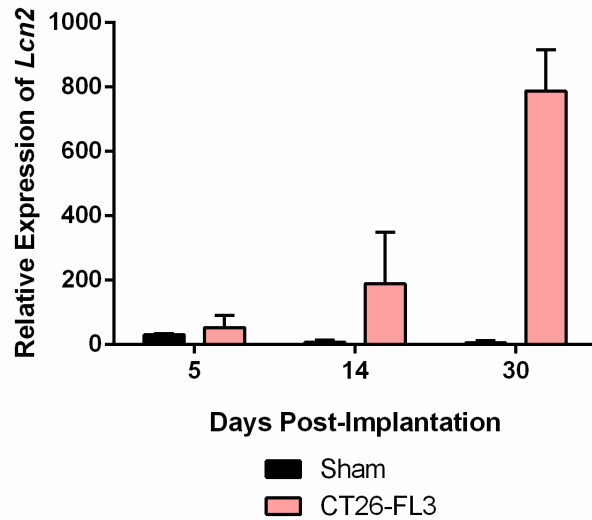


Figure 2.2: Liver “soil” mRNA expression of *Lcn2* in tumor bearing mice. Liver mRNA isolated from sham or tumor-bearing mice analyzed via qRT-PCR for relative *Lcn2* mRNA levels.

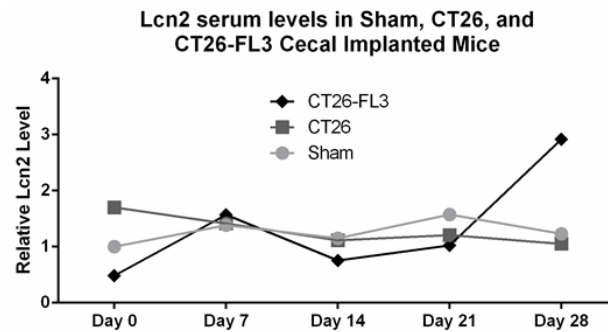
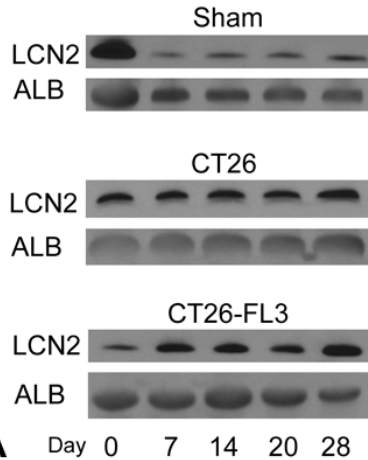


Figure 2.3: Circulating levels of *Lcn2* in tumor progression. A) *Lcn2* levels in serum increase during tumor progression in CT26 and CT26-FL3 bearing mice as compared to sham mice. B) Quantification of the western as performed by Image J analysis.

CHAPTER 3

THE ROLE OF INTRA-TUMOR EXPRESSION OF LIPOCALIN-2 IN COLORECTAL CANCER METASTASIS

3.1 INTRODUCTION

Data from our preliminary *in-vivo* studies indicate that elevated *Lcn2* expression in the liver and *Lcn2* protein levels in circulation was correlated with colorectal cancer metastasis. In this chapter, our goal was to determine if elevated *Lcn2* expression in tumor cells, the “seed”, had an impact on CRC tumor growth and its metastasis to the liver. We performed *in vitro* studies to determine the effect of overexpression or knockdown of *Lcn2* expression in CT26 and MC38 colon adenocarcinoma cell lines that were generated in the BALB/C and C57BL/6 mouse strains. We determined the effects of *Lcn2* expression on tumor growth and invasiveness.

Previous work by Zhang, et al. established CT26-FL3 as a highly metastatic cell line derived from CT26. CT26-FL3 expresses *Lcn2* nearly three times higher than CT26, but CT26-FL3 gave rise to liver metastasis in 90% of host mice as compared to CT26, which only gave rise to metastasis in 10% (Figure 2.1). In addition, the microarray data showed that *Lcn2* levels were 300-fold higher in liver tissue of mice bearing tumors from CT26-FL3 as compared to

sham controls, however, CT26-FL3 only had three fold higher *Lcn2 mRNA* expression as compared to CT26 (Figure 2.1). In this chapter we will investigate if overexpression and knockdown of *Lcn2* in CT26, CT26-FL3, or MC38-luc cells will lead to corresponding increases and decreases in the invasiveness of these tumor cells.

3.2 RESULTS

3.2.1 EFFECT OF OVEREXPRESSION OF LCN2 IN CT26 AND CT26-FL3 CELLS ON GROWTH AND INVASIVENESS

To understand the autocrine effects of *Lcn2* on primary tumor cells we measured cellular growth and invasiveness of stably transfected tumor cells. Figure 3.1 shows *mRNA* and secreted protein overexpression of *Lcn2* in CT26 and CT26-FL3. Figure 3.2 shows that overexpression of *Lcn2* did not significantly impact the growth of either CT26 or CT26-FL3. This data shown also confirms previous observations by Zhang, et al. which showed that CT26-FL3 grows slower *in-vitro* as compared to CT26 cells. To measure the effects of tumor cell secreted *Lcn2* on tumor cell invasiveness, we used an *in-vitro* trans-well invasion assay. The results showed that while CT26-FL3 was more invasive than CT26 cells as previously shown by Zhang, et al, overexpression of *Lcn2* did not significantly alter their invasiveness as compared to the vector transfected cells (Figure 3.2). Thus, *Lcn2* did not affect either the growth rate or the ability of cells to pass through a basement membrane in the transwell assay.

3.2.2 EFFECT OF LCN2 OVEREXPRESSION ON METASTASIS OF CT26 AND CT26-FL3 *IN-VIVO*.

Although we observe that CT26-FL3 is more invasive than CT26 *in-vitro*, it is only by two to three-fold, which does not account for the 9-10 fold higher metastatic capability of CT26-FL3 *in-vivo*. To test the effect of *Lcn2* overexpression in CT26 and CT26-FL3, 2×10^5 cells were injected in the spleen of BALB/C mice and samples were harvested three weeks after the injection. While cecal implantation allows assessment of spontaneous liver metastasis of colorectal cancer, splenic injection can provide a measure for the growth of both poorly and highly metastatic cells upon arrival in the liver, allowing for a comparison of metastatic colonization by CT26 and CT26-FL3. Furthermore, stable transfection of CT26-FL3 and subsequent selection with G418, may cause some loss of its metastatic potency, requiring a number of rounds of selection through the liver to regain the highly metastatic nature of the cells.

In Figure 3.3, mice bearing splenic tumors of CT26 and CT26-FL3 that were overexpressing *Lcn2* showed no significant differences in primary tumor growth or metastatic tumor growth. In another experiment using splenic injection, shown in Figure 3.4, CT26-FL3 overexpressing *Lcn2* and CT26-FL3 vector control were injected in to the spleens of BALB/C and BALB/C *Lcn2*^{-/-} mice. The *Lcn2* overexpressing cell lines have smaller primary tumor sizes (Figure 3.4.A), but the total tumor burden was the same, indicating that *Lcn2* overexpression allowed cells to leave the primary tumor and spread more than the vector control groups. Systemic knockout of *Lcn2*, also seen in in Figure 3.4, increased liver

metastasis in both the vector control and Lcn2 overexpression groups.

Interestingly, when spleen and liver masses are added together, there were no differences, indicating that, in this model total tumor growth was not affected by overexpression of Lcn2 in tumor cells or by systemic Lcn2 knockout. However, primary and secondary tumor growths are different, indicating a role for Lcn2 in metastasis. More specifically, tumor Lcn2 does slightly impact metastasis, but only when systemic Lcn2 is absent.

3.2.3 EFFECT OF TUMOR CELL OVEREXPRESSION OF LCN2 ON TUMOR GROWTH AND INVASIVENESS OF MC38 CELLS

To verify the results seen with the CT26 and CT26-FL3 cells with Lcn2 overexpression, we utilized the MC38 mouse adenocarcinoma cell line, which is syngeneic for the C57BL/6 mice. MC38 is less aggressive than CT26 *in-vivo*, but metastasis from cecum implantation can be increased to nearly 50% by passaging through the liver twice as seen with MC38-FL2 (data not shown).

Figure 3.5 shows that *Lcn2* mRNA levels were 1000-fold higher in the MC38-luc *Lcn2* overexpressing cell line as compared to MC38-luc cells transfected with the empty vector. Cellular growth *in-vitro* was slower in the presence of Lcn2. Interestingly, Lcn2 overexpressing MC38-luc cells actually display a phenotype that is less fibroblastic than typical MC38 cells as seen in Figure 3.5.D. In Figure 3.6, a transwell invasion assay showed that MC38-luc-Lcn2 cells were two-fold more invasive than Mc38-Luc-Vector cells.

3.2.4 EFFECT OF LCN2 OVEREXPRESSION ON METASTASIS OF MC38 IN-VIVO.

To test the effect of *Lcn2* overexpression in MC38-luc cells on metastasis *in-vivo*, the cells were injected into the spleens of C57BL/6 mice and allowed to grow for three weeks. Surprisingly, as shown in Figure 3.7, *Lcn2* overexpression prevented tumor growth in the spleen *in-vivo*.

To begin to understand the contrasting effects of *Lcn2*, we measured secreted levels in both cell lines. The results from ELISA Figure 3.8 showed that CT26 and MC38-luc cells secreted undetectable levels of *Lcn2* protein. On the other hand, the CT26-*Lcn2* cell line secreted 15 pg/mL of *Lcn2*, while the MC38-luc-*Lcn2* secreted 7980 pg/mL of *Lcn2*, approximately 535-fold higher than CT26-*Lcn2*. These extremely high levels of *Lcn2* are consider hyper-physiological since normal mice can typically have 1000 pg/mL of *Lcn2* in serum while tumor bearing mice have approximately 2000-4000 pg/mL of serum *Lcn2*. *Lcn2* is a known neutrophil chemoattractant, and it is possible that such high levels of *Lcn2* being secreted from the primary tumor cells might cause recruitment of anti-tumor immune cells into the spleen to eliminate the tumor cells (Asimakopoulou et al., 2016a). Collectively, the results showed that in MC38-luc cells, overexpression of *Lcn2* slowed cell growth *in-vitro* and prevented tumor growth *in-vivo*. Additionally, MC38-luc-*Lcn2* exhibited altered morphology towards a less-fibroblastic phenotype as compared to MC38-luc-pGL4.13 and MC38-luc-*Lcn2* suggesting a mesenchymal to epithelial transition.

An additional data that warrants future studies is the role of iron and Lcn2 in invasion and metastasis. In Figure 3.8.B, MC38-luc-Lcn2 showed no differences in wound healing as compared to controls. However, when ferric iron was supplement or iron was chelated with deferoxamine (DFO), MC38-luc-Lcn2 took a significantly longer time to heal the scratch. Since Lcn2 can shuttle iron into and out of the cell, it is possible that MC38-luc-Lcn2 exports iron with Lcn2 faster than it can uptake iron, so that the lack of intracellular iron could slow wound healing or migratory activity of cells expressing Lcn2.

3.3 SUMMARY AND DISCUSSION

In previous work by Zhang, et al., we observed that orthotopic implantation of CT26-FL3 produced liver metastasis at a frequency of 90% and under the same conditions, CT26 produced liver metastasis with 10% frequency (Zhang et al., 2013). This 9-10 fold increase in invasion *in-vivo* compared to the 2-3 fold increase in invasiveness *in-vitro* indicated that crosstalk with the primary and secondary tumor microenvironments *in-vivo* contribute to the high metastasis of CT26-FL3. This is not surprising since it is well know that the tumor microenvironment is critical to the growth and development of the primary tumor and metastatic tumor growth (Hanahan and Weinberg, 2011).

The hyper-elevated Lcn2 protein levels observed in MC38-luc-pGL4.13-Lcn2, at around 7000-fold, were hyper-physiological levels that only increased cell invasion by two-fold ($p < 0.05$) *in vitro*. However, when injected into C57/B6 mice, MC38-luc-Lcn2 was unable to produce a tumor after 21 days. MC38-luc-

Lcn2 was also unable to grow in the flank as compared to MC38-luc and only produced a measurable tumor after three months post-injection (data not shown). As a known neutrophil chemoattractant, it is probable that such high levels of Lcn2 from the MC38 primary tumor induced an immune response which eliminated the tumor from the mouse (Asimakopoulou et al., 2016a).

It is possible that the effects of Lcn2 secreted from the primary tumor on metastasis are concentration dependent. The data showed that expression of 50-fold higher Lcn2 in CT26-Lcn2 and did not increase invasion or metastasis, while expression of 1000-fold higher Lcn2 in MC38-luc-Lcn2 only led to a two-fold increase in invasion.

Collectively, these data suggest that Lcn2 does not play a significant role in tumor growth and progression when over-expressed in tumor cells, the seed component of the seed and soil hypothesis. This leads to the question on the role of Lcn2 when expressed in the host parenchymal and stromal compartments.

The current literature suggests that LCN2 expression in human colorectal cancer is positively correlated with poor outcomes, but this association is disputed by a number of studies. Candido, et al. found that colon tumors express *LCN2 mRNA* approximately 66.3% higher than normal colon tissue, and 45% of colon tumors express some LCN2 protein, as detected by immunohistochemistry (IHC) (Candido et al., 2014). Nielsen, et al. showed a positive correlation with tumor transformation (Nielsen et al., 1996) and Marti, et al, suggested that LCN2 can be utilized in the prognosis of metastatic patients (Marti et al., 2013). Catalan, et al described LCN2 as a diagnostic marker, however, Fung and

McLean disagreed that LCN2 can be used as a clinically viable testing option (Catalán et al., 2011; Fung et al., 2013; McLean et al., 2013). Thus, while it seems that LCN2 has the potential for clinical utility, its multifaceted role is unclear and warrants further investigation.

In the subsequent chapters, our goal is to determine if Lcn2 expressed in the host and stromal cells in the microenvironment plays a role in metastasis as using both *in-vitro* and *in-vivo* strategies. An interesting question to dissect would be its role in promoting tumor cell invasion or sustaining tumor growth upon arriving in the secondary environment such as the liver. More recent studies using human colorectal cancer cell lines suggest that intratumoral LCN2 may inhibit metastasis by polarizing tumor cells into an epithelial phenotype (Feng et al., 2016) which seem to be consistent with the MC38-luc-Lcn2 phenotype shown in Figure 3.5.D. Future studies would need to investigate the role that 24p3R, the Lcn2 receptor plays in the primary tumor cells.

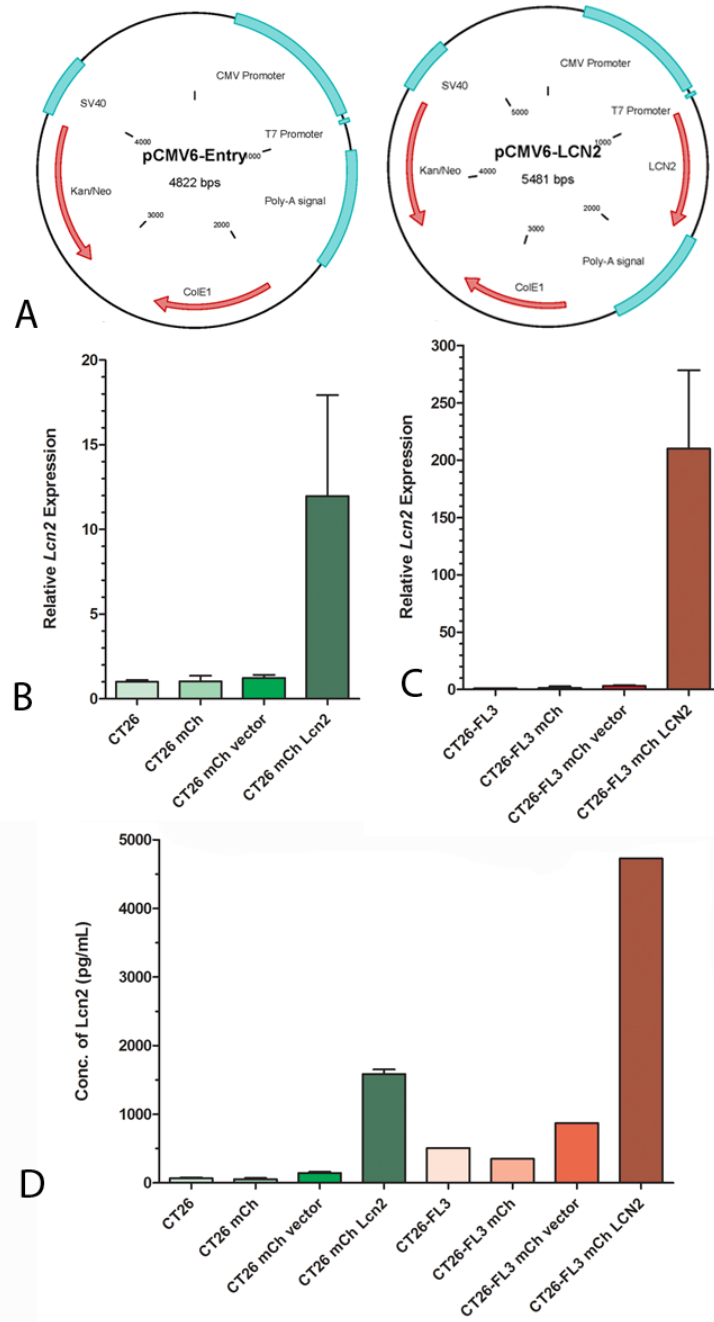


Figure 3.1: Lcn2 overexpression in CT26 and CT26-FL3. A) Plasmids pCMV6-Entry and pCMV6-Lcn2. B) CT26 overexpression of Lcn2. C) CT26-FL3 overexpression of Lcn2. D) ELISA showing secreted Lcn2 protein levels confirming Lcn2 overexpression (Elamparo, 2013).

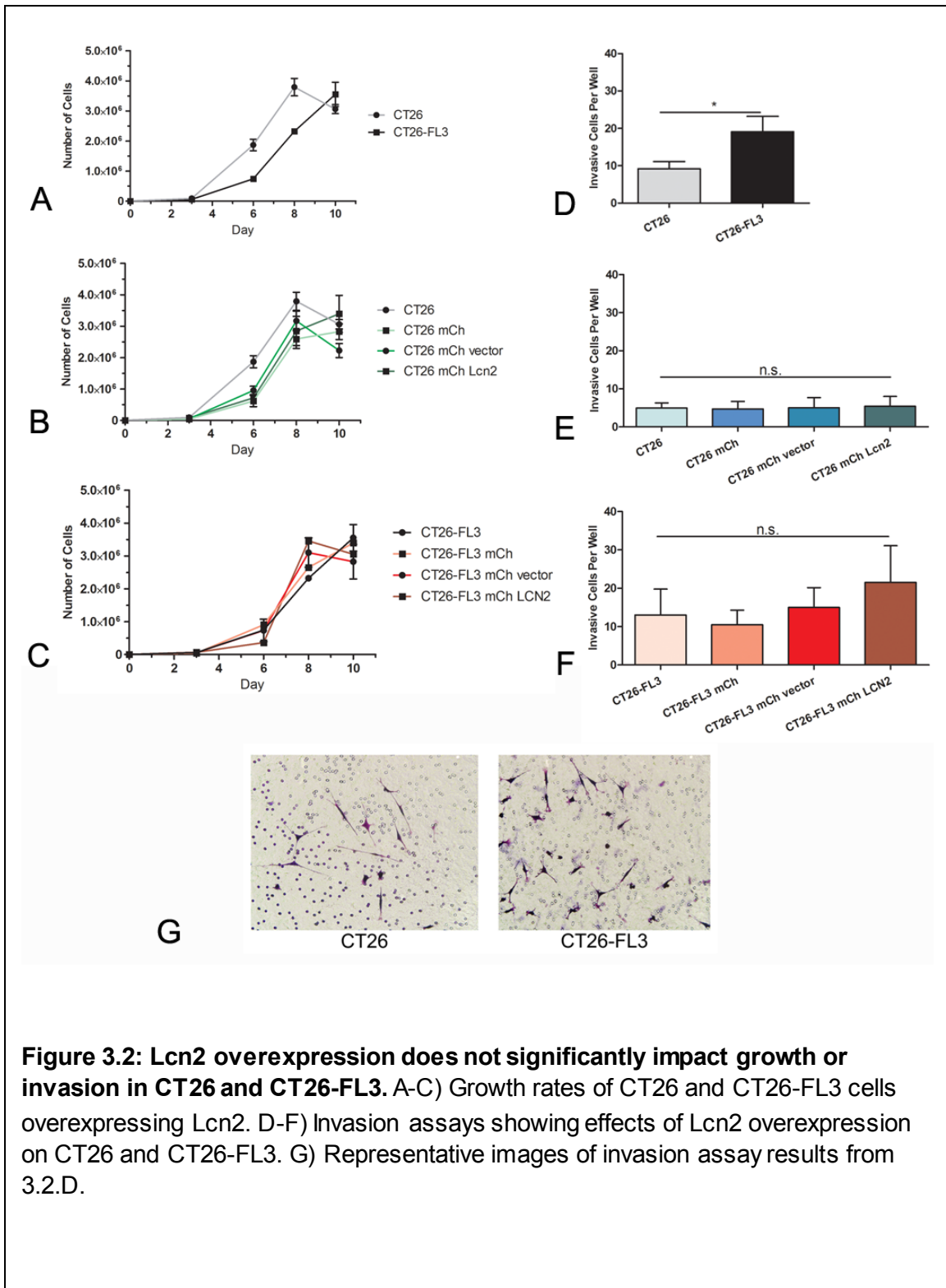
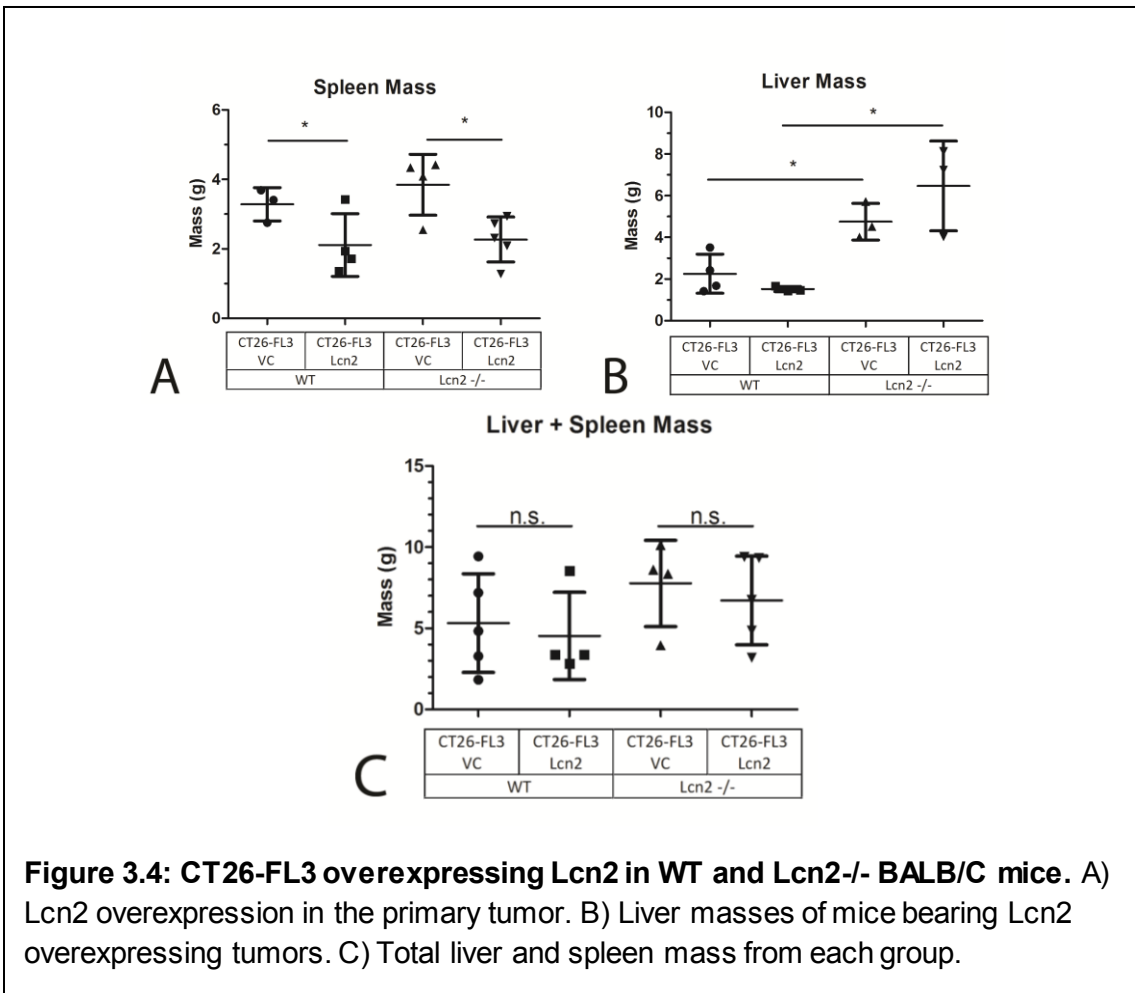
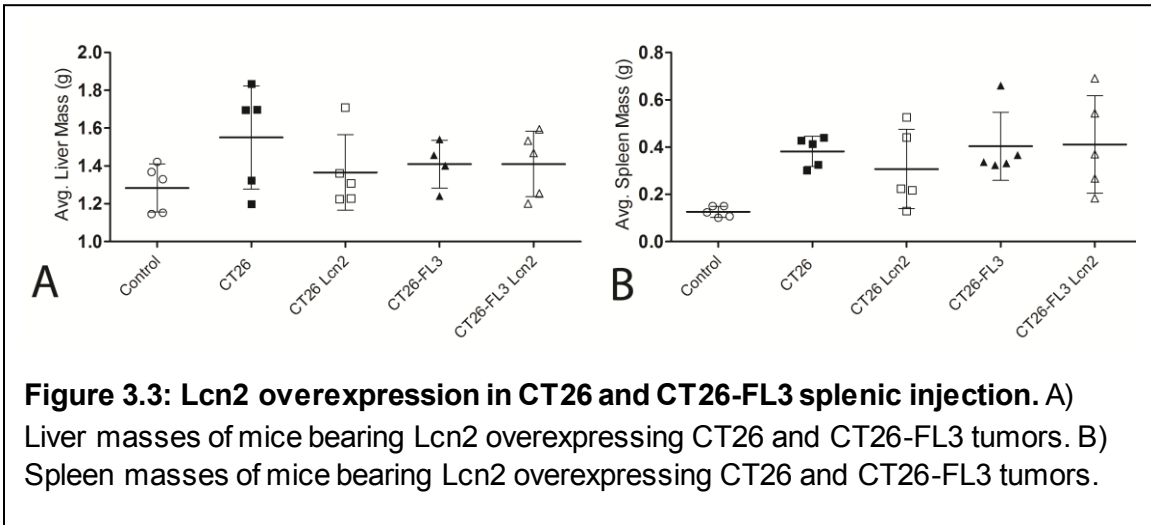


Figure 3.2: Lcn2 overexpression does not significantly impact growth or invasion in CT26 and CT26-FL3. A-C) Growth rates of CT26 and CT26-FL3 cells overexpressing Lcn2. D-F) Invasion assays showing effects of Lcn2 overexpression on CT26 and CT26-FL3. G) Representative images of invasion assay results from 3.2.D.



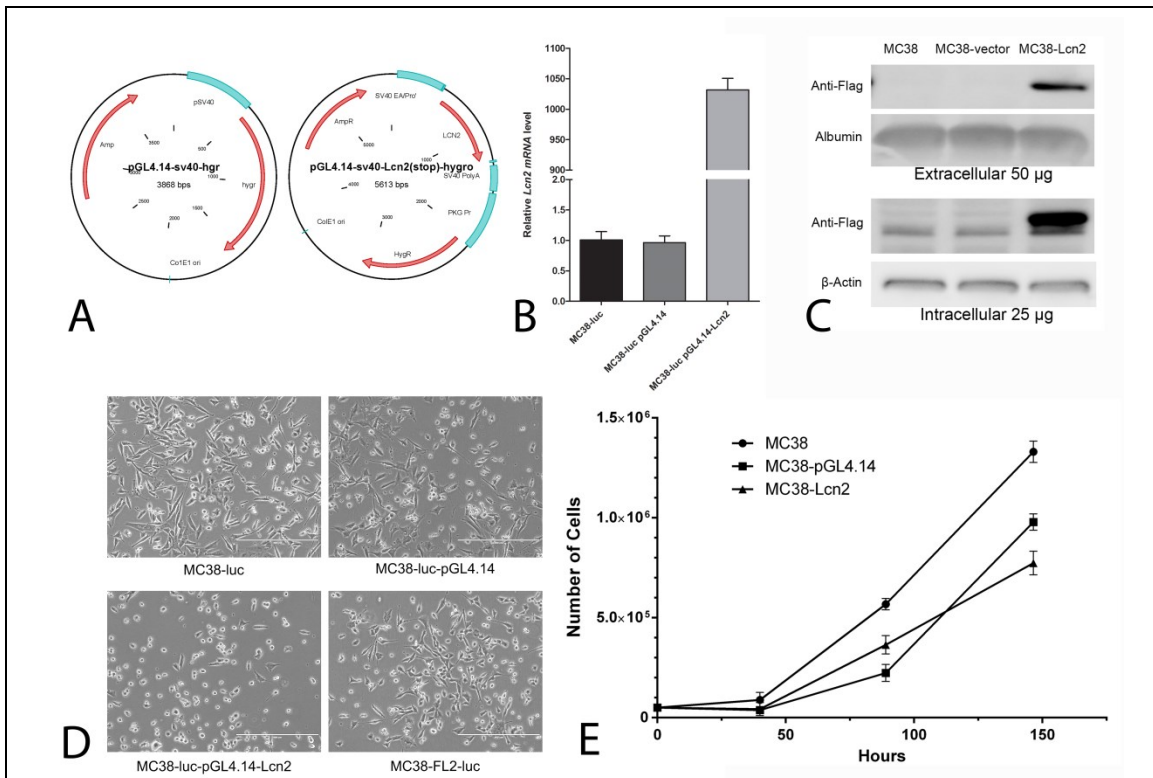


Figure 3.5: MC38-luc cells overexpressing Lcn2. A) Plasmid maps of pGL4.14 and pGL4.14-Lcn2. B) Lcn2 overexpression measured via qRTPCR. C) Western immunoblot showing intracellular and extracellular Lcn2 overexpression. D) Cellular phenotype of MC38-luc cell lines. E) Growth assay of MC38-luc clones.

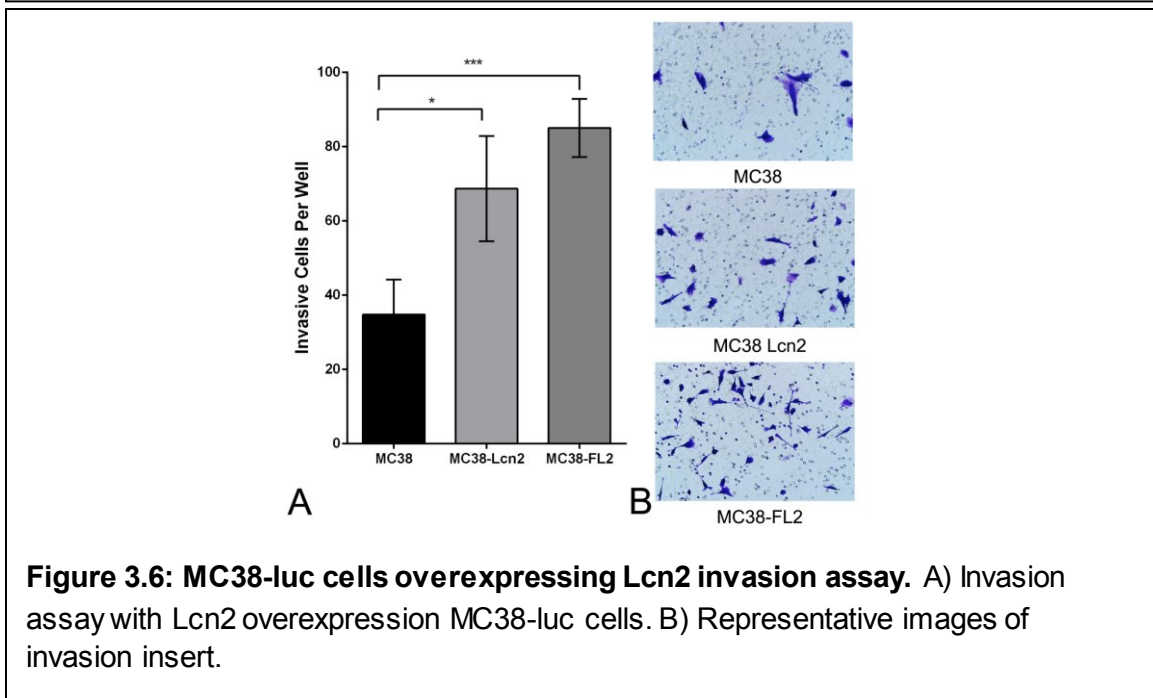
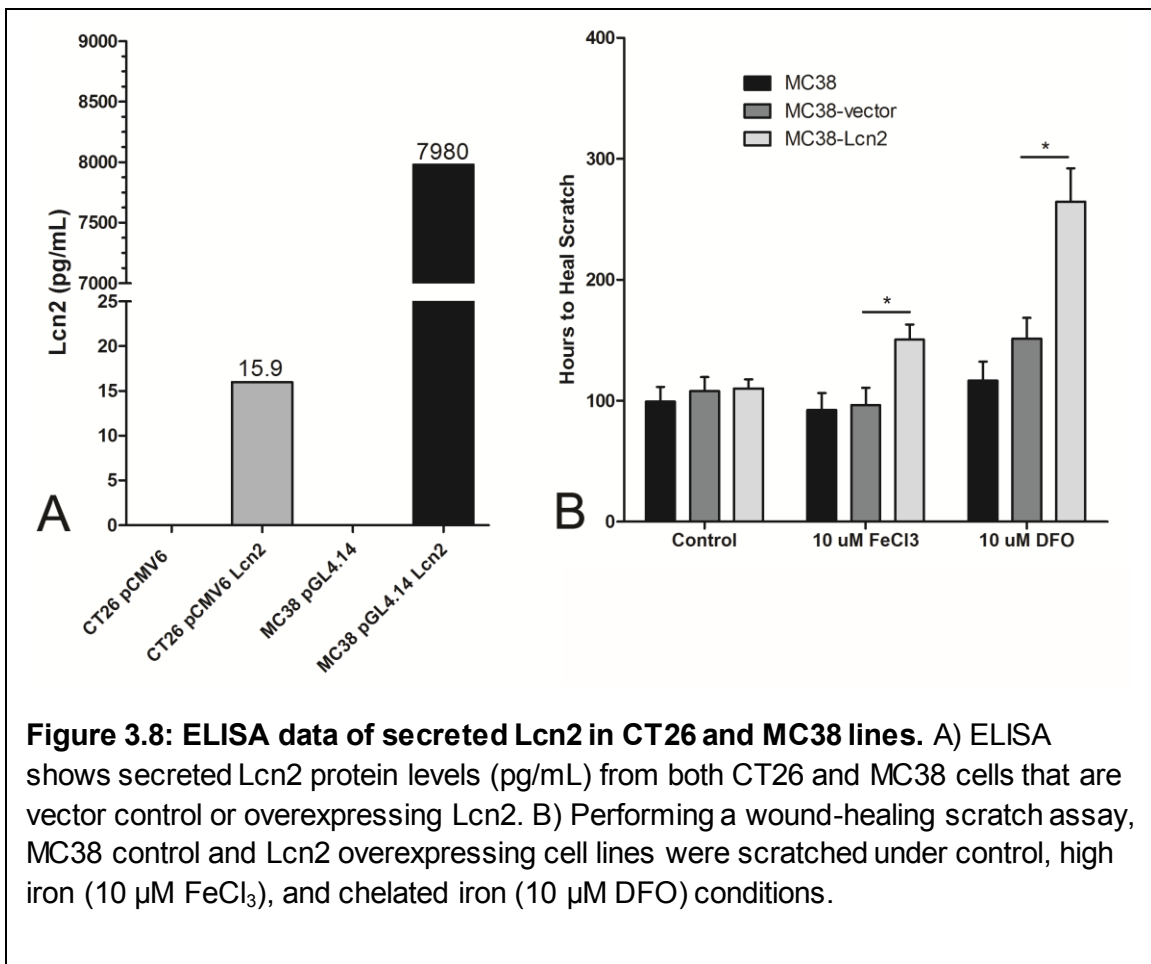
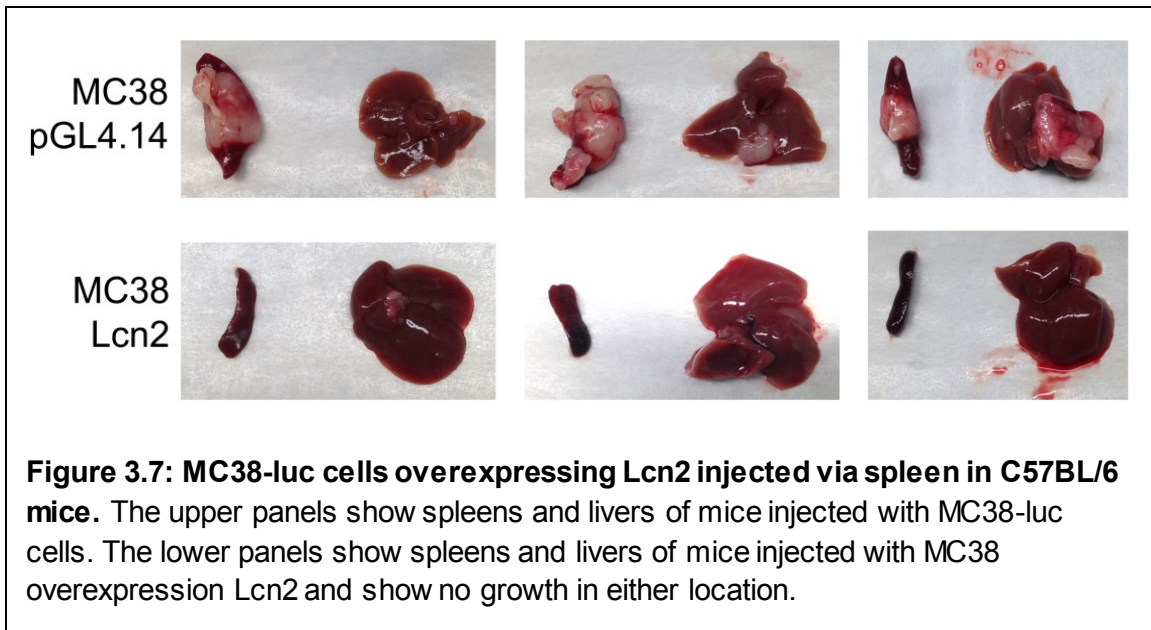


Figure 3.6: MC38-luc cells overexpressing Lcn2 invasion assay. A) Invasion assay with Lcn2 overexpression MC38-luc cells. B) Representative images of invasion insert.



CHAPTER 4

THE *IN-VITRO* ROLE OF TUMOR MICROENVIRONMENT-DERIVED LCN2 IN TUMOR CELL INVASION

4.1 INTRODUCTION

The current literature describing the role of Lcn2 in metastasis is discordant, most likely due to the variety of cancer models used by different labs. Thus, the burden of proof remains to further delineate the effects of Lcn2 on colorectal cancer metastasis through experimental methods. Since hepatocytes comprise the majority of the liver, it is likely that they contribute a significant portion of the Lcn2 found in pre-metastatic and metastatic livers of colorectal cancer bearing mice. In a bacterial infection and hepatectomy model, Xu, et al. showed that hepatocytes secrete ~25% of serum Lcn2 in normal conditions and ~90% of serum Lcn2 levels after infection or injury (Xu et al., 2015).

Macrophages located in the metastatic microenvironment are a likely cell type that may be influencing Lcn2's participation in metastasis. Macrophages are highly plastic immune cells whose gene expression can be modified in response to cues from the microenvironment allowing them to be polarized into a continuum of phenotypes. The two oversimplified phenotypes in the macrophage spectrum are the classically activated pro-inflammatory M1 and the alternatively activated anti-inflammatory M2 (Mosser and Edwards, 2008). The M2

designation contains nearly all alternatively activated macrophages and can be further broken down into the M2a wound healing macrophage and the M2b/c immune regulatory macrophage. The distinctions between different phenotypes are often blurred and macrophages can exist in a hybrid state, expressing genes found in multiple subtypes.

Many papers have shown a role for Lcn2 in the polarization of macrophages, which can further influence the tumor microenvironment in the metastatic setting (Guo et al., 2014; Jung et al., 2015). In a bacterial pneumonia study, LCN2 deactivated macrophages and was a marker of macrophage deactivation and impaired immune clearance of bacteria (Warszawska et al., 2013). Jung, et al. showed that IL-10 in the tumor microenvironment caused downstream production of Lcn2 by tumor associated macrophages that were polarized towards an M2 phenotype (Jung et al., 2012). In an obesity-associated inflammation model, Lcn2 was shown to be an anti-inflammatory regulator of macrophages, skewing towards an M2 phenotype via a feed-forward NF- κ B-STAT3 loop (Guo et al., 2014).

In contrast, using an ischemia-reperfusion model, Lcn2 promoted macrophages towards an M1 phenotype (Cheng et al., 2015). In addition, in a microglial model, Lcn2 polarized microglia, the resident macrophages of the central nervous system, into an M1 phenotype (Jang et al., 2013). Jablonski, et al. showed Lcn2 as one of the most highly upregulated genes (41.8 fold) in M1 vs. undifferentiated M0 undifferentiated macrophages (Jablonski et al., 2015). However, these classical inflammatory models were very different from tumor-

bearing models, which all showed *Lcn2* expression correlating with the M2 phenotype.

Another hematopoietic cell population that is found in the metastatic microenvironment is the neutrophil, which has also been shown to promote liver metastasis (Gordon-Weeks et al., 2017). In healthy humans, neutrophils make up 50-70% of all white blood cells and have been shown to play a role in both anti-tumor and pro-tumor immunity (Galdiero et al., 2013). Similar to macrophages, neutrophils can be polarized into a classical N1, anti-tumor phenotype and a pro-tumor, N2 phenotype. Neutrophils found in tumors are designated as tumor associated neutrophils (TANs), which can be either pro-tumorigenic or anti-tumorigenic (Sionov et al., 2015).

Neutrophils were the first cell type that was found to express high levels of Lipocalin-2, hence the name Neutrophil Gelatinase Associated Lipocalin (NGAL). Gelatinase (MMP9) was found in humans to bind NGAL to prevent the degradation of MMP9 (Koh and Lee, 2015). Schroll, et al. showed that recombinant *Lcn2* can induce neutrophil migration which is reduced in *Lcn2* knockout mice (Schroll et al., 2012).

Our preliminary microarray data showed that *Lcn2* is highly upregulated in the non-tumor area of a murine liver bearing CRC metastasis. The goal of this chapter is to further understand the role that *Lcn2* expressed in the parenchymal hepatocytes and in hematopoietic immune cells plays in promoting or establishing liver metastasis of colorectal cancer using *in-vitro* assays. The immune cell components that are the primary focus in this chapter are the

myeloid lineage-derived neutrophils and macrophages. By utilizing a transwell chamber, we can perform invasion assays by co-culturing the tumor cells with immune cells. This *in-vitro* system allows us to simulate metastasis with the upper chamber representing the primary tumor, or “seed”, and the lower chamber representing the metastatic site, “or soil.” Altering the levels of Lcn2 in the lower chamber “soil” cells allows us to develop a framework for the role of Lcn2 from microenvironmental cell types on colorectal cell invasiveness.

4.2 RESULTS

4.2.1 EFFECT OF HEPATIC LCN2 ON CRC INVASIVENESS

In this study, we utilized the murine hepatocyte cell line TIB-73 (BNL CL.2 (ATCC® TIB-73™)) to test the role of hepatic *Lcn2* expression on CRC cell invasion. It is a reliable cell line that can be altered via transfection or transduction. *Lcn2* overexpression was established in TIB-73 using the previously described pCMV6-Entry-Lcn2 plasmid. As shown in Figure 4.1.A, *Lcn2* mRNA was over-expressed, in Figure 4.1.B, intracellular protein levels decreased for TIB-73 with Lcn2 overexpression, but, most importantly, secreted Lcn2 protein levels increased, as shown by ELISA in Figure 4.1.C. Consistent with previous experiments, intracellular Lcn2 protein levels did not always correspond to mRNA overexpression since Lcn2 is mostly secreted from the cells. In Figure 4.2, we show that the presence of hepatocytes in the lower well of a matrigel invasion assay increased the invasiveness of both CT26 and CT26-FL3. To determine if increased Lcn2 levels in the “soil”, or the TIB-73 liver cells,

in the bottom well would have an effect on tumor cell invasion, TIB-73 cells over-expressing Lcn2 were placed in the bottom well during an invasion assay. The results in Figure 4.2.C showed that increased Lcn2 from the soil (TIB-73 hepatocytes) increased tumor cell invasion.

To determine if increased hepatocyte Lcn2 specifically caused the increased invasiveness of CT26, Lcn2-specific siRNA was transfected into the TIB-73 cells as described in the materials and methods chapter. The results in Figure 4.3 show that siRNA against *Lcn2* diminished mRNA levels as determined by qRT-PCR and extracellular Lcn2 protein levels as determined by ELISA. Lcn2 knockdown via siRNA reduced the invasiveness of CT26, but not to a statistically significant level. However, a Pearson correlation analysis showed that Lcn2 levels from the TIB-73 cells correlated with invasiveness of CT26 cells to some extent ($r=0.58$, $r^2=0.34$).

4.2.2 EFFECT OF LCN2 EXPRESSED BY NEUTROPHILS ON CRC CELL INVASIVENESS.

Another cell type within the metastatic tumor microenvironment that might impact CRC invasion and metastasis through Lcn2 expression is the neutrophil. The cell line MPRO (ATCC® CRL-11422™) can be induced to differentiate into mature neutrophil (NEUT) after four days of exposure to 10 μ M all-trans-retinoic acid (ATRA). These differentiated neutrophils (NEUT) express azurophilic primary granules, the mouse neutrophil antigen 7/4, and possess chloroacetate esterase activity seen in primary neutrophils (Gupta et al., 2014; Tsai and Collins, 1993).

NEUT cells were 72% positive for the cell surface markers Cd11b and Ly6G by flow cytometry analysis as compared to MPRO cells which were only 12% positive for both markers. In Figure 4.3.C, qRT-PCR levels indicated that *Lcn2* expression increased by approximately 150-fold and the *Lcn2* receptor *24p3R* expression increased by approximately 15-fold in NEUT cells as compared to the undifferentiated MPRO cells. Co-culture of NEUT cells with CT26 cells in invasion assays showed that the invasiveness of CT26 cells increases nearly two fold in the presence of NEUT cells as compared to CT26 by itself or with MPRO cells. Experiments to determine if downregulation of *Lcn2* by siRNA transfection or lentiviral shRNA expression were largely unsuccessful due to the difficulty in diminishing the very highly elevated *Lcn2* mRNA levels in NEUT cells.

4.2.3 EFFECT OF LCN2 IN MACROPHAGES ON CRC CELL INVASIVENESS

Macrophages are one of the most prevalent immune cell types in the metastatic microenvironment and our goal was to determine the influence of *Lcn2* in macrophages on colorectal cancer cell invasion (Qian and Pollard, 2010). Using the Raw 264.7 macrophage-like cell line, we tested some of the effects of macrophages on cell invasiveness *in-vitro*. Similar to primary macrophages, Raw264.7 cells can be polarized into an 'anti-tumor' M1 phenotype with LPS or a 'pro-tumor' M2 phenotype with IL-4 (Davis et al., 2013). Utilizing the transwell invasion assay with CT26 or CT26-FL3 in the upper chamber and Raw264.7 co-cultured in the bottom well, tumor cell invasion increased dramatically in the presence of macrophages, as shown in Figure 4.5. Subsequent attempts to

knockdown Lcn2 via siRNA or shRNA were unsuccessful as Raw264.7 is one of the most difficult cell types to reliably transfect. To circumvent this difficulty, we utilized primary bone marrow derived macrophages (BMDMs) from BALB/C mice or C57BL/6 mice as previously described (Jung et al., 2016; Singh et al.). Bone marrow was extracted from WT C57BL/6 and C57BL/6 Lcn2^{-/-} mice and incubated in 15% L-929 conditioned media for 7 days, after which the F4/80+/Cd11b+ population, corresponding to macrophages, was determined to be 97.2% by flow cytometry. In Figure 4.5.C, MC38-luc cells were placed in the top chamber, while the bottom chamber contained either wild type C57BL/6 BMDM or C57BL/6 Lcn2^{-/-} BMDM. Both wild type and Lcn2^{-/-} BMDM were treated with either LPS or IL-4 to polarize them into an M1 or M2 phenotype, respectively. Consistent with the previous results obtained with the Raw264.7 cells in co-culture invasion assays, the presence of BMDMs increased the invasiveness of MC38-luc cells dramatically (Figure 4.5.C). The loss of Lcn2 from BMDMs had no impact on the invasion rates for unstimulated or LPS-treated BMDMs, however, BMDM cell from Lcn2^{-/-} mice, treated with IL-4 showed the highest levels of MC38-luc invasion. This data suggested that in the M2 phenotype, a factor other than Lcn2 may be contributing to the high levels of tumor cell invasion.

Figure 4.5.D shows results from ELISA analysis for Lcn2 levels in media taken from the wells of the invasion assays performed in Figure 4.4.C. Lcn2 levels were highest in B6 BMDM's treated with LPS (>4,500 µg/mL). The other wells showed Lcn2 levels of approximately 200 pg/mL, including IL-4 treated

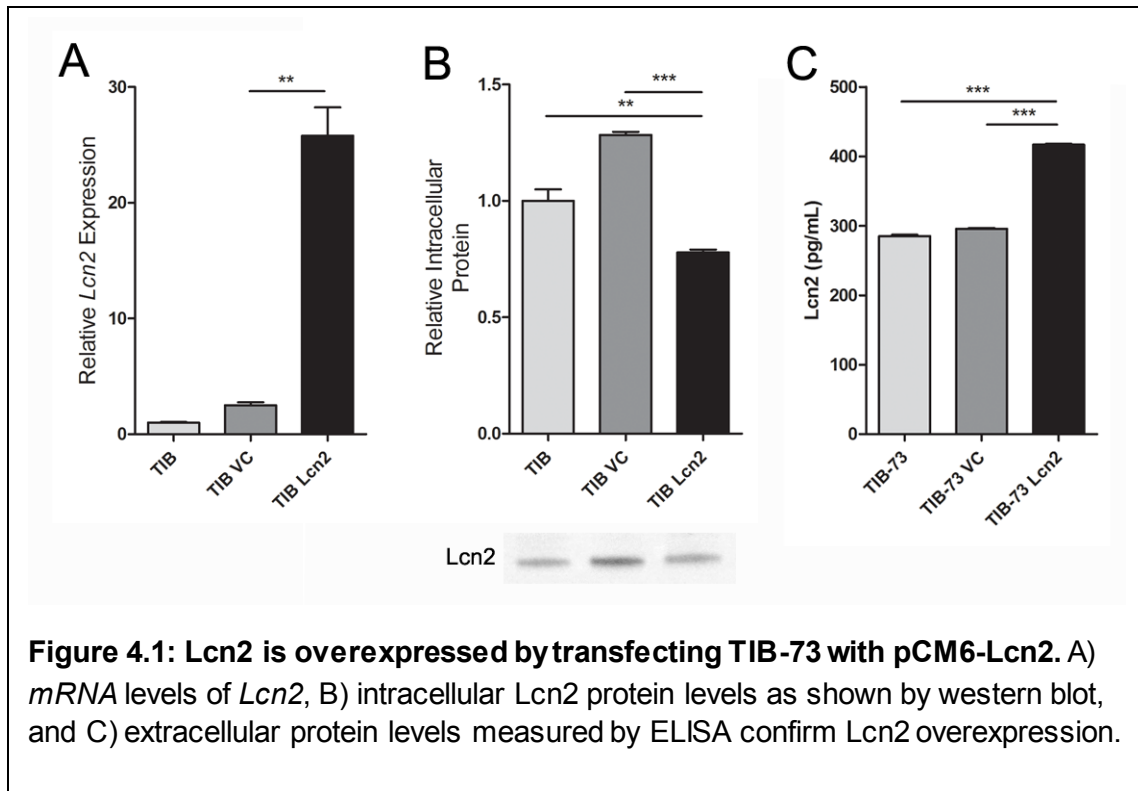
Lcn2^{-/-} BMDMs, which gave the highest levels of MC38-luc invasion.

Interestingly media from C57BL/6 Lcn2^{-/-} BMDM's treated with LPS and incubated with MC38-Luc cells contained 1000 pg/mL Lcn2, which suggested that in response to LPS stimulation of BMDMs into an M1 state, the MC38-luc cells secreted higher levels of Lcn2, however, this has no effect on MC38-luc invasiveness. The Pearson correlation shown in figure 4.5.E revealed that there was no association in between Lcn2 levels in the media and MC38-luc tumor cell invasiveness ($r=0.086$, $r^2= 0.007$).

4.3 SUMMARY AND DISCUSSION

The results shown in these experiments confirmed the data from the microarray analysis, which suggested that high levels of Lcn2 from cells in the metastatic microenvironment may be partially responsible for the growth of liver metastasis of colorectal cancer. Elevated levels of Lcn2 secreted by TIB-73 hepatocytes increased the invasion of CT26 colorectal tumor cells. The differentiated NEUT neutrophils, which expressed very high levels of Lcn2 also increased the invasiveness of CT26. On the other hand, while the Raw264.7 macrophages and the BMDMs isolated from wild type or Lcn2^{-/-} mice caused large increases in tumor cell invasion, loss of Lcn2 in these cells or elevated levels in the media did not affect tumor cell invasiveness. Collectively, the data shown here indicated that Lcn2 from specific cells in the tumor microenvironment and host influenced the invasiveness of CT26, CT26-FL3, and MC38-luc colorectal tumor cells while Lcn2 from other cells have no effect and may exert

their effects on tumor growth and invasiveness through other factors. For example, Raw264.7 cells express less Lcn2 than TIB-73 cells in both their native states; however, Raw264.7 induced more tumor cell invasion than TIB-73 in the co-culture invasion assay. This is reasonable as there are a host of cytokines and chemokines that are involved in the crosstalk between tumor cells and stromal cells, thus, it is unlikely that any one protein (Lcn2) can be primarily responsible for singlehandedly driving cellular invasion or tumor phenotype. The focus of this chapter was to investigate the Lcn2 specific effects on tumor cell invasion, but it remains possible that *in-vivo*, Lcn2 may have an effect on the metastatic cascade in liver metastasis that is not the invasiveness of the colorectal tumor cells. The subsequent chapter aims to investigate Lcn2 *in-vivo* in the hepatic tumor microenvironment.



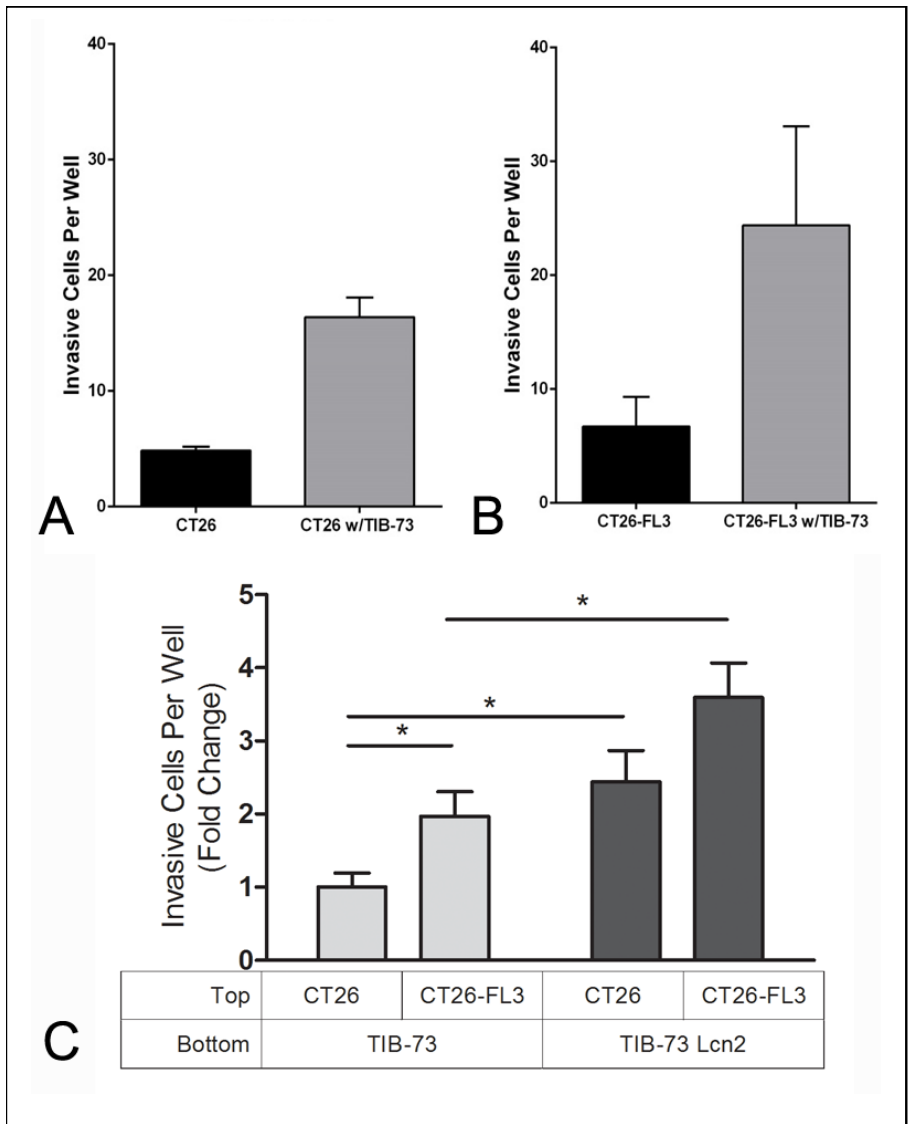


Figure 4.2: Lcn2 overexpression from TIB-73 cells in the “seed” compartment in a co-culture invasion assay increases invasiveness of CT26 and CT26-FL3.
 A) CT26 and B) CT26-FL3 are co-cultured with TIB-73 for an invasion assay. C) Lcn2 overexpression in TIB-73 increases invasion of both CT26 and CT26-FL3.

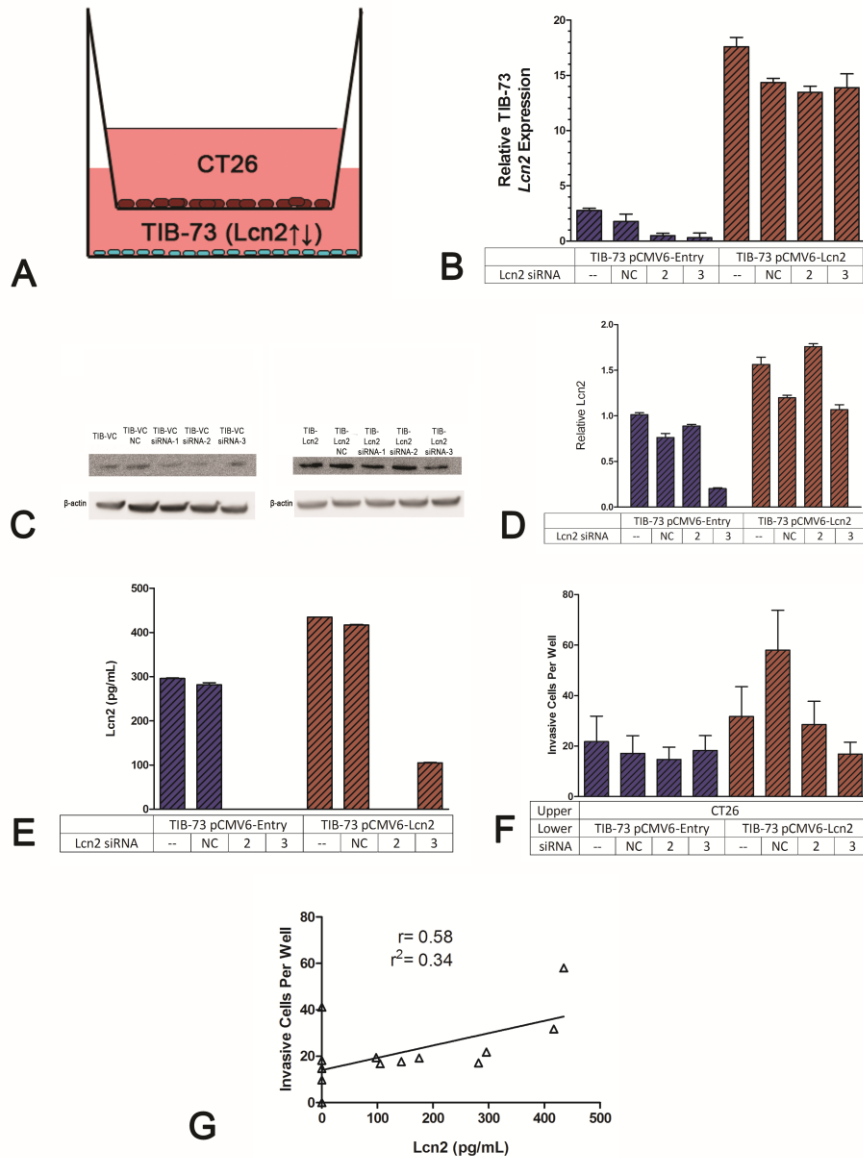
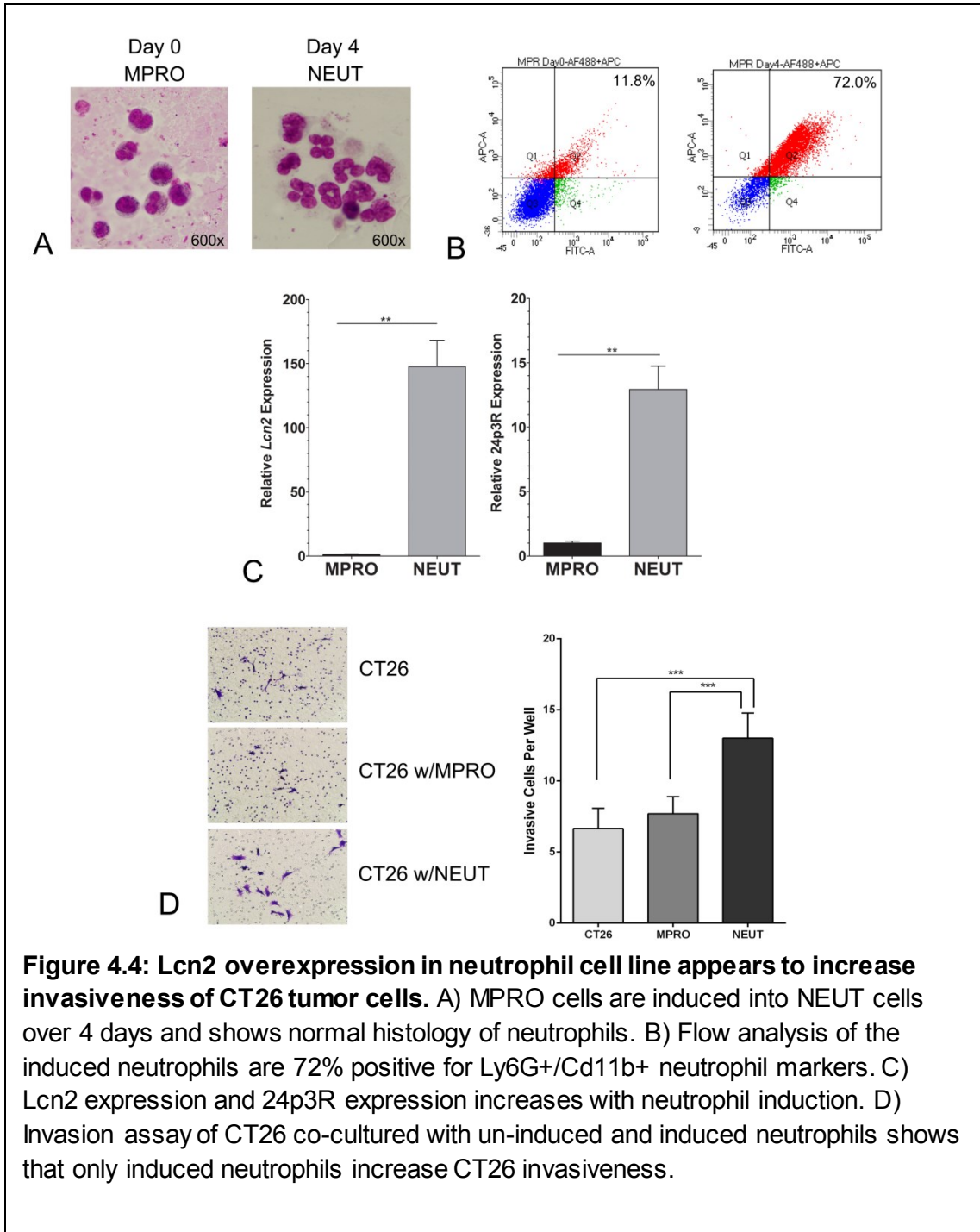


Figure 4.3: Lcn2 expression from TIB-73 hepatocytes directly affects invasiveness of CT26 tumor cells. A) Invasion assay schematic shows the layout of a co-culture invasion assay with CT26 tumor cells in the upper chamber. To confirm siRNA knockdown of Lcn2 we observe: B) mRNA levels via qRT-PCR, C) western blots showing intracellular Lcn2 protein levels, D) quantification of the intracellular western blots, and E) extracellular protein via ELISA. F) CT26 invasiveness in co-cultured invasion assay is shown for all TIB-73 pVM6-Entry and TIB-73 pCMV6-Lcn2 clones untransfected or given NC siRNA (non-targeting control), Lcn2 siRNA 2, or Lcn2 siRNA 3. G) The correlation between Lcn2 extracellular protein in TIB-73 co-culture wells and CT26 invasiveness is shown.



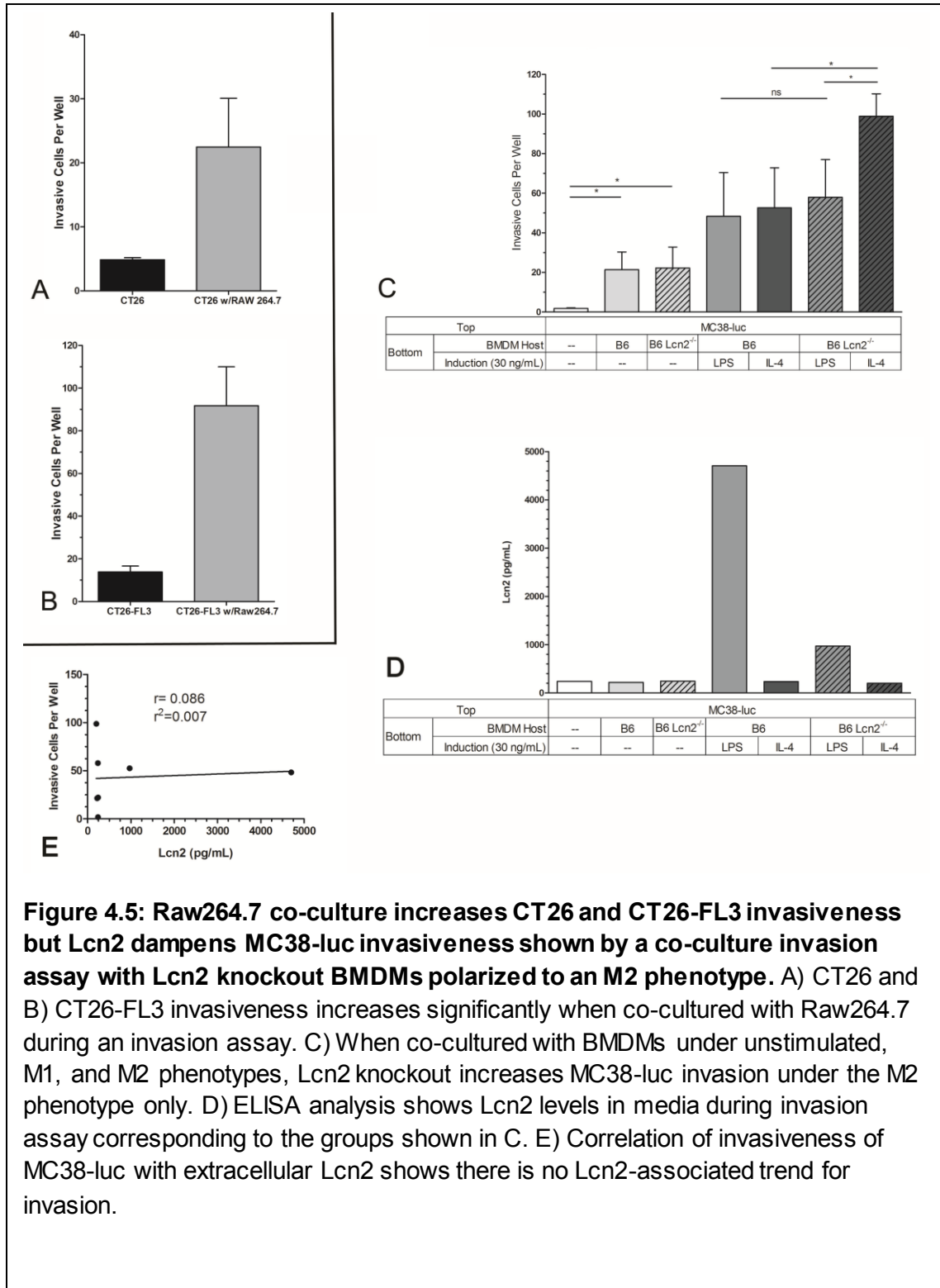


Figure 4.5: Raw264.7 co-culture increases CT26 and CT26-FL3 invasiveness but Lcn2 dampens MC38-luc invasiveness shown by a co-culture invasion assay with Lcn2 knockout BMDMs polarized to an M2 phenotype. A) CT26 and B) CT26-FL3 invasiveness increases significantly when co-cultured with Raw264.7 during an invasion assay. C) When co-cultured with BMDMs under unstimulated, M1, and M2 phenotypes, Lcn2 knockout increases MC38-luc invasion under the M2 phenotype only. D) ELISA analysis shows Lcn2 levels in media during invasion assay corresponding to the groups shown in C. E) Correlation of invasiveness of MC38-luc with extracellular Lcn2 shows there is no Lcn2-associated trend for invasion.

CHAPTER 5

THE ROLE OF LIPOCALIN-2 IN SHAPING THE METASTATIC STROMA OF COLORECTAL CANCER *IN-VIVO*

5.1 INTRODUCTION

To better understand the role of Lipocalin-2 in the hepatic tumor microenvironment in advanced colorectal cancer metastasis, we utilized an immune-competent mouse model to experimentally recapitulating a comprehensive tumor microenvironment, which closely represents clinical tumor physiology. As previously described, we observed increased levels of systemic Lcn2 and elevated hepatic *Lcn2* mRNA levels in our orthotopic cecal implantation mouse model of colorectal cancer progression and metastasis,. In studies described in this chapter, we utilized *in-vivo* electroporation of endotoxin-free plasmid DNA to increase systemic levels of Lcn2 in tumor-bearing and non-tumor-bearing mice. The goal was to determine the effect of increased serum levels of Lcn2 on the localization of immune cell populations in the metastatic liver microenvironment.

5.2 RESULTS

5.2.1 PV1J-LCN2 UTILIZATION IN MULTIPLE MOUSE MODELS

Previous work in the laboratory by John Bonaparte showed that mice electroporated with 50 ug of pV1J-Lcn2 had ~30% higher serum Lcn2 levels than mice electroporated with pV1J vector only (Bonaparte, 2015, unpublished data). The higher Lcn2 levels were sustained for 2-3 weeks until gradually dropping back to pre-electroporation levels. When the electroporation was performed in mice that have been implanted with MC38-luc cells in the spleen, elevated Lcn2 had no effect on the primary tumor volumes in the spleen. However, elevated Lcn2 levels resulted in a two-fold increase in liver mass due to increase metastasis, as compared to mice electroporated with the empty vector (Bonaparte, 2015). These data suggested that elevated systemic levels of Lcn2 either (1) accelerated the establishment of metastasis or (2) supported the growth of colorectal cancer tumor cells in the liver after they have disseminated from the primary tumor. The goal of the experiments in this chapter is to begin to elucidate the changes in the stromal immune cell populations in the metastatic liver microenvironment in the presence of high systemic levels of Lcn2 in tumor-bearing mice.

To determine if increased CRC metastatic burden from systemic Lcn2 increase is specific to liver metastasis or causes non-specific increases in metastasis in other cancers, we electroporated pV1J-Lcn2 into a breast cancer and a melanoma mouse model. These experiments were performed in collaboration with Lauren Stryzewski as part of her undergraduate Honor's

Thesis. In the melanoma model, B16-F10 melanoma cells were injected subcutaneously into C57BL/6 mice. In the breast cancer model, 4T1-RFP-luc breast cancer cells were injected into the left 4th mammary fat pad of BALB/C mice. In both models, tumor cell implantation was followed by electroporation of pV1J-LCN2 plasmid or pV1J empty vector. Tumors were allowed to grow for 6 weeks to assess growth and the presence of metastases.

The results in Figure 5.1.A showed the 4T1-luc-RFP tumor bioluminescence in mice electroporated with pV1J and pV1J-Lcn2. Figure 5.1.B showed that the primary tumor volume is greater in mice electroporated with pV1J-Lcn2 during all weeks of tumor progression. Figure 5.1.C showed the metastatic tumor bioluminescence appears to trend towards being higher in the pV1J-Lcn2 group, but there is no difference in metastatic burden in these mice. It is likely that allowing the primary tumors to grow longer may provide more insight into the effects of high systemic Lcn2 on breast cancer metastasis. Figure 5.1.D and 5.1.E showed that in C57BL/6 mice injected subcutaneously with B16-F10-luc melanoma cells and electroporated with pV1J or pV1J-Lcn2, the pV1J-Lcn2 group showed higher primary tumor mass, but there was no difference in lung metastasis as shown by IVIS imaging in photons/second.

Taken together, these data showed that elevated systemic Lcn2 levels enhanced primary tumor growth of both melanoma and breast cancers. In the splenic model of CRC liver metastasis, which quickly produces liver metastasis via drainage through the splenic vein, elevated Lcn2 increased liver metastasis but did not impact primary growth. On the other hand, both breast and melanoma

primary tumors grew very aggressively and the mice had to be sacrificed due to the large tumor burden before significant metastasis occurred. Future studies should utilize a slower growing melanoma and breast cancer mouse cell lines in conjunction with Lcn2 electroporation, to better gauge the impact of Lcn2 on the incidence of metastatic growth in other target organs. In conclusion, elevated systemic Lcn2 levels increased the growth rate of primary breast and melanoma tumors, and but did not increase incidence of metastasis to lung and liver.

5.2.2 LOCALIZATION OF LCN2 EXPRESSION IN THE LIVER OF METASTASIS-BEARING MICE

In the microarray experiment described in Chapter 2, *Lcn2* was identified as a gene of high interest in liver metastasis because it was one of the most highly upregulated in the liver “soil”. *Lcn2* mRNA levels in the microarray was over-expressed in the non-tumor regions of the liver, as confirmed by the exclusion of mCherry protein, which was expressed only in the tumor cells. However, while this analysis showed that *Lcn2* is highly expressed in the non-tumor region, there was no indication of the specific cell type(s) producing Lcn2. To identify the cells producing Lcn2 in the liver of colorectal cancer bearing mice, immunohistochemistry (IHC) and in-situ hybridization (ISH) were utilized.

IHC staining for Lcn2 on metastasis-bearing mouse liver tissue showed diffuse staining, which is consistent with its role as a secreted protein (Figure 5.2). Lcn2 staining appeared darker on the edges of the tumor region. Although

myeloperoxidase positive (MPO+) cells, or neutrophils, were found around the tumor periphery, there was no punctate co-localization of MPO with Lcn2.

In-situ RNA hybridization was used to determine the sites of hepatic *Lcn2* transcription. The results in Figure 5.3 showed that *Lcn2* is mostly over-expressed around the periphery of the tumor with very few transcripts expressed within the tumor cells. Figure 5.4 further showed that when adjacent metastatic liver sections were stained by IHC for the CD45 pan-leukocyte marker (total immune cells), F4/80+ marker for macrophages, MRP-8 for mast cells, and MPO for neutrophils, these cellular markers are found in cells within the same region as the *Lcn2 mRNA*, however, there was no distinct cellular staining pattern correlating *Lcn2* expression with any one type of immune cells *in-situ*.

5.2.3 EFFECTS OF INCREASED SYSTEMIC LCN2 ON THE IMMUNE CELL COMPOSITION OF THE METASTATIC LIVER MICROENVIRONMENT

After localizing the *Lcn2 mRNA* expression to the tumor periphery *in-situ*, more cell specific *Lcn2* co-localization was necessary to determine which stromal cells were expressing *Lcn2*. We also wanted to determine how an increase in systemic *Lcn2* levels in tumor-bearing mice affected the metastatic tumor microenvironment, specifically with respect to the recruitment of macrophages and neutrophils. CRC patients with high serum levels of *Lcn2* had poorer prognosis and outcomes, thus, it is critical to understand if elevated *Lcn2* in CRC-bearing mice was contributing to CRC metastasis or if it is a downstream byproduct of the high inflammation seen in tumor bearing mice.

We used a splenic injection model in these experiments by injecting MC38-luc CRC cells directly into the spleen. The high vascular drainage from the spleen into the liver allows metastasis to occur in all animals injected. MC38-luc is a very useful tumor model because it is less aggressive than CT26 and provided a more fine-tuned window in which to observe changes due to high systemic Lcn2 expression. *In-vivo* electroporation of pV1J-Lcn2 was used to elevate systemic Lcn2 in tumor-bearing mice given a splenic implantation of MC38-luc. Lcn2 and immune cell co-localization were analyzed using fluorescence confocal microscopy. Analysis by flow cytometry was used to further quantitate the cell populations identified by confocal microscopy including leukocytes (Cd45+), macrophages (F4/80+), neutrophils/MDSCs (Cd11b+/Ly6G+), and mast cells (Cd117+/FcεR1α+). Figures 5.8-5.11 show that electroporation of Lcn2 caused minimal to no change in immune cell populations in non-tumor bearing mice, therefore, only the results obtained from tumor-bearing mice are described below. Figure 5.7 shows the fold change in immune cell populations in the spleen, liver, and liver metastases of tumor-bearing mice electroporated with either pV1J or pV1J-Lcn2.

TOTAL IMMUNE CELLS

As shown in Figure 5.5.D, analysis by confocal microscopy showed no differences in the CD45+ cell population between pV1J and pV1J-Lcn2 electroporated mice. Flow cytometry analysis of the CD45+ population showed that, as expected, tumor bearing mice electroporated with pV1J or pV1J-Lcn2

had more spleen and liver immune cells than non-tumor bearing mice, due to the role of immune cells in supporting the tumor microenvironment. Figure 5.8.B shows two populations in pV1J-Lcn2 tumor bearing mice at sacrifice because the two mice being analyzed varied in tumor burden.

MACROPHAGES

The results in Figure 5.5.C showed that in the pV1J-Lcn2 electroporated mice, a significantly higher number of macrophages infiltrated the tumors at the tumor-liver periphery, as compared to mice electroporated with the pV1J vector. Analysis of resected tumors by flow cytometry analysis for the F4/80+ cell populations are shown in Figure 5.9. Tumor-bearing mice showed a significant decrease in spleen F4/80+ cells, but an increase in liver F4/80+ cells. In these tumor-bearing mice, only pV1J-Lcn2 electroporated mice showed a 1.7-fold increase in the number of macrophages in the liver as compared to vector electroporated mice. In addition, metastatic liver tumors in mice electroporated with pV1J-Lcn2 were infiltrated with 1.75-fold more macrophages than those electroporated with the pV1J vector.

NEUTROPHILS

Analysis of tumor bearing liver sections by confocal microscopy showed that there were no differences in MPO+ neutrophil populations within the tumors of mice electroporated with pV1J (Figure 5.5,C). Quantification of the MPO+ populations showed no changes in their numbers at the tumor periphery when

systemic Lcn2 level was increased by electroporation with pV1J-LCN2 (Figure 5.6). In contrast, we observed a change in the number of Cd11b+/Ly6G+ neutrophil/G-MDSC population between the spleen and liver (Figure 5.10). Flow cytometry analysis of single cell suspensions from spleen and liver taken from tumor bearing mice four weeks after electroporation showed that mice with elevated Lcn2 had fewer neutrophils in the spleen and a higher number of neutrophils in the liver (Figure 5.10). These changes in population suggest that neutrophils may be recruited into the metastasis bearing liver in response to Lcn2, but not into the metastatic tumor bed.

MAST CELLS

A similar analysis of tumor bearing liver sections by confocal microscopy to examine the number of Mct+ mast cells and flow analysis of single cell suspensions from spleen and liver for Cd117+/FceR1a+ mast cells showed no significant differences in their numbers in mice electroporated with pV1J or pV1J-Lcn2 (Figure 5.11). Notably, the flow analysis showed fewer mast cells infiltrating liver metastatic tumors in mice electroporated with pV1J-Lcn2 as compared to pV1J; however, their numbers were so low such that their role in the tumor microenvironment in relation to Lcn2 overexpression may not be significant.

QUANTITATION OF CELL POPULATIONS BY CONFOCAL MICROSCOPY.

In Figure 5.6.A, we quantitated the Lcn2+ cells in metastasis bearing liver and found that there were higher numbers of Lcn2+ neutrophils in mice

electroporated with pV1J. When Lcn2 systemic levels were elevated by electroporating with pV1J-LCN2, the population shifted such that there was a higher number of Lcn2+ macrophages in the liver. Overall examination of Lcn2+ cells however, indicated that most of these cells were neither neutrophils nor macrophages (Figure 5.6.B). Although there is no reliable cellular marker for mouse hepatocytes, the histology and morphology of the Lcn2+ cells in the tissue sections indicate that these are mostly hepatocyte cells. Although we observe a change from more neutrophils expressing Lcn2 to more macrophages expressing Lcn2 in response to pV1J-Lcn2 electroporation, most of the macrophages within the tissue sections did not express Lcn2, (Figure 5.5). These observations suggest that in all tumor-bearing mice, Lcn2 is predominantly produced by hepatocytes around the periphery of the metastatic lesion, and when systemic Lcn2 is elevated, infiltration of metastatic tumors by macrophages increases to potentially sustain metastatic proliferation.

To assess the effects of macrophages infiltration of metastatic tumors under high Lcn2 conditions, we subcutaneously injected MC38 CRC cells admixed with BMDMs in to C57BL/6 mice. As shown in Figure 5.12, addition of undifferentiated BMDMs had no impact on tumor burden. However, addition of BMDMs conditioned with IL-4 that polarized the macrophages to the M2 phenotype caused a dramatic increase in tumor burden. Furthermore, loss of Lcn2 in macrophages conditioned to the M2 phenotype, by using Lcn2^{-/-} BMDMs isolated from Lcn2^{-/-} mice, reduced the magnitude of tumor growth seen in WT M2 BMDMs, but this reduction was non-significant due to the high variance.

Follow up experiments repeating this M2 BMDM co-injection with MC38 in the splenic injection model may show the impact of macrophage infiltration in proliferation of metastatic lesion in the presence of elevated Lcn2.

5.3 SUMMARY AND FUTURE DIRECTIONS

The data show that elevated systemic Lcn2 in a tumor-bearing mouse increased tumor burden in colon, breast, and melanoma cancers in mice, but increased primary tumor growth only in breast and melanoma models and increased metastatic burden in the MC38 spleen injection model. This suggests that high systemic Lcn2 increases tumor burden in mice, but whether it manifests in increased metastasis depends on the kinetics of the specific tumor model. The flow cytometry data suggest that under conditions of high systemic Lcn2 expression, total immune cell and mast cell populations do not change; however, a percentage of macrophages and neutrophils decreases in the spleen and increase in the liver, but only macrophages invaded the tumor margins under high systemic Lcn2 conditions. Confocal microscopy showed that in mice electroporated with pV1J-Lcn2, there is an increase in the number of macrophages infiltrating the metastatic tumor margins in the liver. These macrophages correlated with increased metastasis, however, more work needs to be done to show that macrophages directly promote metastatic growth.

Our data further showed that hepatocytes are the predominant Lcn2-producing cells in the metastatic liver microenvironment. This is supported by the observations that 1) Lcn2 mRNA transcripts were localized around the periphery

of metastatic tumors *in-situ*, 2) intracellular Lcn2 protein was colocalized with hepatocyte cells in confocal microscopy analyses, and 3) minimal Lcn2 protein colocalized with non-hepatocyte cells in confocal images.

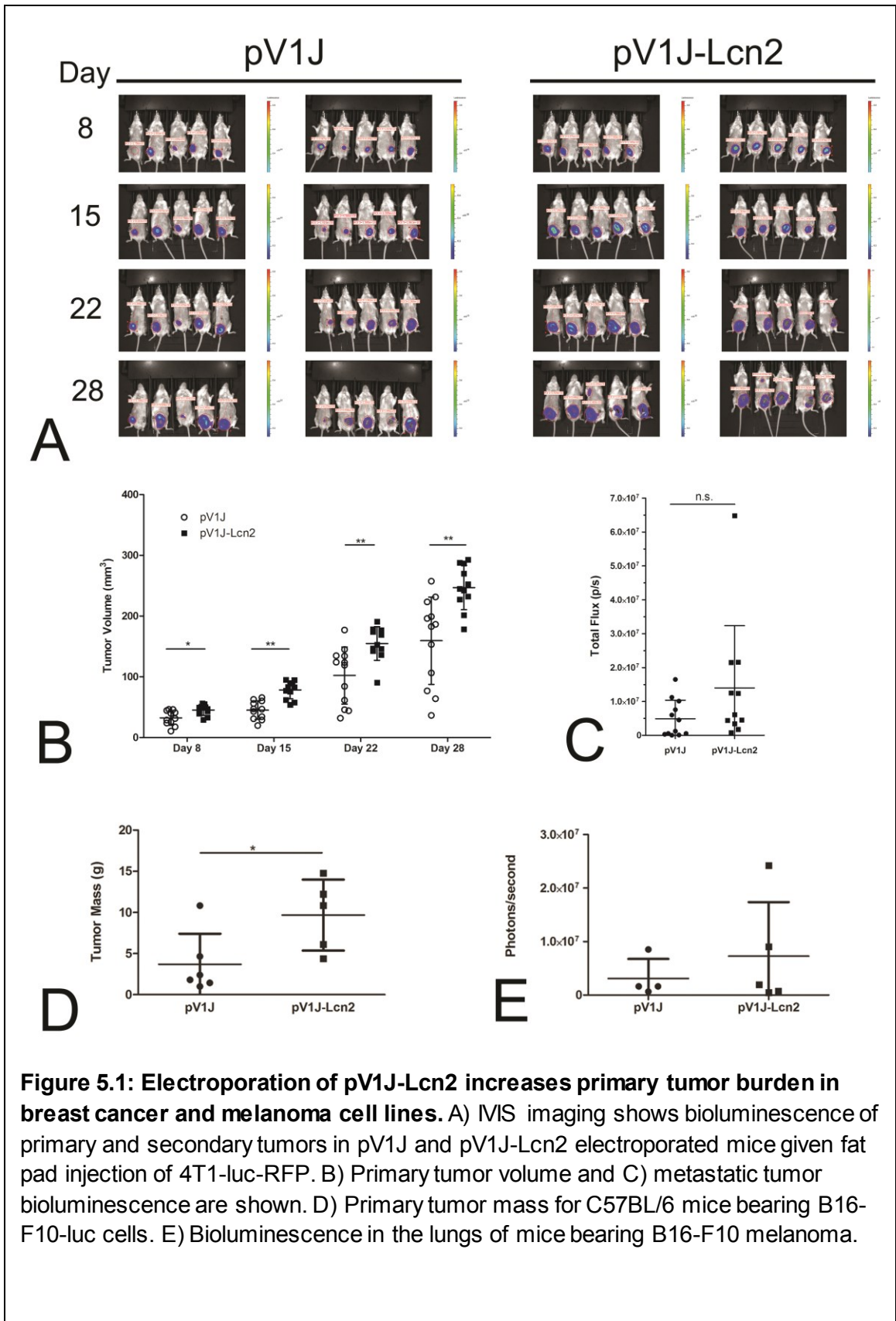
The data suggests that elevated systemic Lcn2 may increase inflammation, which may cause increased infiltration of macrophages into the metastatic tumors. Lcn2 in the hepatocytes around the edges of the tumor may support tumor growth through this recruitment. Lcn2 may also support tumor growth by acting as an alternative iron-transport mechanism by increasing the iron available to metastatic tumor cells (Gomez-Chou et al., 2017; Jung et al., 2017).

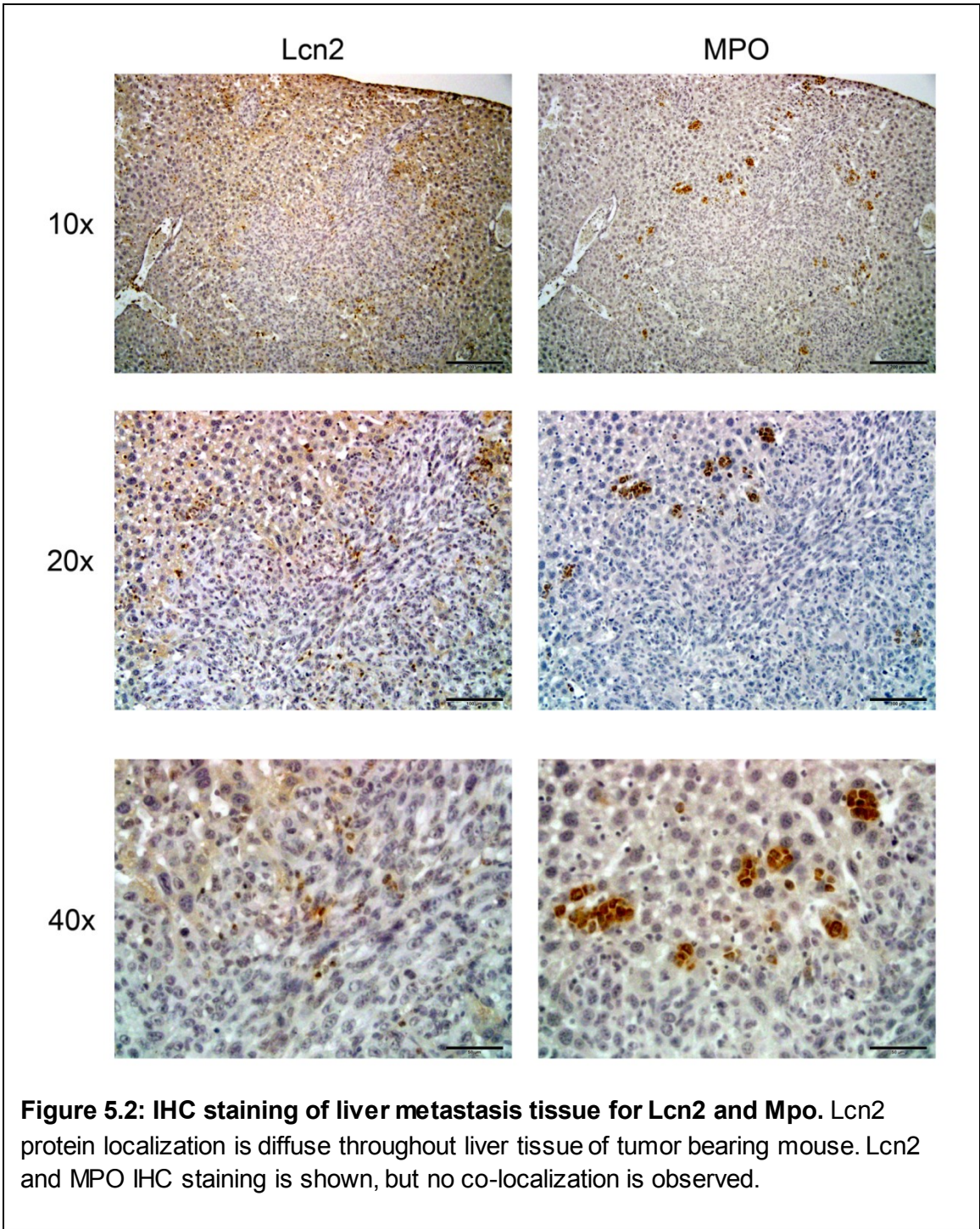
Lcn2 has been described as a downstream product of the IL-6/STAT-3 axis in hepatocytes and macrophages, and IL-1 β as a positive regulator of Lcn2 production via NF- κ B (Asimakopoulou et al., 2016b; Feng et al., 2016; Gineste et al., 2016; Guo et al., 2014; Kienzl-Wagner et al., 2015; Moschen et al., 2017; Warszawska et al., 2013; Xu et al., 2015). Since IL-6 is a well-established cytokine upregulated in many tumors, including CT26 and MC38, tumor-derived IL-6 may contribute to downstream Lcn2 expression in hepatocytes, among many other proteins driven by IL-6/STAT-3 signaling (Miller et al., 2016)(Li et al., 2012).

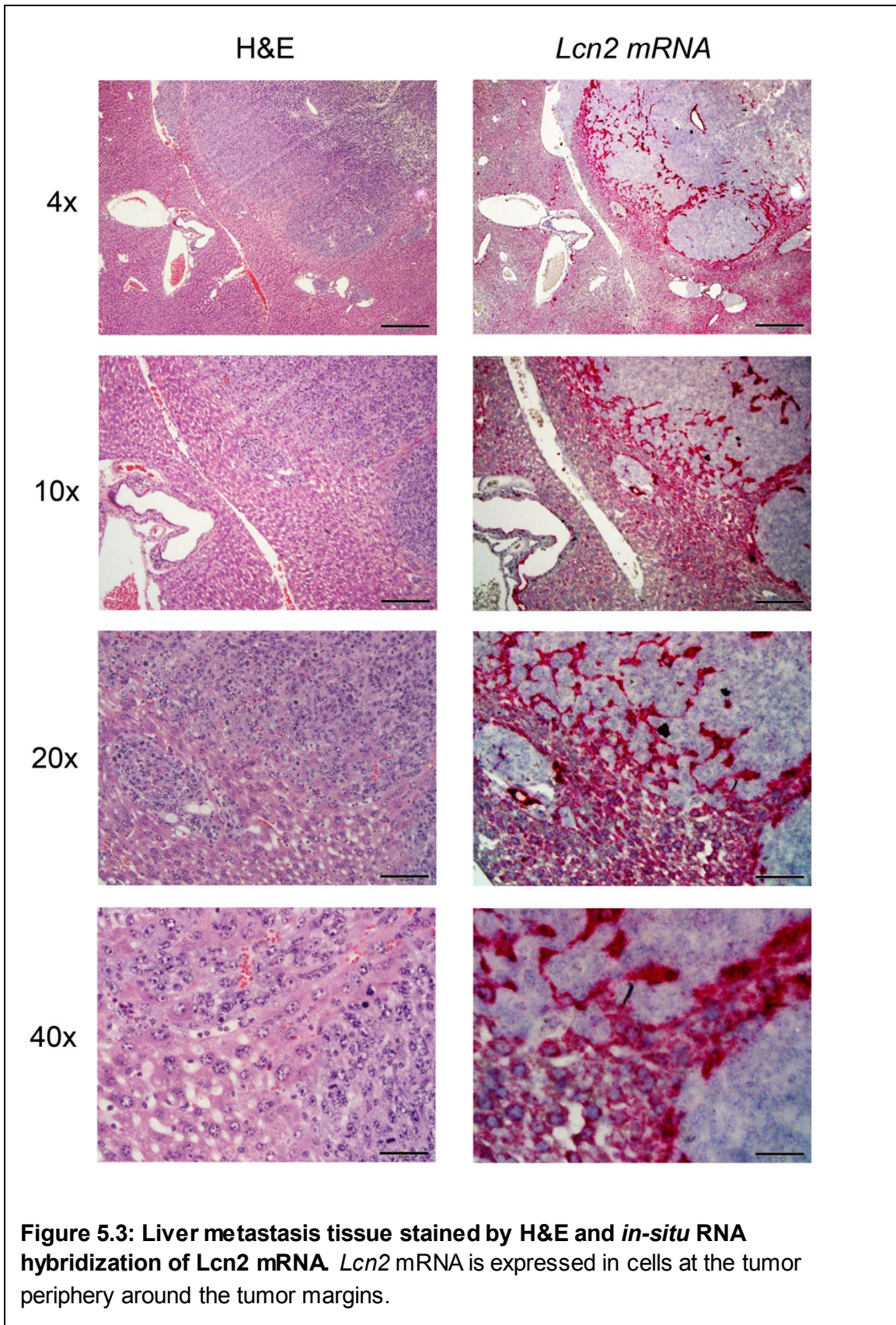
Other studies have investigated the role of iron and Lcn2 in macrophages and the data suggest that M1-polarized macrophages tend to store iron in ferritin and M2-polarized macrophages store iron in a labile iron pool, wherein iron is more accessible to chelation by Lcn2 and a siderophore (Corna et al., 2010). A

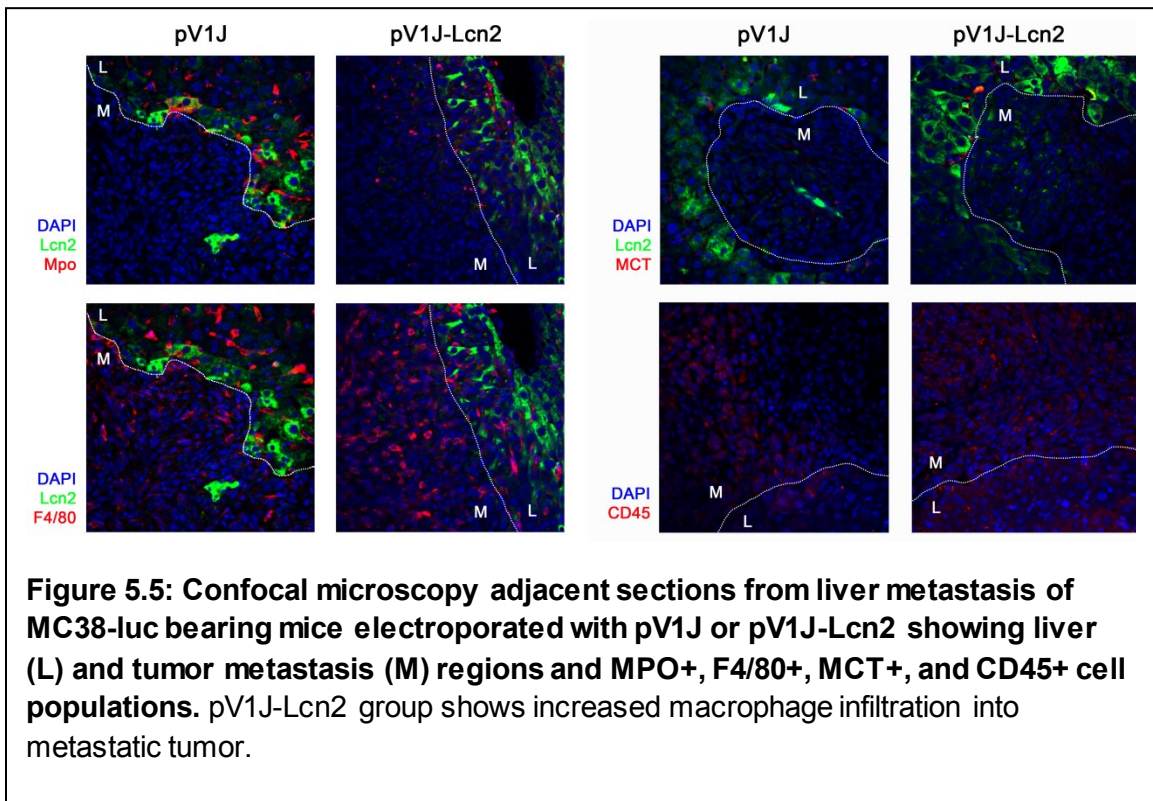
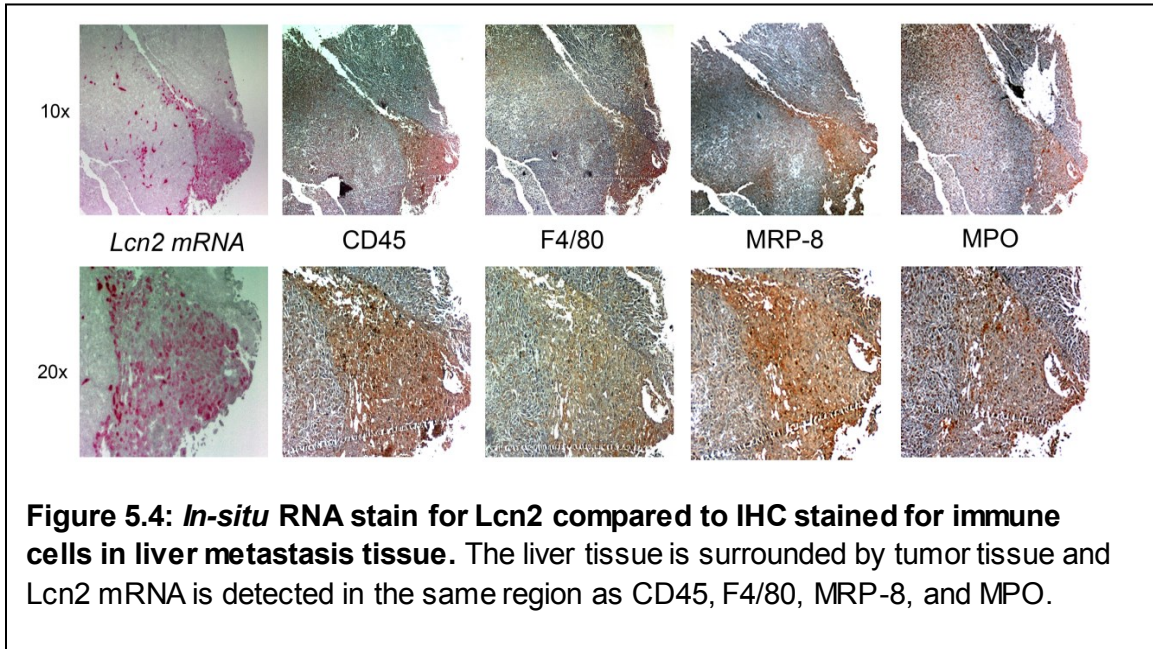
recent study showed that macrophages with an 'iron-releasing' phenotype in the tumor microenvironment aid in tumor progression (Mertens et al., 2016). Future studies utilizing these BMDMs and CRC cell lines could investigate the role that Lcn2 and STAT3 play in conjunction with macrophages and iron.

Future directions for this study should look to differentiate between the effects of Lcn2 on metastasis when Lcn2 is synthesized only in hepatocytes or immune cells. Utilizing a hepatocyte specific Lcn2 knockout model, we could determine if systemic Lcn2 causes hepatocytes to secrete Lcn2, or if hepatocyte Lcn2 caused macrophage infiltration of the tumor margins (Xu et al., 2015). Bone marrow transplantation of Lcn2^{-/-} BM into WT mice and vice-versa would further reveal the effects of knocking out Lcn2 specifically in immune cells. To further investigate the role of macrophages in these processes, clodronate liposomes could be used in tumor-bearing mice to eliminate all macrophages. Finally, Lcn2 can be transported into cells via the Lcn2 receptor 24p3R. 24p3R^{-/-} mice are embryonic lethal, but if a drug or antibody were able to inhibit this this receptor, it would reveal the extent of Lcn2 transport between hepatocytes and immune cells and if that affected liver metastasis of CRC.









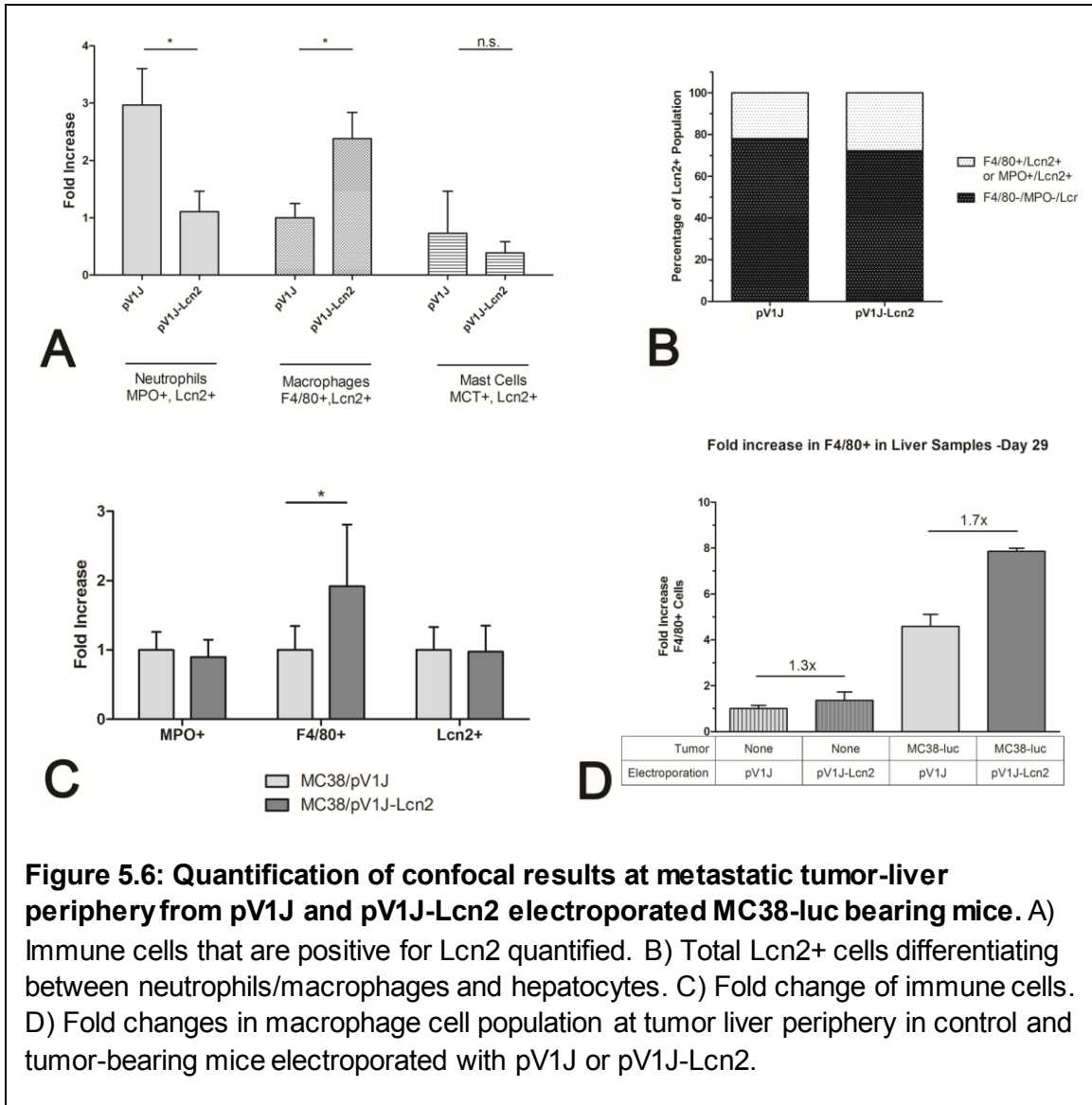


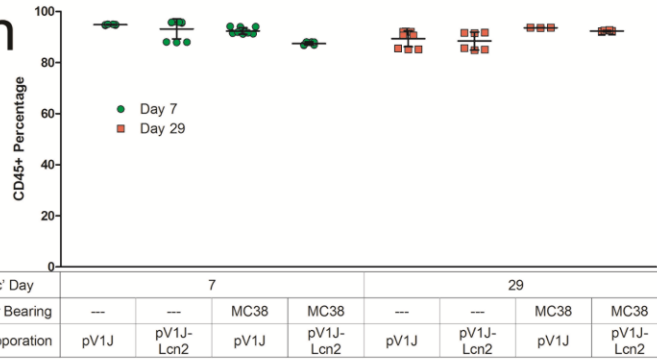
Figure 5.6: Quantification of confocal results at metastatic tumor-liver periphery from pV1J and pV1J-Lcn2 electroperated MC38-luc bearing mice. A) Immune cells that are positive for Lcn2 quantified. **B)** Total Lcn2+ cells differentiating between neutrophils/macrophages and hepatocytes. **C)** Fold change of immune cells. **D)** Fold changes in macrophage cell population at tumor liver periphery in control and tumor-bearing mice electroperated with pV1J or pV1J-Lcn2.

	Spleen		Liver		Liver Mets	
	pV1J	pV1J-Lcn2	pV1J	pV1J-Lcn2	pV1J	pV1J-Lcn2
Leukocytes (CD45+)	1.00	0.99	1.00	1.16	1.00	1.07
Macrophages (F4/80+)	1.00	0.86	1.00	1.70	1.00	1.75
Neutrophils (Cd11b+/Ly6G+)	1.00	0.59	1.00	3.08	1.00	0.33
Mast Cells (Cd117+/FcεR1α+)	1.00	1.60	1.00	1.25	1.00	0.50

Figure 5.7: Quantification of flow cytometry results shows fold change of pV1J-Lcn2 over pV1J electroperation in cell populations of the spleen, liver, and liver metastasis compartments of tumor-bearing mice only.

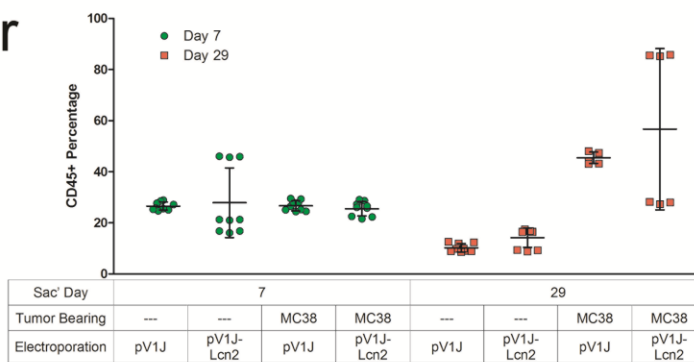
Spleen

A



Liver

B



Tumors

C

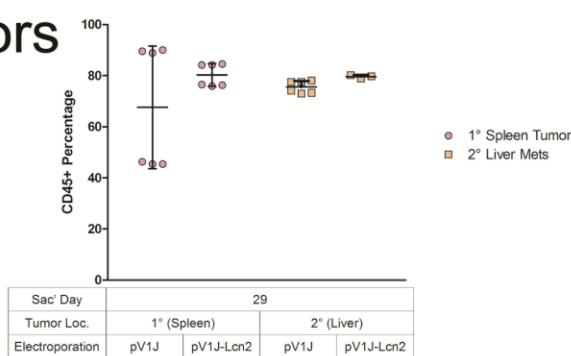
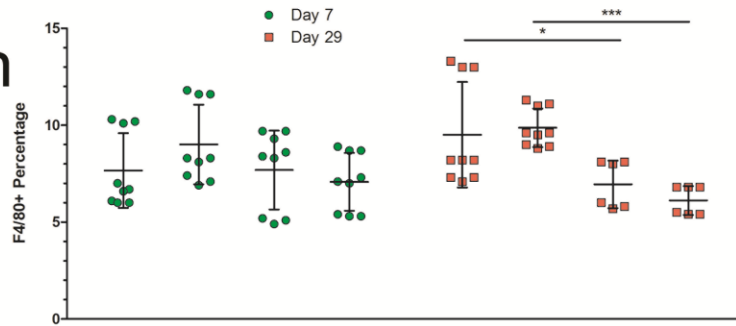


Figure 5.8: Flow analysis of Cd45+ immune cells. Mice given a sham or MC38-luc splenic injection were electroporated with pV1J or pV1J-Lcn2 and the Cd45+ cell populations were quantified in the (A) spleen, (B) liver, and (C) primary or metastatic tumors.

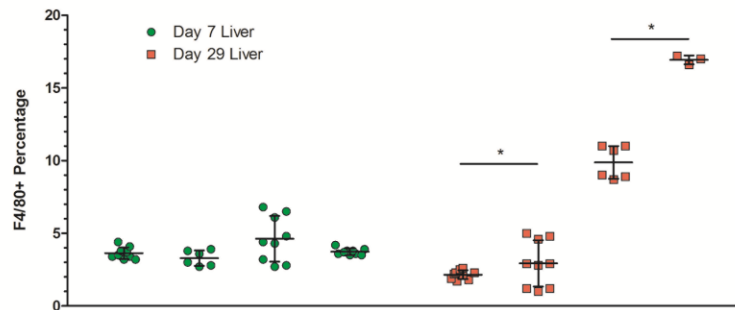
Spleen

A



Liver

B



Tumors

C

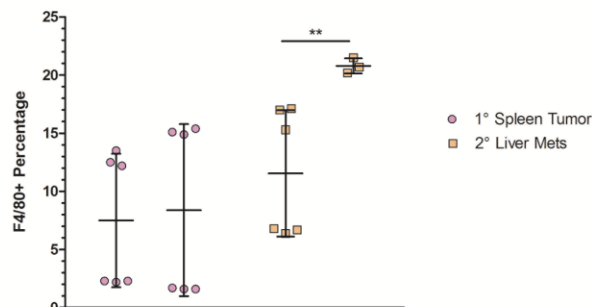


Figure 5.9: Flow analysis of F4/80+ macrophages. Mice given a sham or MC38-luc splenic injection were electroporated with pV1J or pV1J-Lcn2 and the F4/80+ cell populations were quantified in the (A) spleen, (B) liver, and (C) primary or metastatic tumors.

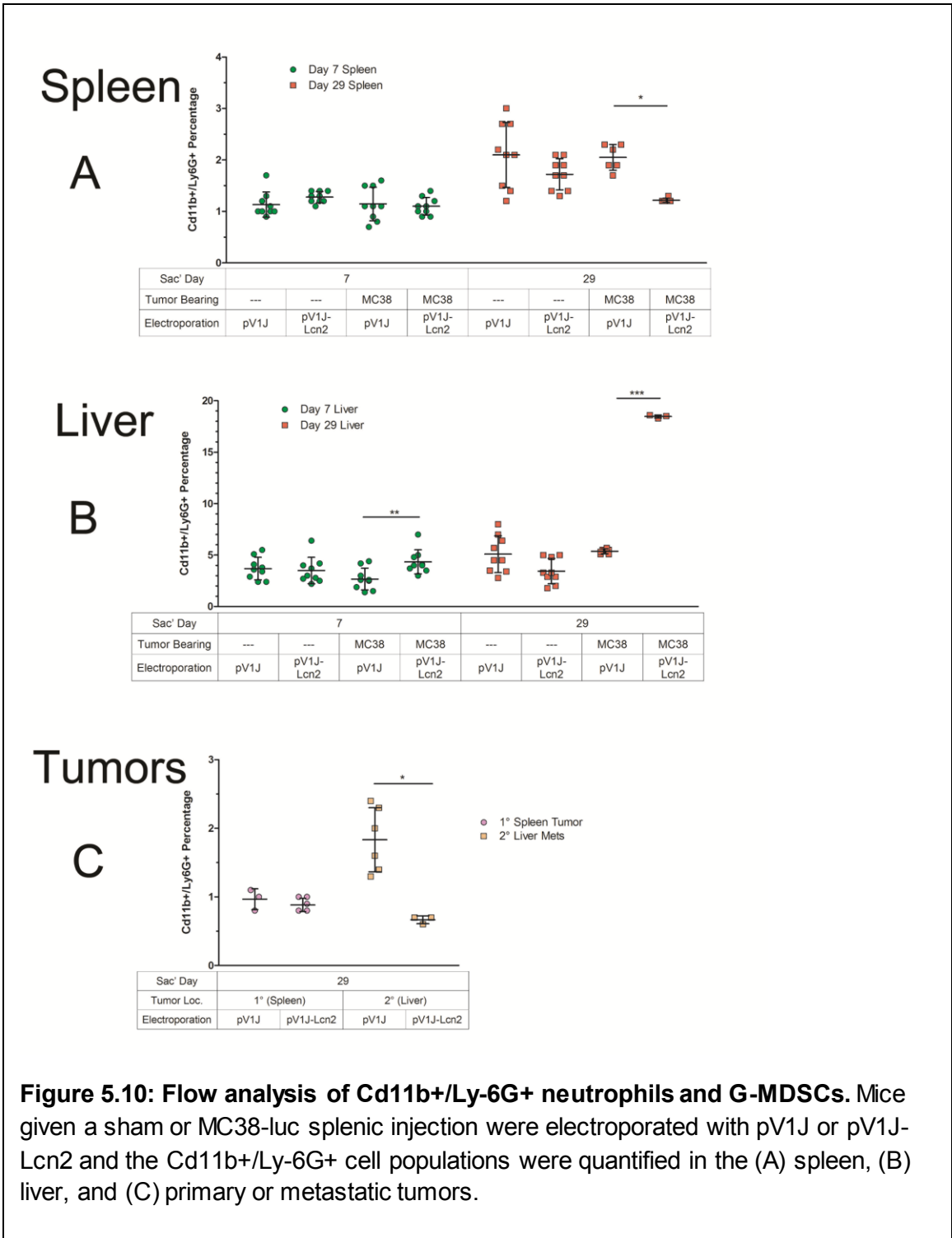
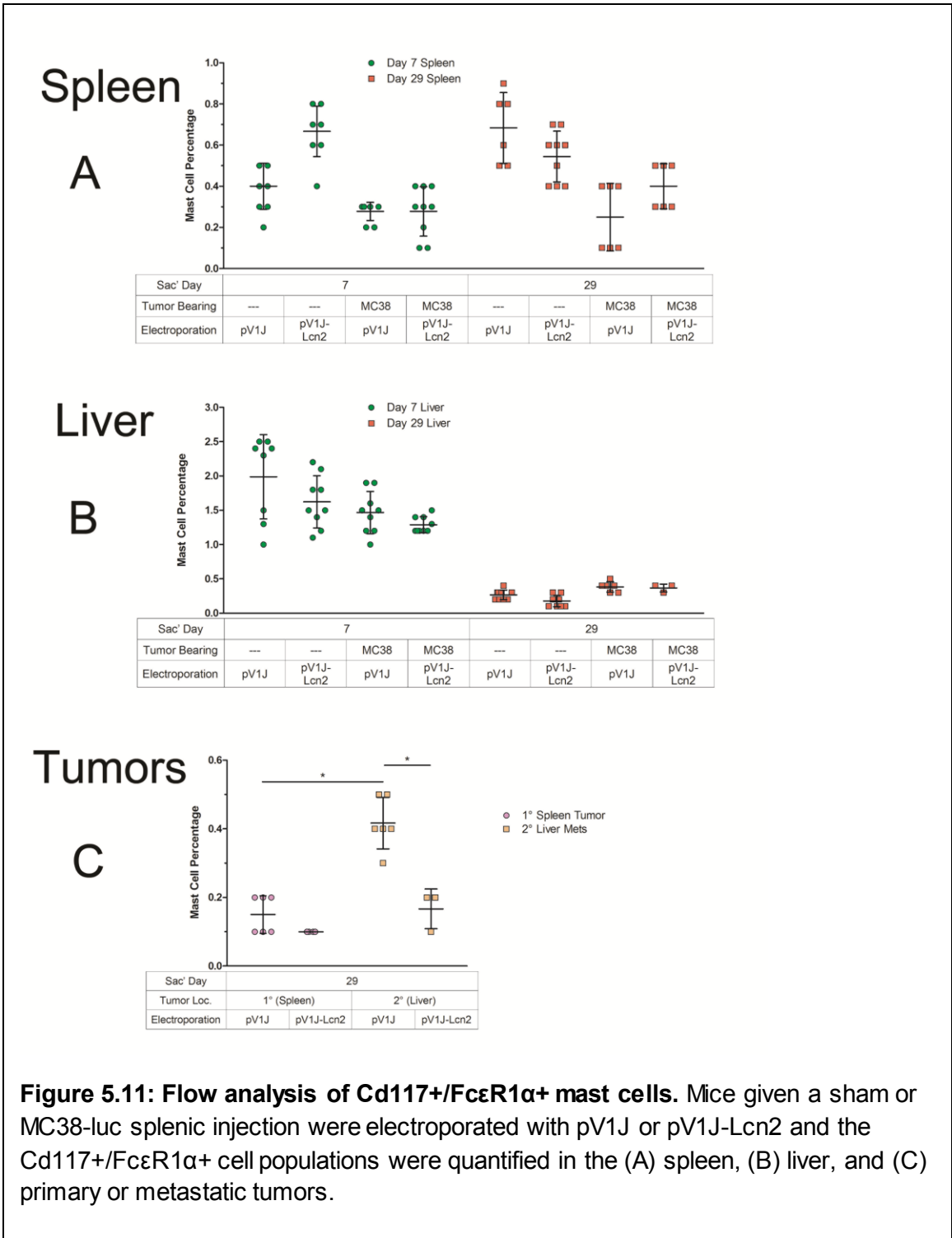
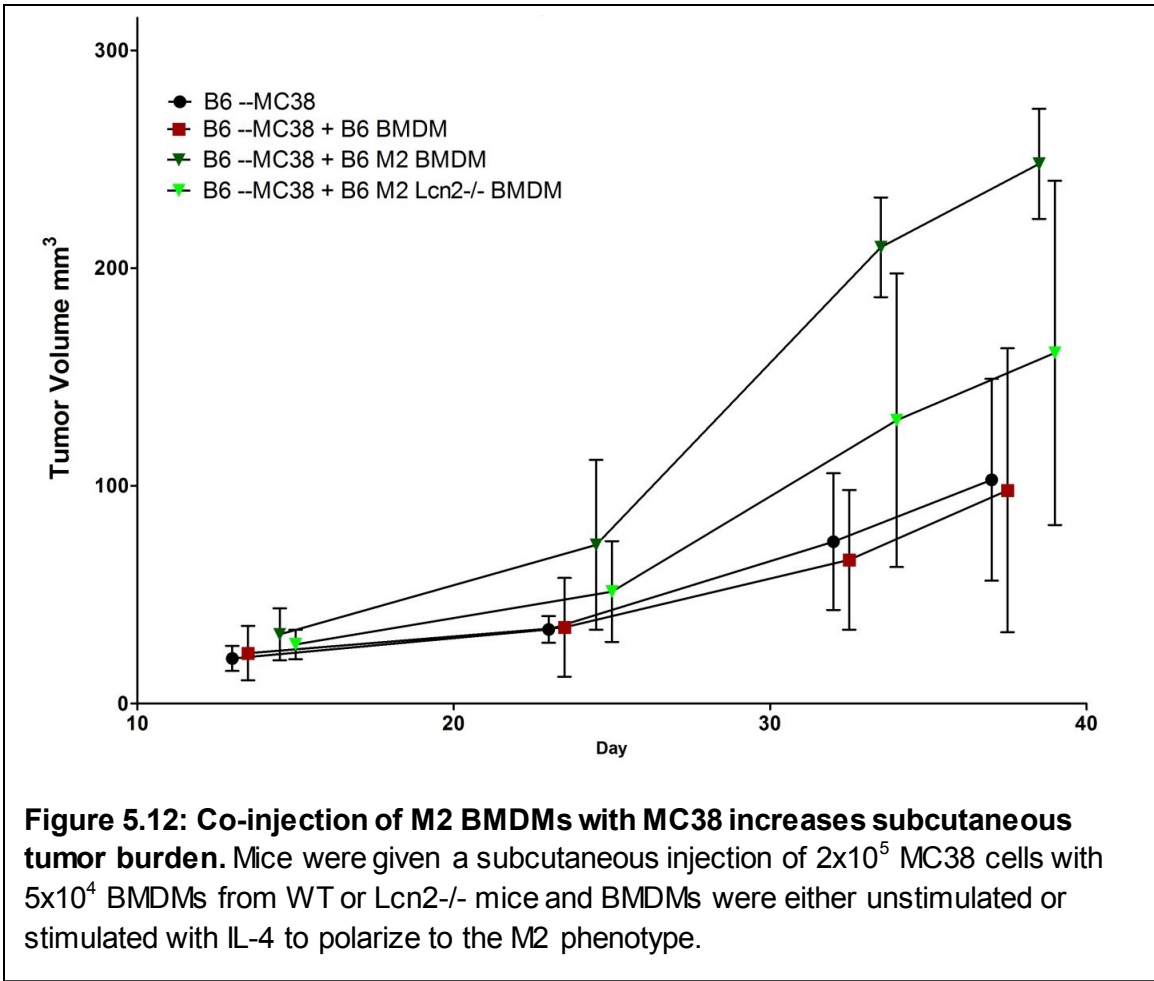


Figure 5.10: Flow analysis of Cd11b+/Ly-6G+ neutrophils and G-MDSCs. Mice given a sham or MC38-luc splenic injection were electroporated with pV1J or pV1J-Lcn2 and the Cd11b+/Ly-6G+ cell populations were quantified in the (A) spleen, (B) liver, and (C) primary or metastatic tumors.





CHAPTER 6

MATERIALS AND METHODS

Mouse Strains

BALB/C mice were used as orthotopic homograft recipients for the syngeneic CT26 and CT26-FL3 adenocarcinoma cell lines. C57BL/6 mice were used as the orthotopic homograft recipient for MC38-luc adenocarcinoma cell lines. Lipocalin-2 knockout mice in the C57/BL6 background were obtained from Tak Mak (Princess Margaret Cancer Center, University Health Network, Toronto, ON). These mice were backcrossed to the BALB/C background over 10 generations. A commercial Lipocalin-2 knockout mouse strain (B6.129P2-Lcn2tm1Aade/AkiJ) was obtained from Jackson Laboratories (Bar Harbor, ME). All BALB/C, C57BL/6, and B6.129P2-Lcn2tm1Aade/AkiJ mice were purchased from Jackson Laboratories and were bred and maintained at the Mouse Experimentation Core Facility of the Center for Colon Cancer Research at the University of South Carolina in Columbia, SC. All animal experiments were conducted according to the guidelines and approval of USC Institutional Animal Care and Use Committee.

Cell culture

The cell lines CT26 (ATCC® CRL-2638™), MPRO (ATCC® CRL-11422™), B16-F10 (ATCC® CRL-6475™), and 4T1 (ATCC® CRL2539™) were purchased from American Type Culture Collection (ATCC®). The cell lines Raw264.7 (ATCC® Tib-71™), BNL CL.2 (ATCC® Tib-73™), and MC38-luc cells were kindly given as a gift from Dan Dixon. The highly-metastatic CT26-FL3 was isolated from the parental CT26 cell line by in vivo selection by injecting into the cecum and passaging three times through the liver as described (Zhang et al., 2013). Cell lines CT26, MC38-luc, BNL CL.2, B16-F10, and Raw264.7 were grown in DMEM (4.5 g/L glucose, 110 mg sodium pyruvate/L and L-glutamine)(Mediatech, Inc. Corning, Manassas, VA) with 10% FBS and 1% Penicillin-Streptomycin (HyClone, Thermo Scientific, Logan, UT). Cell line 4T1 was grown in RPMI-1640 (Mediatech, Inc. Corning, Manassas, VA) with 10% FBS and 1% Penicillin-Streptomycin. Dissociation of adherent cells was performed with Trypsin EDTA 1x (Mediatech, Inc. Corning, Manassas, VA) after washing cells in Hanks' Balanced Salt Solution (HBSS) (Mediatech, Inc. Corning, Manassas, VA). MPRO cells were grown in DMEM supplemented with 10% FBS, 1% Penicillin-Streptomycin, 10 ng/mL Recombinant Mouse GM-CSF (Biolegend, San Diego, CA). Induction of MPRO into a differentiated neutrophil (NEUT) was performed by adding 10µM all-trans-retinoic acid (ATRA, Acros Organics, Morris Plains, NJ) over a minimum of 3 days. Differentiation into NEUT was confirmed with wright-giemsa staining and flow cytometry. 4T1 cells (ATCC® CRL-2539™) were grown in RPMI-1640 (Corning, Manassas, VA). All cells were transfected

using Lipofectamine 2000 (Invitrogen, Waltham, MA). MC38-luc was transfected with pGL4.14-Lcn2-Hygro and selected with 400 $\mu\text{g}/\text{mL}$ Hygromycin (Hygrogold, Invivogen, San Diego, CA). CT26 and CT26-FL3 were transfected with pCMV6-Lcn2 (Origene, Rockville, MD) and selected with 400 $\mu\text{g}/\text{mL}$ G418 Sulfate (Mediatech, Inc. Corning, Manassas, VA).

Cecal Implantation of Colon Cancer Cells

Surgical laparotomy was performed for cecal implantation of syngeneic colon tumor cells on mice that were 8 to 12 weeks of age. Cell lines were dispersed into a single cell suspension and washed twice with PBS immediately before implantation. Mice were anesthetized with 2% isoflurane in oxygen by inhalation using a nose cone. Mice were placed in a supine position, and covered with a surgical drape. A midline sagittal incision was created and the cecum was exteriorized. 2×10^6 tumor cells in a volume of 10-20 μL were injected into the cecal subserosa, sealed with VetBond™ tissue adhesive (3M™, St. Paul, MN) and sterilized with 70% ethanol to remove any tumor cells that may have leaked out. The cecum was replaced into the peritoneal cavity and the skin was sutured in two layers with 6-0 polyglycolic acid absorbable sutures (CP Medical, Portland, OR). The peritoneum was sutured with a continuous subcuticular pattern, and the epithelium sutured with a simple cutaneous interrupted pattern. Sham mice were given the surgical laparotomy with PBS injected into the cecal subserosa. Postoperative care for the mice included an intraperitoneal (IP) bolus injection of 0.5 cc PBS and 0.1 cc Buprenorphine (0.03%) to manage post-operative pain.

Splenic Implantation of Colon Cancer Cells

Surgical laparotomy was performed for splenic implantation of syngeneic colon tumor cells on mice that were 8 to 12 weeks of age. CT26 cells were implanted into BALB/C mice and MC38 cells were implanted into C57BL/6 mice. Cell lines were trypsinized into a single cell suspension and washed twice with PBS before implantation. Mice were anesthetized with 2% isoflurane in oxygen by inhalation using a nose cone. Mice were placed in a supine position, and covered with a surgical drape. A dorsoventral incision was made in the left upper quadrant of the abdomen and the spleen was exteriorized. 2×10^5 tumor cells in a volume of 10-20 μL were injected into the spleen, sealed with VetBond™ tissue adhesive (3M™, St. Paul, MN) and sterilized with 70% ethanol to remove any tumor cells that may have leaked out. The spleen was inserted back into the peritoneal cavity and the skin was sutured in two layers with 6-0 polyglycolic acid absorbable sutures (CP Medical, Portland, OR). The peritoneum was sutured with a continuous subcuticular pattern, and the epithelium sutured with a simple cutaneous interrupted pattern. Sham mice were given the identical surgical procedure with PBS injection into the spleen. Postoperative care for the mice included an intraperitoneal (IP) bolus injection of 0.5 cc PBS and 0.1 cc Buprenorphine (0.03%) to manage post-operative pain.

Mammary Fat-Pad Implantation of Breast Cancer Cells

A subcutaneous injection into the fourth mammary fat pad was performed on BALB/C mice using syngeneic 4T1 breast cancer tumor cells on mice that were

8 to 12 weeks of age. Cell lines were trypsinized into a single cell suspension and washed twice with PBS before implantation. Mice were anesthetized with 2% isoflurane in oxygen by inhalation using a nose cone. Mice were placed in a supine position. 5×10^3 tumor cells in a volume of 50 μ L were injected into the fat pad. Sham mice were given the identical surgical procedure with PBS injection into the spleen. Postoperative care for the mice included an intraperitoneal (IP) bolus injection of 0.5 cc PBS and 0.1 cc Buprenorphine (0.03%) to manage post-operative pain.

Subcutaneous Implantation of Tumor Cells

Subcutaneous implantation of tumor cells was performed using CT26 cells in BALB/C mice, MC38 cells in C57BL/6 mice, and B16-F10 melanoma cells in C57/bl6 mice. Tumor cells were placed in single cell suspension and washed with PBS twice. 1×10^6 cells were injected with a 31G in 50 μ L under the cutaneous layer of the mouse in the lumbar region on the dorsal surface of the mouse. The injection site was sealed with a drop of VetBond™ tissue adhesive (3M™, St. Paul, MN).

Transwell Migration and Invasion Assay

The invasion assay measures tumor cell capacity for breaking through a matrigel™-coated transwell insert (BD Biosciences, San Jose, CA). 1×10^5 cells were starved 24 hours in 0.1% FBS in DMEM and seeded in the top chamber in 0.1% FBS in DMEM. The lower chamber contained 10% FBS in DMEM and the

cells were allowed to migrate for 20 hours. The matrigel to DMEM dilution was 1:6 (1.43 mg/mL) for CT26 and 1:10 (0.91 mg/mL) for MC38 cells. Co-culture transwell assays were completed as described above with 1×10^5 cells of interest seeded on the bottom well to nearly 75% confluency prior to the start of the assay. To harvest the assay, cells were fixed in 4% paraformaldehyde and stained in 1% crystal violet. Cells were imaged and counted in five field views at 40x for each transwell chamber.

Migration assays were performed in 6-well plates, growing cells to 75% confluence. At the start of the assay, media was switched to 2% FBS in DMEM and each well was scratched three times using a p200 pipette tip. Cells were imaged every 24 hours at 40x using the EVOS imager until the wound was recovered with cell growth or 120 hours. Iron supplementation with 10 μ M ferric chloride (Sigma, St. Louis, MO) and iron chelation with 10 μ M deferoxamine (Sigma, St. Louis, MO) were added to the media of cells after initial scratch was performed for MC38-luc cells.

Cell proliferation assay

To determine the growth rate of MC38-luc, CT26, CT26-FL3, and their Lcn2 overexpressing lines in culture, 10,000 cells per well containing 2 ml of DMEM with 10% FBS were plated into 6-well plates. CT26, CT26-FL3, and their Lcn2 overexpressing lines were plated at 1×10^5 cells per well in 6 well dishes in triplicate and counted at 72 hours, 144 hours, 192 hours, and 240 hours. MC38-

luc and MC38-luc-Lcn2 lines were plated at 5×10^5 cells per well in 6 well dishes in triplicate and counted at 40 hours, 90 hours, and 145 hours.

RNA Isolation

Total RNA was isolated either from cells or murine tissues using the RNeasy RNA isolation kit (Qiagen, Valencia, CA) or E.Z.N.A.® Total RNA Kit I (Omega BioTek, Norcross, GA). cDNA was synthesized from the total RNA extract using iScript cDNA synthesis Kit (Bio-Rad, Hercules, CA). The kits were used following manufacturer's instructions.

Microarray Analyses

Liver samples for microarray analyses were obtained from three groups of mice. The first group mice, called the sham surgery control underwent the surgery for cecal implantation but PBS was injected into cecum instead of tumor cells. The pre-metastatic liver samples were taken from mice with cecal tumors but no liver metastases. The metastatic liver samples were taken from tumor bearing mice with liver metastases. Tumor cells were labeled with red fluorescence. Care was taken that the liver samples were free of tumor tissues by verifying that the samples did not contain red fluorescent proteins by confocal microscopy and by ensuring that RNA samples did not contain transcripts from red fluorescent protein by RT-PCR. In addition, liver samples were confirmed to be free of tumor cells by analyzing DNA extracted from the tissue for mCherry sequence via PCR amplification. The RNA samples for microarray analysis were

isolated, prepared, and analyzed as described in Zhang et.al (Zhang, 2013). RNA purity was determined by measuring an RNA Integrity Number (RIN) of at least 8.

Analysis by Quantitative Real-Time PCR

Quantitative Real-Time PCR (qRT-PCR) was performed on cDNA samples using an Applied Biosystems 7300 Real Time PCR System (Thermo Fisher Scientific Inc., Waltham, MA) with PowerSYBR® green reagent (Life Technologies, Carlsbad, CA). qRT-PCR Primers against mouse transcripts for β -actin and Lcn2 were designed and obtained from Integrated DNA Technologies (IDT, Coralville, IA). The primer sequences are as follows:

β -actin-F, 5'-AAGAGCTATGAGCTGCCTGA-3',

β -actin-R, 5'-TACGGATGTCAACGTCACAC-3';

Lcn2-F, 5'-CTACAATGTCACCTCCATCCTG-3',

Lcn2-R, 5'-ACCTGTGCATATTTCCCAGAG-3'.

Measurements were run in triplicate and transcription levels were determined relative to β -actin expression levels.

Serum Isolation

Blood serum was collected in Heparin-coated capillary tubes or EDTA-coated vials (Thermofisher, Pittsburg, PA; Becton Dickinson, Franklin Lakes, NJ) via retro-orbital puncture from mice anesthetized with 2% isoflurane in oxygen. Samples were centrifuged at 13,700 rcf for four minutes using the ADAMS Micro-

Hematocrit II centrifuge (Becton Dickinson, Franklin Lakes, NJ) to separate the serum from red blood cells. Sera were stored in microcentrifuge tubes at -80°C prior to analysis.

Western Blotting

Protein extracts were obtained from whole cell lysates or murine blood sera. Isolation of protein in-vitro was performed using M-PER (mammalian protein extraction reagent, Thermofisher, Grand Island, NY) with a protease inhibitor (Sigma, St. Louis, MO) following manufacturer's instructions. Proteins were separated on 4-15% precast acrylamide gels (Bio-Rad, Hercules, CA), transferred to nitrocellulose blots, and probed with primary with antibodies against Lcn2 (1:500 to 1:1000, Goat pAb and Rat mAb, R&D Systems, Minneapolis, MN or Rabbit pAb, Abcam, Cambridge, MA). Blots were incubated with primary antibodies overnight at 4°C, washed with PBS/0.01% Tween-20, probed with HRP-conjugated secondary antibody (Bio-rad, Hercules, CA) for 1 hour at room temperature, washed, and visualized with ECL enhanced chemiluminescence kit (GE Healthcare, Piscataway, NJ). Blots were visualized using either the GE ImageQuant LAS 4000 (GE Healthcare Bio-Sciences, Pittsburgh, PA) or the Konica Minolta SRX-101A tabletop radiograph machine (Konica Minolta Medical Imaging, Wayne, NJ). As internal controls for equal loading, blots were re-probed with either Hrp-conjugated Anti- β -actin (Abcam, Cambridge, MA) or Anti-Albumin Rabbit pAb (Santa Cruz Biotechnology, Santa

Cruz, CA) after stripping the blot with a mild stripping buffer. Western images were quantified using ImageJ software (NIH, Bethesda, MA).

Enzyme-Linked Immunosorbent Assay

ELISA was performed on serum and cell culture supernatant using the Mouse Lipocalin-2/NGAL Quantikine ELISA Kit (R&D Systems, Minneapolis, MN). Serum was diluted 100-fold before analysis. Cell culture supernatant was diluted if needed to produce a result in the working range of the assay. ELISA wells were read using the Epoch microplate spectrophotometer (Biotek, Winooski, VT). Absorbance was read at 450 nm, and optical imperfections in the plate were read at 540 nm and subtracted from the 450 nm read. Four parameter logistic ELISA curve fitting analysis was performed on ELISAanalysis.com.

Plasmid Construction and Overexpression of Lipocalin-2 in pCMV6 vector

The pCMV6-Entry plasmid expressing murine Lcn2 was purchased from Origene and transfected in CT26 and CT26-FL3 cells. A pCMV6-Entry vector control plasmid was created by excising the Lcn2 sequence from the plasmid and subsequently transfecting into the CT26 and CT26-FL3 cells as well. The cells were analyzed for intracellular and extracellular protein levels using western blotting and ELISA; relative mRNA levels were measured via qRT-PCR.

Plasmid Construction and Overexpression of Lipocalin-2 in pGL4.14 vector

The Lcn2 gene was excised from the pCMV6-Entry-Lcn2 plasmid with EcoRI and SmaI (New England Biosciences, Ipswich, MA). The Lcn2 fragment

was ligated into pBluescript KS(-). Subsequent digestion was performed with HindIII and XbaI to insert Lcn2 into pGL4.13-hygro to make pGL4.14-Lcn2. To construct the vector control pGL4.14-Lcn2 was digested with BglII and BamHI to produce pGL4.14. MC38 cells obtained were already transfected with a plasmid expressing luciferase that was G418 resistant. The pGL4.14-Lcn2 or the pGL4.14 empty vector was stably transfected into MC38-Luc cells by selection in Hygromycin.

Histology

Tumor-bearing mice were sacrificed and the liver, spleen, and cecum were excised and fixed in freshly prepared 4% paraformaldehyde in PBS, pH 7.2. Tissue blocks were embedded in paraffin, 5 µm sections obtained and then stained with hematoxylin and eosin (H&E) (VWR, West Chester, PA) for visual examination.

Immunohistochemistry and RNA in-situ hybridization

The paraformaldehyde-fixed, paraffin-embedded tissue sections were deparaffinized, rehydrated, and incubated in a microwave oven with 0.01M citrate buffer, pH 6.0 for 10 minutes for antigen retrieval. Nonspecific epitopes were blocked with IgG-free bovine serum albumin (Jackson ImmunoResearch, West Grove, PA) for 1 hour. The sections were incubated overnight at 4°C with antibodies against Lcn2 (R&D) at 1:200 dilution). This was followed by incubation with the corresponding secondary antibody conjugated to horseradish peroxidase

(HRP) (Bio-Rad, Hercules, CA) for 1 hour at room temperature (RT). Antigen signals were detected using the 2-Solution Diaminobenzidine (DAB) Kit (Invitrogen, Frederick, MD), counterstained with hematoxylin, mounted in Acrymount (StatLab, McKinney, TX), and visualized under a light microscope.

For RNA-ISH, slides were prepared as described for immunohistochemistry and then using the mouse Lcn2 RNAscope[®] kit from ACD (Advanced Cell Diagnostics, Newark, CA) and slides were visualized under a light microscope.

Confocal microscopy

The liver was excised from mice given a splenic injection and electroporated with pV1J or pV1J-Lcn2 at 29 days when mice present with advanced metastatic disease. The samples were fixed in freshly prepared 4% paraformaldehyde in PBS, pH 7.2. Following fixation, the tissues were rinsed with PBS and vibratome sections were cut at 100 μ m thickness. Adjacent sections were cut and stained for H&E and samples were selected to view tumors and liver tissue in the same sample. Samples were stained with primary antibodies: Lcn2 (Rab Pab, Boster Biological Technology, Pleasanton, CA), MPO, F4/80, Mast cell tryptase. Secondary antibodies AF488 anti-rabbit, AF647 anti-goat, and Dylight405 anti-rat (Jackson ImmunoResearch, West Grove, PA) were used. Nuclei were stained with 1:10,000 dilution of 4',6-diamidino-2-phenylindole (DAPI) (Invitrogen, Carlsbad, CA) or Propodium Iodide at a dilution of 1:1000.

Samples were imaged on a Zeiss LSM510 META confocal scanning laser microscope.

Bioluminescent Imaging of mice

Mice were imaged for bioluminescence of luciferase-expressing tumor cells using the MIS Lumina instrument (Perkin Elmer, Waltham, MA). Mice were placed under 2% isoflurane inhalation anesthesia via nose cone both in the preparatory chamber and in the MIS imaging chamber. Mice were given an i.p. injection of 150 mg/kg of XenoLight D-Luciferin (Perkin Elmer) and imaged at least 10 minutes post-injection. Imaging was captured using Living Image software (Perkin Elmer) and adjusting the exposure time to fall within the saturation limits of the acquisition camera. Regions of interest were cordoned off and the bioluminescent counts were converted to photons/second for analysis of tumors in the mice.

siRNA Knockdown of Lcn2

Lcn2 knockdown was achieved using the TriFECTa[®] RNAi kit from IDT (Integrated DNA Technologies, Coralville, IA) comprised of Dicer-substrate short interfering RNAs (DsiRNAs). Primers consisting of 3 Lcn2 specific DsiRNAs, 1 TYE563 transfection control, and 1 negative control (NC). siRNA primers were transfected using Lipofectamine[®] RNAiMAX transfection reagent (ThermoFisher, Pittsburg, PA). TIB-73 and MPRO were given 10 mM siRNA in 6 well plates three

times before harvesting conditioned media, intracellular protein, and mRNA to analyze Lcn2 transcription and translation levels.

Electroporation

BALB/C or C57BL/6 mice that were 8 to 12 weeks of age depending on the application, were used. The lower abdominal quadrant and adjacent leg were shaved. Mice were anesthetized with 2% isoflurane in oxygen by inhalation using a nose cone and placed in a supine position. A longitudinal incision is made with scissors on the ventral surface of the hind limb between the knee and hip of a mouse. 50 μ G of plasmid DNA is injected with a 30G needle in a total volume of 50 μ L (1 μ g/ μ L) into the quadriceps muscles of the mice. Electrodes are placed both sides of the leg muscles and electroporated for 8 pulses at 100 mV for 50 ms. Electroporated mice have serum isolated and ELISA was performed to determine that Lcn2 is upregulated in the blood circulation.

Harvesting and Culturing BMDMs

Bone marrow derived macrophages were isolated from C57BL/6 or B6.129P2-Lcn2tm1Aade/AkiJ Lcn2 knockout mice by flushing femur and tibia bone marrow into RPMI under sterile conditions. Bone marrow was plated on uncoated petri dishes and allowed to grow for 8 days under RPMI with 15% L929 conditioned media. Media with macrophage colony stimulating factor (M-CSF) was prepared by growing L929 (ATCC[®] CCL-1[™]) mouse fibroblast cells in 175mm flask for 1 week and harvesting all conditioned media. After 8 days,

BMDMs were analyzed via flow cytometry for Cd11b+ and F4/80+ population to be over 95%. These BMDMs can be cultured and used for up to 21 days after isolation from the mice.

Statistical Analysis

All data are shown as the mean \pm standard deviation (SD); comparisons of two groups were analyzed using the two-tailed t-test with Welch's correction using GraphPad Prism version 5.00 for Windows, (GraphPad Software, San Diego California USA, www.graphpad.com). P-values of $p < 0.05$, $p < 0.01$, and $p < 0.001$ are indicated with (*), (**), and (***), respectively, and all considered statistically significant.

REFERENCES

American Cancer Society (2014). American Cancer Society recommendations for colorectal cancer early detection.

American Cancer Society (2015). What is colorectal cancer?

Arbab, A.S., and Achyut, B. (2016). Myeloid cell signatures in tumor microenvironment predicts therapeutic response in cancer. *OncoTargets Ther.* 1047.

Asimakopoulou, A., Weiskirchen, S., and Weiskirchen, R. (2016a). Lipocalin 2 (LCN2) Expression in Hepatic Malfunction and Therapy. *Front. Physiol.* 7, 430.

Asimakopoulou, A., Borkham-Kamphorst, E., Tacke, F., and Weiskirchen, R. (2016b). Lipocalin-2 (NGAL/LCN2), a “help-me” signal in organ inflammation. *Hepatology*. Baltimore, Md 63, 669–671.

Azizidoost, S., Ahmadzadeh, A., Rahim, F., Shahjahani, M., Seghatoleslami, M., and Saki, N. (2015). Hepatic metastatic niche: from normal to pre-metastatic and metastatic niche. *Tumour Biol. J. Int. Soc. Oncodevelopmental Biol. Med.*

Bao, G., Clifton, M., Hoette, T.M., Mori, K., Deng, S.-X., Qiu, A., Viltard, M., Williams, D., Paragas, N., Leete, T., et al. (2010). Iron traffics in circulation bound to a siderocalin (Ngal)-catechol complex. *Nat. Chem. Biol.* 6, 602–609.

Barresi, V., Lucianò, R., Vitarelli, E., Labate, A., Tuccari, G., and Barresi, G. (2010). Neutrophil gelatinase-associated lipocalin immunoexpression in colorectal carcinoma: A stage-specific prognostic factor? *Oncol. Lett.* 1, 1089–1096.

Barresi, V., Reggiani-Bonetti, L., Di Gregorio, C., Vitarelli, E., Ponz De Leon, M., and Barresi, G. (2011). Neutrophil gelatinase-associated lipocalin (NGAL) and matrix metalloproteinase-9 (MMP-9) prognostic value in stage I colorectal carcinoma. *Pathol. Res. Pract.* 207, 479–486.

Bonaparte, J.G. (2015). The Effects of Elevated Circulating Levels of Lipocalin 2 on Liver Metastasis of Colorectal Cancer. M.S. University of South Carolina.

Candido, S., Maestro, R., Polesel, J., Catania, A., Maira, F., Signorelli, S.S., McCubrey, J.A., and Libra, M. (2014). Roles of neutrophil gelatinase-associated lipocalin (NGAL) in human cancer. *Oncotarget* 5, 1576–1594.

Catalán, V., Gómez-Ambrosi, J., Rodríguez, A., Ramírez, B., Silva, C., Rotellar, F., Hernández-Lizoain, J.L., Baixauli, J., Valentí, V., Pardo, F., et al. (2011). Up-regulation of the novel proinflammatory adipokines lipocalin-2, chitinase-3 like-1 and osteopontin as well as angiogenic-related factors in visceral adipose tissue of patients with colon cancer. *J. Nutr. Biochem.* 22, 634–641.

Chaplin, D.D. (2010). Overview of the immune response. *J. Allergy Clin. Immunol.* 125, S3–S23.

Cheng, L., Xing, H., Mao, X., Li, L., Li, X., and Li, Q. (2015). Lipocalin-2 Promotes M1 Macrophages Polarization in a Mouse Cardiac Ischaemia-Reperfusion Injury Model. *Scand. J. Immunol.* 81, 31–38.

Conrotto, P., Roesli, C., Rybak, J., Kischel, P., Waltregny, D., Neri, D., and Castronovo, V. (2008). Identification of new accessible tumor antigens in human colon cancer by ex vivo protein biotinylation and comparative mass spectrometry analysis. *Int. J. Cancer J. Int. Cancer* 123, 2856–2864.

Corna, G., Campana, L., Pignatti, E., Castiglioni, A., Tagliafico, E., Bosurgi, L., Campanella, A., Brunelli, S., Manfredi, A.A., Apostoli, P., et al. (2010). Polarization dictates iron handling by inflammatory and alternatively activated macrophages. *Haematologica* 95, 1814–1822.

Corning Incorporated (2013). Assay Methods - Protocol: Cell Invasion Assay.

Correnti, C., and Strong, R.K. (2012). Mammalian siderophores, siderophore-binding lipocalins, and the labile iron pool. *J. Biol. Chem.* 287, 13524–13531.

Davis, M.J., Tsang, T.M., Qiu, Y., Dayrit, J.K., Freij, J.B., Huffnagle, G.B., and Olszewski, M.A. (2013). Macrophage M1/M2 Polarization Dynamically Adapts to Changes in Cytokine Microenvironments in *Cryptococcus neoformans* Infection. *MBio* 4, e00264-13-e00264-13.

De Vlaeminck, Y., González-Rascón, A., Goyvaerts, C., and Breckpot, K. (2016). Cancer-Associated Myeloid Regulatory Cells. *Front. Immunol.* 7.

Ewing, J. (1928). *A Treatise on Tumors* (W.B. Saunders Compay).

Feng, M., Feng, J., Chen, W., Wang, W., Wu, X., Zhang, J., Xu, F., and Lai, M. (2016). Lipocalin2 suppresses metastasis of colorectal cancer by attenuating NF- κ B-dependent activation of snail and epithelial mesenchymal transition. *Mol. Cancer* 15.

Fidler, I.J., and Hart, I.R. (1982). Biological diversity in metastatic neoplasms: origins and implications. *Science* 217, 998–1003.

- Flo, T.H., Smith, K.D., Sato, S., Rodriguez, D.J., Holmes, M.A., Strong, R.K., Akira, S., and Aderem, A. (2004). Lipocalin 2 mediates an innate immune response to bacterial infection by sequestering iron. *Nature* 432, 917–921.
- Fung, K.Y.C., Priebe, I., Purins, L., Tabor, B., Brierley, G.V., Lockett, T., Nice, E., Gibbs, P., Tie, J., McMurrick, P., et al. (2013). Performance of serum lipocalin 2 as a diagnostic marker for colorectal cancer. *Cancer Biomark. Sect. Dis. Markers* 13, 75–79.
- Galdiero, M.R., Bonavita, E., Barajon, I., Garlanda, C., Mantovani, A., and Jaillon, S. (2013). Tumor associated macrophages and neutrophils in cancer. *Immunobiology* 218, 1402–1410.
- Gineste, A., Martin, P., Oswald, E., Coppin, H., and Roth, M.-P. (2016). Evidence for IL-6/STAT3-independent induction of lipocalin-2 in the liver of mice infected with *Escherichia coli*. *Hepatology* 63, 673–674.
- Goetz, D.H., Holmes, M.A., Borregaard, N., Bluhm, M.E., Raymond, K.N., and Strong, R.K. (2002). The neutrophil lipocalin NGAL is a bacteriostatic agent that interferes with siderophore-mediated iron acquisition. *Mol. Cell* 10, 1033–1043.
- Gomez-Chou, S.B., Swidnicka-Siergiejko, A.K., Badi, N., Chavez-Tomar, M., Lesinski, G.B., Bekaii-Saab, T., Farren, M.R., Mace, T.A., Schmidt, C., Liu, Y., et al. (2017). Lipocalin-2 Promotes Pancreatic Ductal Adenocarcinoma by Regulating Inflammation in the Tumor Microenvironment. *Cancer Res.* 77, 2647–2660.
- Goodrich, F., Hackett, A., Capra, F., and Swerling, J. It's a Wonderful Life.
- Gordon-Weeks, A.N., Lim, S.Y., Yuzhalin, A.E., Jones, K., Markelc, B., Buzelli, J.N., Fokas, E., Cao, Y., Smart, S., and Muschel, R. (2017). Neutrophils Promote Hepatic Metastasis Growth Through fibroblast growth factor (FGF)2-dependent Angiogenesis. *Hepatology*.
- Guo, H., Jin, D., and Chen, X. (2014). Lipocalin 2 is a regulator of macrophage polarization and NF- κ B/STAT3 pathway activation. *Mol. Endocrinol.* 28, 1616–1628.
- Gupta, D., Shah, H.P., Malu, K., Berliner, N., and Gaines, P. (2014). Differentiation and Characterization of Myeloid Cells. *Curr. Protoc. Immunol.* Ed. John E Coligan AI 104, Unit-22F.5.
- Hanahan, D., and Weinberg, R.A. (2011). Hallmarks of cancer: the next generation. *Cell* 144, 646–674.
- Howlander, N., Noone, A., Krapcho, M., Garshell, J., Miller, D., Altekruse, S., Kosary, C., Yu, M., Ruhl, J., Tatalovich, Z., et al. (2014). Cancer Statistics Review, 1975-2012 - SEER Statistics.

- Hugen, N., van de Velde, C.J.H., de Wilt, J.H.W., and Nagtegaal, I.D. (2014). Metastatic pattern in colorectal cancer is strongly influenced by histological subtype. *Ann. Oncol. Off. J. Eur. Soc. Med. Oncol. ESMO* 25, 651–657.
- Jablonski, K.A., Amici, S.A., Webb, L.M., Ruiz-Rosado, J. de D., Popovich, P.G., Partida-Sanchez, S., and Guerau-de-Arellano, M. (2015). Novel Markers to Delineate Murine M1 and M2 Macrophages. *PLOS ONE* 10, e0145342.
- Jang, E., Lee, S., Kim, J.-H., Kim, J.-H., Seo, J.-W., Lee, W.-H., Mori, K., Nakao, K., and Suk, K. (2013). Secreted protein lipocalin-2 promotes microglial M1 polarization. *FASEB J.* 27, 1176–1190.
- Jung, M., Weigert, A., Tausendschön, M., Mora, J., Ören, B., Sola, A., Hotter, G., Muta, T., and Brüne, B. (2012). Interleukin-10-induced neutrophil gelatinase-associated lipocalin production in macrophages with consequences for tumor growth. *Mol. Cell. Biol.* 32, 3938–3948.
- Jung, M., Mertens, C., and Brüne, B. (2015). Macrophage iron homeostasis and polarization in the context of cancer. *Immunobiology* 220, 295–304.
- Jung, M., Ören, B., Mora, J., Mertens, C., Dziumbila, S., Popp, R., Weigert, A., Grossmann, N., Fleming, I., and Brüne, B. (2016). Lipocalin 2 from macrophages stimulated by tumor cell-derived sphingosine 1-phosphate promotes lymphangiogenesis and tumor metastasis. *Sci. Signal.* 9, ra64.
- Jung, M., Mertens, C., Bauer, R., Rehwald, C., and Brüne, B. (2017). Lipocalin-2 and iron trafficking in the tumor microenvironment. *Pharmacol. Res.* 120, 146–156.
- Justus, C.R., Leffler, N., Ruiz-Echevarria, M., and Yang, L.V. (2014). In vitro Cell Migration and Invasion Assays. *JoVE J. Vis. Exp.* e51046–e51046.
- Kaplan, R.N., Riba, R.D., Zacharoulis, S., Bramley, A.H., Vincent, L., Costa, C., MacDonald, D.D., Jin, D.K., Shido, K., Kerns, S.A., et al. (2005). VEGFR1-positive haematopoietic bone marrow progenitors initiate the pre-metastatic niche. *Nature* 438, 820–827.
- Kienzl-Wagner, K., Moschen, A.R., Geiger, S., Bichler, A., Aigner, F., Brandacher, G., Pratschke, J., and Tilg, H. (2015). The role of lipocalin-2 in liver regeneration. *Liver Int. Off. J. Int. Assoc. Study Liver* 35, 1195–1202.
- Kim, J., and Bae, J.-S. (2016). Tumor-Associated Macrophages and Neutrophils in Tumor Microenvironment. *Mediators Inflamm.* 2016, 1–11.
- Kjeldsen, L., Johnsen, A.H., Sengeløv, H., and Borregaard, N. (1993). Isolation and primary structure of NGAL, a novel protein associated with human neutrophil gelatinase. *J. Biol. Chem.* 268, 10425–10432.

- Koh, S.A., and Lee, K.H. (2015). HGF mediated upregulation of lipocalin 2 regulates MMP9 through nuclear factor- κ B activation. *Oncol. Rep.* *34*, 2179–2187.
- Li, S., Wang, N., and Brodt, P. (2012). Metastatic cells can escape the proapoptotic effects of TNF- α through increased autocrine IL-6/STAT3 signaling. *Cancer Res.* *72*, 865–875.
- Lv, Z., Xu, L.-Y., Shen, Z.-Y., Zhang, F.-R., Xu, X.-E., and Li, E.-M. (2010). Overexpression of neutrophil gelatinase-associated lipocalin and its receptor in colorectal carcinoma: Significant correlation with cell differentiation and tumour invasion. *Oncol. Lett.* *1*, 103–108.
- Maciel, T.T., Moura, I.C., and Hermine, O. (2015). The role of mast cells in cancers. *F1000Prime Rep.* *7*.
- Martí, J., Fuster, J., Hotter, G., Solà, A.M., Deulofeu, R., Modolo, M.M., Loera, M.A., Ferrer, J., Fondevila, C., and García-Valdecasas, J.C. (2010). Serum neutrophil gelatinase-associated lipocalin in patients with colorectal liver metastases: preliminary results of an exploratory prospective study. *Int. J. Biol. Markers* *25*, 21–26.
- Marti, J., Fuster, J., Sola, A.M., Hotter, G., Molina, R., Pelegrina, A., Ferrer, J., Deulofeu, R., Fondevila, C., and Garcia-Valdecasas, J.C. (2013). Prognostic value of serum neutrophil gelatinase-associated lipocalin in metastatic and nonmetastatic colorectal cancer. *World J. Surg.* *37*, 1103–1109.
- McLean, M.H., Thomson, A.J., Murray, G.I., Fyfe, N., Hold, G.L., and El-Omar, E.M. (2013). Expression of neutrophil gelatinase-associated lipocalin in colorectal neoplastic progression: a marker of malignant potential? *Br. J. Cancer* *108*, 2537–2541.
- Mertens, C., Akam, E.A., Rehwald, C., Brüne, B., Tomat, E., and Jung, M. (2016). Intracellular Iron Chelation Modulates the Macrophage Iron Phenotype with Consequences on Tumor Progression. *PloS One* *11*, e0166164.
- Miller, S., Senior, P.V., Prakash, M., Apostolopoulos, V., Sakkal, S., and Nurgali, K. (2016). Leukocyte populations and IL-6 in the tumor microenvironment of an orthotopic colorectal cancer model. *Acta Biochim. Biophys. Sin.* *48*, 334–341.
- Moschen, A.R., Adolph, T.E., Gerner, R.R., Wieser, V., and Tilg, H. (2017). Lipocalin-2: A Master Mediator of Intestinal and Metabolic Inflammation. *Trends Endocrinol. Metab.* TEM.
- Moses, K., and Brandau, S. (2016). Human neutrophils: Their role in cancer and relation to myeloid-derived suppressor cells. *Semin. Immunol.* *28*, 187–196.

- Mosser, D.M., and Edwards, J.P. (2008). Exploring the full spectrum of macrophage activation. *Nat. Rev. Immunol.* 8, 958–969.
- Neilands, J.B. (1995). Siderophores: structure and function of microbial iron transport compounds. *J. Biol. Chem.* 270, 26723–26726.
- Nielsen, B.S., Borregaard, N., Bundgaard, J.R., Timshel, S., Sehested, M., and Kjeldsen, L. (1996). Induction of NGAL synthesis in epithelial cells of human colorectal neoplasia and inflammatory bowel diseases. *Gut* 38, 414–420.
- Obenauf, A.C., and Massagué, J. (2015). Surviving at a distance: organ specific metastasis. *Trends Cancer* 1, 76–91.
- Oh, B.Y., Hong, H.K., Lee, W.Y., and Cho, Y.B. (2016). Animal models of colorectal cancer with liver metastasis. *Cancer Lett.*
- Oldford, S.A., and Marshall, J.S. (2015). Mast cells as targets for immunotherapy of solid tumors. *Mol. Immunol.* 63, 113–124.
- Ören, B., Urosevic, J., Mertens, C., Mora, J., Guiu, M., Gomis, R.R., Weigert, A., Schmid, T., Grein, S., Brüne, B., et al. (2016). Tumour stroma-derived Lipocalin-2 promotes breast cancer metastasis: Stroma-derived Lcn2 and metastasis. *J. Pathol.* n/a-n/a.
- Paget, S. (1989). Stephen Paget's paper reproduced from *The Lancet*, 1889: The Distribution of Secondary Growths in Cancer of the Breast. *Cancer Metastasis Rev.* 8, 98–101.
- Qian, B.-Z., and Pollard, J.W. (2010). Macrophage diversity enhances tumor progression and metastasis. *Cell* 141, 39–51.
- Rafii, S., and Lyden, D. (2006). S100 chemokines mediate bookmarking of premetastatic niches. *Nat. Cell Biol.* 8, 1321–1323.
- Reilly, P.T., Teo, W.L., Low, M.J., Amoyo-Brion, A.A., Dominguez-Brauer, C., Elia, A.J., Berger, T., Greicius, G., Pettersson, S., and Mak, T.W. (2013). Lipocalin 2 performs contrasting, location-dependent roles in APCmin tumor initiation and progression. *Oncogene* 32, 1233–1239.
- Richardson, D.R. (2005). 24p3 and its receptor: dawn of a new iron age? *Cell* 123, 1175–1177.
- Schroll, A., Eller, K., Feistritzer, C., Nairz, M., Sonnweber, T., Moser, P.A., Rosenkranz, A.R., Theurl, I., and Weiss, G. (2012). Lipocalin-2 ameliorates granulocyte functionality. *Eur. J. Immunol.* 42, 3346–3357.

- Sebens, S., and Schafer, H. (2012). The tumor stroma as mediator of drug resistance--a potential target to improve cancer therapy? *Curr. Pharm. Biotechnol.* *13*, 2259–2272.
- Shinriki, S., Jono, H., Ueda, M., Obayashi, K., Nakamura, T., Ota, K., Ota, T., Sueyoshi, T., Guo, J., Hayashi, M., et al. (2014). Stromal expression of neutrophil gelatinase-associated lipocalin correlates with poor differentiation and adverse prognosis in oral squamous cell carcinoma. *Histopathology* *64*, 356–364.
- Singh, V., Yeoh, B.S., Chassaing, B., Zhang, B., Saha, P., Xiao, X., Awasthi, D., Shashidharamurthy, R., Dikshit, M., Gewirtz, A., et al. Microbiota-Inducible Innate Immune Siderophore Binding Protein Lipocalin 2 Is Critical for Intestinal Homeostasis. *CMGH Cell. Mol. Gastroenterol. Hepatol.*
- Sionov, R.V., Fridlender, Z.G., and Granot, Z. (2015). The Multifaceted Roles Neutrophils Play in the Tumor Microenvironment. *Cancer Microenviron.* *8*, 125–158.
- Soares, K.C., Foley, K., Olino, K., Leubner, A., Mayo, S.C., Jain, A., Jaffee, E., Schulick, R.D., Yoshimura, K., Edil, B., et al. (2014). A Preclinical Murine Model of Hepatic Metastases. *J. Vis. Exp.*
- Spicer, J.D., McDonald, B., Cools-Lartigue, J.J., Chow, S.C., Giannias, B., Kubes, P., and Ferri, L.E. (2012). Neutrophils promote liver metastasis via Mac-1-mediated interactions with circulating tumor cells. *Cancer Res.* *72*, 3919–3927.
- Srikrishna, G. (2011). S100A8 and S100A9: New Insights into Their Roles in Malignancy. *J. Innate Immun.* *4*, 31–40.
- Sun, Y., Yokoi, K., Li, H., Gao, J., Hu, L., Liu, B., Chen, K., Hamilton, S.R., Fan, D., Sun, B., et al. (2011). NGAL expression is elevated in both colorectal adenoma-carcinoma sequence and cancer progression and enhances tumorigenesis in xenograft mouse models. *Clin. Cancer Res. Off. J. Am. Assoc. Cancer Res.* *17*, 4331–4340.
- Suzuki, S., Ishida, T., Yoshikawa, K., and Ueda, R. (2016). Current status of immunotherapy. *Jpn. J. Clin. Oncol.*
- Tandara, L., and Salamunic, I. (2012). Iron metabolism: current facts and future directions. *Biochem. Medica* *22*, 311–328.
- Tsai, S., and Collins, S.J. (1993). A dominant negative retinoic acid receptor blocks neutrophil differentiation at the promyelocyte stage. *Proc. Natl. Acad. Sci. U. S. A.* *90*, 7153–7157.
- Valastyan, S., and Weinberg, R.A. (2011). Tumor Metastasis: Molecular Insights and Evolving Paradigms. *Cell* *147*, 275–292.

Warszawska, J.M., Gawish, R., Sharif, O., Sigel, S., Doninger, B., Lakovits, K., Mesteri, I., Nairz, M., Boon, L., Spiel, A., et al. (2013). Lipocalin 2 deactivates macrophages and worsens pneumococcal pneumonia outcomes. *J. Clin. Invest.* *123*, 3363–3372.

Welch, J.P., and Donaldson, G.A. (1979). The clinical correlation of an autopsy study of recurrent colorectal cancer. *Ann. Surg.* *189*, 496–502.

WHO GLOBOCAN 2012: Estimated Cancer Incidence, Mortality and Prevalence Worldwide in 2012.

Xu, M.-J., Feng, D., Wu, H., Wang, H., Chan, Y., Kolls, J., Borregaard, N., Porse, B., Berger, T., Mak, T.W., et al. (2015). Liver is the major source of elevated serum lipocalin-2 levels after bacterial infection or partial hepatectomy: a critical role for IL-6/STAT3. *Hepatology*. *Baltimore, Md* *61*, 692–702.

Yamamoto, M., Kikuchi, H., Ohta, M., Kawabata, T., Hiramatsu, Y., Kondo, K., Baba, M., Kamiya, K., Tanaka, T., Kitagawa, M., et al. (2008). TSU68 prevents liver metastasis of colon cancer xenografts by modulating the premetastatic niche. *Cancer Res.* *68*, 9754–9762.

Zhang, Y. (2013). The Role of Host-Tumor Interactions In Liver Metastasis of Colorectal Cancer. Theses Diss.

Zhang, X.-F., Zhang, Y., Zhang, X.-H., Zhou, S.-M., Yang, G.-G., Wang, O.-C., Guo, G.-L., Yang, G.-Y., and Hu, X.-Q. (2009). Clinical significance of Neutrophil gelatinase-associated lipocalin(NGAL) expression in primary rectal cancer. *BMC Cancer* *9*, 134.

Zhang, Y., Davis, C., Ryan, J., Janney, C., and Peña, M.M.O. (2013). Development and characterization of a reliable mouse model of colorectal cancer metastasis to the liver. *Clin. Exp. Metastasis* *30*, 903–918.

APPENDIX A – PERMISSION TO REPRINT

ELSEVIER LICENSE TERMS AND CONDITIONS

Jun 21, 2017

This Agreement between Daniel Hughes ("You") and Elsevier ("Elsevier") consists of your license details and the terms and conditions provided by Elsevier and Copyright Clearance Center.

License Number	4133650255036
License date	Jun 21, 2017
Licensed Content Publisher	Elsevier
Licensed Content Publication	Cell
Licensed Content Title	Tumor Metastasis: Molecular Insights and Evolving Paradigms
Licensed Content Author	Scott Valastyan, Robert A. Weinberg
Licensed Content Date	Oct 14, 2011
Licensed Content Volume	147
Licensed Content Issue	2
Licensed Content Pages	18
Start Page	275
End Page	292
Type of Use	reuse in a thesis/dissertation
Portion	figures/tables/illustrations
Number of figures/tables /illustrations	2
Format	both print and electronic
Are you the author of this Elsevier article?	No
Will you be translating?	No
Order reference number	
Original figure numbers	Figures 1, 3
Title of your thesis/dissertation	The Role of Lipocalin-2 in the Hepatic Microenvironment of Colorectal Cancer Metastasis
Expected completion date	Jul 2017
Estimated size (number of pages)	110
Elsevier VAT number	GB 494 6272 12
Requestor Location	Daniel Hughes [REDACTED] [REDACTED] United States Attn: Daniel Hughes
Publisher Tax ID	98-0397604
Total	0.00 USD

THESIS COPYRIGHT PERMISSION FORM

Title(s) of the Image(s): Terese Winslow LLC owns the copyright to the following image(s):

“Lower Gastrointestinal Anatomy”

Description of the Work: Terese Winslow LLC hereby grants permission to reproduce the above image(s) for use in the work specified:

Thesis title: The Role of Lipocalin-2 in the Hepatic Microenvironment of Colorectal Cancer Metastasis

University: The University of South Carolina, College of Arts and Sciences

License Granted: Terese Winslow LLC hereby grants limited, non-exclusive worldwide print and electronic rights only for use in the Work specified. Terese Winslow LLC grants such rights “AS IS” without representation or warranty of any kind and shall have no liability in connection with such license.

Restrictions: Reproduction for use in any other work, derivative works, or by any third party by manual or electronic methods is prohibited. Ownership of original artwork, copyright, and all rights not specifically transferred herein remain the exclusive property of Terese Winslow LLC. Additional license(s) are required for ancillary usage(s).

Credit must be placed adjacent to the image(s) as follows:

For the National Cancer Institute © 2011 Terese Winslow LLC, U.S. Govt. has certain rights

Permission granted to:

Author name: Daniel Titus Hughes

Mailing address: [REDACTED]

Email address: [REDACTED]

Phone number: [REDACTED]



Digitally signed by Daniel Hughes
Date: 2017.06.20 17:31:24 -04'00'

Author Signature

Date



Digitally signed by TERESE WINSLOW
Date: 2017.06.20 21:05:04 -04'00'

Terese Winslow, CMI, Member

Date

Terese Winslow LLC Medical Illustration

714 South Fairfax Street, Alexandria, Virginia 22314

703.836.9121 Fax 571.429.3603

terese@teresewinslow.com

www.teresewinslow.com